

DISSERTATION

PERFORMANCE MODELING OF STORMWATER BEST MANAGEMENT
PRACTICES WITH UNCERTAINTY ANALYSIS

Submitted by

Daeryong Park

Department of Civil and Environmental Engineering

In partial fulfillment of the requirements

For the Degree of Doctor of Philosophy

Colorado State University

Fort Collins, Colorado

Fall 2009

UMI Number: 3401004

All rights reserved

INFORMATION TO ALL USERS

The quality of this reproduction is dependent upon the quality of the copy submitted.

In the unlikely event that the author did not send a complete manuscript and there are missing pages, these will be noted. Also, if material had to be removed, a note will indicate the deletion.



UMI 3401004

Copyright 2010 by ProQuest LLC.

All rights reserved. This edition of the work is protected against unauthorized copying under Title 17, United States Code.



ProQuest LLC
789 East Eisenhower Parkway
P.O. Box 1346
Ann Arbor, MI 48106-1346

COLORADO STATE UNIVERISTY

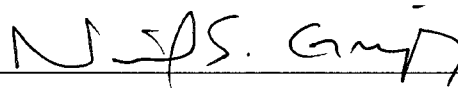
October 8, 2009

WE HEREBY RECOMMEND THAT THE DISSERTATION PREPARED UNDER OUR SUPERVISION BY DAERYONG PARK ENTITLED PERFORMANCE MODELING OF STORMWATER BEST MANAGEMENT PRACTICES WITH UNCERTAINTY ANALYSIS BE ACCEPTED AS FULFILLING IN PART REQUIREMENTS FOR THE DEGREE OF DOCTOR OF PHILOSOPHY.

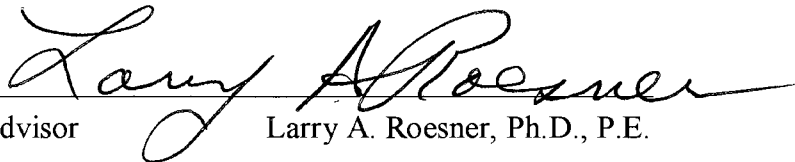
Committee on Graduate Work



Melinda J. Laituri, Ph.D.

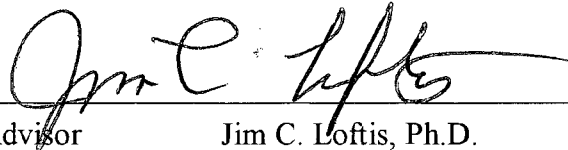


Neil S. Grigg, Ph.D., P.E.



Advisor

Larry A. Roesner, Ph.D., P.E.



Co-Advisor

Jim C. Loftis, Ph.D.



Department Head

Luis A. Garcia, Ph.D.

ABSTRACT OF DISSERTATION

PERFORMANCE MODELING OF BEST MANAGEMENT PRACTICES WITH UNCERTAINTY ANALYSIS

Best management practices (BMPs) contain many uncertainties that make it difficult to determine their performance with a model. Moreover, predicting BMP performance with existing methods is not easy. The major research objective of this dissertation is to incorporate uncertainty analysis in a BMP performance model to better represent its treatment performance.

The k - C^* model is used in this study to simulate BMP performance, and the study assumes that the influent event mean concentration (C_{in}) and aerial removal constant (k) include uncertainty. Both C_{in} and k represent data and model uncertainty. To evaluate the model, three different uncertainty cases, uncertainty in C_{in} , k , and both C_{in} and k , are applied to the total suspended solid (TSS) data of detention basins and retention ponds. To evaluate uncertainty values, three different uncertainty analysis methods, the derived distribution method (DDM), the first-order second-moment method (FOSM), and the latin hypercube sampling (LHS), are applied to each case. TSS, as a representative pollutant, and detention basins and retention ponds, as representative BMPs, are utilized in this study. The observed datasets are selected from the International Stormwater BMP database.

By incorporating uncertainty analysis into the $k-C^*$ model, the effect of BMP surface area and inflow on the effluent event mean concentration (C_{out}) of TSS can be quantified for detention basins and retention ponds. These effects are not large in detention basins but are noticeable in retention ponds.

In addition, the $k-C^*$ model with uncertainty analysis is applied to a hypothetical watershed to show how uncertainty might be used improve the probability of compliance with TMDLs

Daeryong Park

Department of Civil and Environmental Engineering

Colorado State University

Fort Collins, CO 80523

Fall 2009

ACKNOWLEDGEMENTS

I would like to thank my advisor Dr. Larry Roesner and co-advisor Dr. Jim Loftis for the support, guidance, and encouragement throughout my time at CSU. I also would like to extend my appreciation to my committee members; Dr. Neil Grigg, and Dr. Melinda Laituri for their helpful comments and generous assistance during my study.

My deepest and special thanks go to Jennifer Davis, Dr. Jorge Gironás, and Dr. Christine Pomeroy not only for their support and encouragement throughout my studies but also for their true friendship. They have made my life at CSU wonderful and successful. I would also like to extend my appreciation to other members of Dr. Larry Roesner's; Dr. Ramadan Alkhatib, John Edgerly, Ivan Rivas, Liz Kidner, Adam Jokerst, Chris Olson, Xiaoju Zhang, Yongdeok Cho, Steve Roznowski and Simon Lauwo. In addition, I would like to thank Korean graduate students and visiting scholars; Dr. Dongryul Lee, Dr. Suk Hwan Jang, Dr. Hyun-Suk Shin, Dr. Reeho Kim, and Dr. Young-il Song, Dr. Keeuk Cha, Dr. Youngho Shin, Dr. Hangu Lee, Dr. Young-Dae Cho, Dr. Dong-Jin Lee, Dr. Taesam Lee, Dr. Gwangup Lim, Dr. Jognbeom Kang, Dr. Sungchul Kim, Youngjoo Shin, Byoungho Yoo, Yongbae Jung, Kyung Mo Lim, Tae Jung Song, Jaehoon Kim, Sangki Park, Sungsu Bae, Sangdo Ahn, Soojung Hong, Joon Cheol Lee, Jungkyu Ahn, Kyung-Seop Sin, Jonghyun Lee, Ki Chul Jung, Ji-Hee Son, Hyeyun Ku, and Hee Cheol Bou. I also would like to thank other office members including Heather Hill, Emily Boyd, Tony Spencer, Pranay Sanadhya, Haw Yen, Barmak Moghaddam, Mehdi Ahmadi, Masih Akhbari for their patience and kindness. I also would like to express my appreciations to my colleagues: Kyu Hyuk Kyung, Yi-Young Jung, Taejun

Seo, In-Sung Lee, Jong-Wha Bai, Yunchul Cho, Hoki Ban, Ah-Young Cho, and Sookyung Kim.

I would also like to thank the Yonsei University, Dr. Woncheol Cho, Dr. Jun-Haeng Heo, and Dr. Sung-Uk Choi who supported and provided the opportunity to study at CSU.

Most of all, I would like to thank to my wife, Soohyun Kim, who has supported me unfailingly and given so much to this work, especially in encouragement and impetus. Thanks to my babies, Saewoong Park, and Saeyool Park, who make me happy from the stress of the study. Thanks to my sister, Ja Yong Park, my sister-in-law, Ji Hyun Kim, and my brother-in-law, Eui Jae Kim, for sharing happiness and sadness during my study. Finally, Thanks to my parents and parents-in-law, Jongsoon Lee, Bongsik Park, Geumjoo Choi, and Gangjun Kim for the support, love, and patience to wait for me in Korea.

From the help of all these people and those I have not mentioned above, I was able to successfully graduate from CSU.

TABLE OF CONTENTS

1	INTRODUCTION	1
1.1	Study Motivation and Background	1
1.2	Reference	3
2	PERFORMANCE MODELING OF BEST MANAGEMENT PRACTICE WITH UNCERTAINTY ANALYSIS	4
2.1	Introduction.....	4
2.2	Background.....	5
2.2.1	Performance of BMP	5
2.2.2	Uncertainty Analysis	7
2.3	Methods.....	10
2.3.1	Model of Storage BMP Performance	10
2.3.2	Methods for Uncertainty Analysis.....	12
2.3.2.1	Prediction Intervals in Estimating k from the Regression Line	12
2.3.2.2	Derived Distribution Method (DDM)	13
2.3.2.3	First Order Second Moment Method (FOSM).....	13
2.3.2.4	Latin Hypercube Sampling (LHS)	15
2.4	Data Selection and Model Organization	16
2.4.1	Data Selection	16
2.4.2	Statistical Description of Stormwater Constituents.....	18
2.4.3	Model Selection and Organization for BMP Performance	19
2.5	Results and Discussion.....	22
2.5.1	Uncertainty in C_{in}	24
2.5.2	Uncertainty in k	30
2.5.2.1	Sensitivity of Uncertainty in k to C_{in}	31
2.5.2.2	Sensitivity of Uncertainty in k to q	34

2.5.3	Uncertainty in Both C_{in} and k	37
2.6	Conclusions	42
2.7	References	45
2.8	Appendix I. FOSM Application	50
3	EFFECT OF BMP SIZE AND RUNOFF ON THE PERFORMANCE OF BEST MANAGEMENT PRACTICES WITH UNCERTAINTY ANALYSIS.....	52
3.1	Introduction.....	52
3.2	Background.....	53
3.2.1	Performance Effects of BMP Geometry and Inflow	53
3.2.2	Latin Hypercube Sampling	54
3.3	Method	56
3.3.1	Data Selection	56
3.3.2	Model of Storage BMP Performance	60
3.3.3	Relating Hydraulic Loading Rate and Areal Removal Rate Constant.....	60
3.3.4	Uncertainty Analysis and LHS.....	65
3.4	Results	65
3.4.1	Effect of BMP Surface Area	66
3.4.2	Effect of Inflow	70
3.4.3	Analysis of BMP Performance between Detention Basins and Retention Ponds	74
3.4.3.1	Correlation of Concentration, BMP Geometry and Inflow	74
3.4.3.2	Analysis from the k-C* Model	76
3.4.3.3	Analysis of Probability Plots	76
3.5	Conclusions	78
3.6	References	79
4	PROBABILISTIC ESTIMATION OF POLLUTANT LOAD TO RECEIVING WATER FROM BMPS USING UNCERTAINTY ANALYSIS.....	82

4.1	Introduction	82
4.2	Background	83
4.2.1	Stormwater Storage-Release Systems	83
4.2.2	The Storage-Treatment-Overflow-Runoff Model	84
4.2.3	BMP Performance Model	85
4.2.4	Uncertainty Analysis	86
4.2.5	Load Duration Curve	87
4.3	Methods	88
4.3.1	Outline of Urban Stormwater System.....	88
4.3.2	Precipitation Data	89
4.3.3	BMP Performance Data	90
4.3.4	BMP Performance Model	90
4.3.5	Relationship between Hydraulic Loading Rate and Areal Removal Coefficient	90
4.3.6	Generation of Probabilistic Outcomes	90
4.3.7	First Order Second Moment (FOSM) Method.....	91
4.3.8	Steps for Pollutant Load Estimation with Uncertainty	91
4.3.8.1	Log Transformation of Original EMC Data	92
4.3.8.2	Estimation of Mean and Standard Deviation of Log Transformed EMC data	92
4.3.8.3	Computation of Pollutant Load.....	93
4.3.9	Computation of the Event-Based Pollutant Load Frequency Curve.....	95
4.3.9.1	Separation of Flows into BMP and Overflow Bypass.....	96
4.3.9.2	Development of Load Frequency Curve (LFC).....	96
4.4	Results	99
4.4.1	Load Frequency Curves (LFCs).....	99
4.4.2	Generic Procedure for BMP Design.....	103
4.5	Discussion	107
4.6	Conclusions	109
4.7	References	110
5	CONCLUSIONS, CONTRIBUTIONS, AND RECOMMENDATIONS	114

5.1	Conclusions	114
5.2	Summary of Contribution	116
5.3	Recommendation	117
5.4	References	117
	Appendix II. Collected Data for Detention Basins	118
	Appendix III. Collected Data for Retention Ponds	119

List of Figures

Figure 2.1 Overview of data categories in the International Stormwater BMP Database (www.bmpdatabase.org) (ASCE & US EPA, (2002))	16
Figure 2.2 Histogram of observed data and lognormal fitting for detention basins;	18
Figure 2.3 Estimated k vs. q using individual storm events for detention basins	21
Figure 2.4 Schematic for generation of probabilistic C_{out} ;	23
Figure 2.5 Probability density functions for C_{out} as function of q for detention basins; (a) DDM; (b) LHS; (c) FOSM.....	26
Figure 2.6 Comparison of $f(C_{out})$ considering uncertainty in C_{in} among DDM, LHS and FOSM for detention basins	28
Figure 2.7 Uncertainty in C_{in} : probability density functions of LHS including confidence intervals and observed data for detention basins.....	29
Figure 2.8 The comparison of confidence intervals between LHS and FOSM on considering uncertainties in C_{in} for detention basins	30
Figure 2.9 $f(C_{out})$ as a function of C_{in} using $q=0.1$ m/day when considering uncertainty in k for detention basins (a) DDM; (b) LHS	32
Figure 2.10 Comparison of $f(C_{out})$ as a function of C_{in} using $q=0.1$ m/day on considering uncertainty in k for detention basins between DDM and LHS	33
Figure 2.11 Uncertainty in k to C_{in} : probability density functions from LHS including confidence intervals and observed data for detention basins	33
Figure 2.12 $f(C_{out})$ as a function of q using $C_{in}=170$ mg/L on considering uncertainty in k for detention basins (a) DDM; (b) LHS	35
Figure 2.13 Comparison of $f(C_{out})$ as a function of q using $C_{in}=170$ mg/L and considering uncertainty in k for detention basins between DDM and LHS	36
Figure 2.14 Uncertainty in k to q : probability density functions from LHS including confidence intervals and observed data for detention basins	37
Figure 2.15 $f(C_{out})$ as a function of q on considering uncertainty in both C_{in} and k for detention basins ;(a) LHS, (b) FOSM.....	38

Figure 2.16 Comparison of $f(C_{out})$ as a function of q on considering uncertainty in k for detention basins between LHS and FOSM	39
Figure 2.17 Uncertainty in both C_{in} and q : probability density functions of LHS including confidence intervals and observed data for detention basins	40
Figure 2.18 The comparison of confidence intervals between LHS and FOSM on considering uncertainties in C_{in} and k for detention basins	41
Figure 3.1 Outline of the international stormwater BMP database and data collection of this study (www.bmpdatabase.org)	57
Figure 3.2 Lognormal probability plots of observed EMCs;	59
Figure 3.3 q vs. k with 95% prediction interval;	63
Figure 3.4 Schematic for generation of probabilistic C_{out}	66
Figure 3.5 Probability density functions for TSS effluent EMCs in detention basins as a function of BMP Surface area	68
Figure 3.6 Probability density functions for TSS effluent EMCs in retention ponds as a function of BMP Surface area	69
Figure 3.7 Probability density functions for TSS effluent EMCs in detention basins as a function of average inflow	71
Figure 3.8 Probability density functions for TSS effluent EMCs in retention ponds as a function of average inflow	73
Figure 3.9 Correlations in detention basins and retention ponds	75
Figure 4.1 Schematic process of urban runoff through the BMP	89
Figure 4.2 Schematic for generation of probabilistic C_{out}	91
Figure 4.3 Schematic of Load Frequency Curve and 95% Confidence Intervals	98
Figure 4.4. Comparison of LFCs as function of BMP volume (=2.03 cm) and imperviousness (=40%) and with median and 95% confidence intervals in detention basins.	100
Figure 4.5 Comparison of LFCs as function of BMP volume (=2.03 cm times watershed) and imperviousness (=40%) and with median and 95% confidence intervals in retention ponds.	102

Figure 4.6 Load frequency curves including confidence intervals for requirements of load and exceedance.....	104
Figure 4.7 Flowchart of generic BMP design for a given target and safety.....	106

List of Tables

Table 2.1 Selected Best Management Practices in this study.....	17
Table 2.2 Typical background concentration values proposed in literature.....	20
Table 2.3 Required parameters information of C_{in} and k for uncertainty analyses	21
Table 3.1 Geometric information of BMPs and assembled number of dataset in this study	57
Table 3.2 Statistical variables of influent and effluent EMCs in detention basins and retention ponds	58
Table 3.3 Required parameters information of k for detention basins and retention ponds	64
Table 3.4 Typical background concentration values proposed in literatures	65
Table 4.1 QuickSTORM Input Parameters	96
Table 4.2 STORM parameters depending on conditions for no target pollutant values .	103

Abbreviations

The following abbreviations are used in this chapter:

AFOSM= Advanced First-Order Second-Moment;

ASCE = American Society of Civil Engineers;

BMP = Best Management Practice;

EMC = Event Mean Concentration;

CalTrans = California Department of Transportation;

CDF = Cumulative Density Function;

CSTR = Continuously-Stirred Tank Reactor;

DDM = Derived Distribution Method;

EMC = Event Mean Concentration;

EPM = Effluent Probability Method;

FDC = Flow Duration Curve;

FOE = First Order Error;

FOSM = First Order Second Moment;

FOVE = First Order Variance Estimation;

GLUE = Generalized Likelihood Uncertainty Estimation;

HLR = Hydraulic Loading Rate;

HYSIM = Hydrological Simulation Model (HYSIM)

IWA = International Water Association;

LDC = Load Duration Curve;

LFC = Load Frequency Curve

LHS = Latin Hypercube Sampling;

MCS = Monte Carlo Simulation;

MFOSM = Mean-value First-Order Second-Moment;

MOS = Margin of Safety;

NURP = Nationwide Urban Runoff Program;

OAT = One-factor-At-a-Time;

PDF = Probability Density Function;

PPE = Probabilistic Point Estimation;

STORM = Storage, Treatment, Overflow, Runoff Model;

SWAT = Soil and Water Assessment Tool;

TAN = Total Ammonium Nitrogen;

TMDL = Total Maximum Daily Load;

TN = total nitrogen;

TP = Total Phosphorus;

TSS = Total suspended solid;

UDFCD = Urban Drainage and Flood Control District;

US EPA = United States Environmental Protection Agency.

1 INTRODUCTION

1.1 Study Motivation and Background

Urbanization impacts the rainfall-runoff process in a variety of ways by modifying the natural conditions of a watershed. As a watershed becomes more developed, peak flows, runoff volumes, and nonpoint source pollution increase while the time of concentration decreases. Best Management Practices (BMPs) reduce these negative effects of urbanization by controlling peak flows and removing pollutants from the runoff. The hydrologic aspects of their operation have been extensively studied for several decades, resulting in the generation of design criteria manuals; however only the hydrologic performance into account. Pollutant removal is not considered in the design guidance even though the primary purpose of BMPs is pollutant removal.

BMP design based on water quality is still controversial and existing BMP design methods are too inaccurate to be applied with confidence. The inaccuracy of the predictive models is so poor, that experts in the field (Strecker et al., 2001 and 2004) recommend that measured effluent data taken from International BMP Database (www.bmpdatabase.org) be used to estimate water quality discharge concentrations from BMP rather than model simulations. This is mainly due to the many uncertainties associated with the performance of a BMP in terms of pollutant removal and the inability of existing models to represent those uncertainties. Therefore, the development of BMP design methodology based on BMP performance models continues to be a task that needs to be addressed (UDFCD, 2001).

This study examines the uncertainty in the main variables affecting the pollutant removal in extended detention and retention pond BMPs, with the intention of generating risk-based BMP design methodologies. In particular, this research investigates uncertainty in the BMP design parameters, characterizing pollutant removal by using risk-based probabilistic methods. The specific objectives are the following:

- (1) Incorporate uncertainty analysis to the $k-C^*$ model, a BMP performance model originated as a wetland model, but commonly used to model performance of other types of BMPs, and verify its performance with observed data.
- (2) Investigate the sensitivity of this uncertainty-based $k-C^*$ model to inflow discharge (Q) and the BMP surface area (A_{BMP}), a representative physical parameter of BMPs.
- (3) Characterize the variability of pollutant load reduction simulated by the uncertainty-based $k-C^*$ model in order to evaluate the performance of BMPs in terms of the Total Maximum Daily Load (TMDL) goals.

The BMP performance data sets for this study were obtained from the International Stormwater BMP Database (www.bmpdatabase.org), which has been assembled since 1996 by the American Society of Civil Engineering (ASCE) and the U.S. Environmental Protection Agency (US EPA). The database was established to foster a better understanding of factors influencing BMP performance and to promote improvements in BMP design, selection and implementation. This study uses the data from that database to examine the removal of total suspended solids (TSS) for detention basins and retention ponds.

The dissertation comprises three chapters followed by a final chapter of conclusions and recommendations. In Chapter 2, uncertainty is incorporated into the $k-C^*$ model, and used to assess the BMP performance. Uncertainty in three variables of the model is explored: C_{in} , k and both C_{in} and k . The methods used in the uncertainty analysis include the Derived distribution method (DDM), the First-Order Second-Moment (FOSM) method, and the Latin Hypercube Sampling (LHS) method. Chapter 3 investigates the effects of BMP surface area and inflow discharge on the BMP performance based on pollutant concentration removal using the BMP performance model developed in Chapter 2. Chapter 4 demonstrates the potential applicability of the $k-C^*$ model with uncertainty analysis to a hypothetical stormwater system and demonstrates how it might be used to reduce the uncertainty associated with designing a BMP to meet a specific TMDL. Finally, Chapter 5 presents the main conclusions and a summary of the contributions of this study followed by recommendations for future research.

1.2 Reference

Urban Drainage and Flood Control District (UDFCD). (2001). "Urban Drainage and Flood Control District Drainage Criteria Manual (USWDCM)." Volume 3, Denver, Colorado.

2 PERFORMANCE MODELING OF BEST MANAGEMENT PRACTICE WITH UNCERTAINTY ANALYSIS

2.1 Introduction

Many elements of uncertainty exist in nature, and obtaining accurate information about natural systems becomes a challenge. Mays and Tung (1992) defined uncertainty as the occurrence of events that are beyond one's control. Due to these uncertainties, it is difficult to design and build a model that predicts results similar to the observed ones. Most of the widely-used urban hydrologic models are deterministic and ignore uncertainty, but uncertainty analysis shows a range of results, offering the decision maker more information. Water quality modeling has even more uncertainties and is very unpredictable. This includes uncertainties in models representing pollutant removals in stormwater BMPs, which are widely used for the reduction of nonpoint-source pollutants.

A lot of information on the hydrologic performance of BMPs has been published (Urbonas and Roesner, 1993; ASCE, 1994; Guo and Urbonas, 1996; Guo, 1999; Guo and Urbonas, 2002). However, BMP performance in the treatment of pollutants is still a topic of much research. It is extremely important to improve the current paradigm which assumes a BMP is a deterministic system characterized by a percent-concentration reduction. The objective of this chapter is to present a BMP performance model that incorporates uncertainty analysis in its evaluation of TSS removal in detention basins. This chapter describes the construction of a BMP performance model with uncertainty

analysis and evaluates this model's performance by comparing its results with observed data available from the International Stormwater BMP Database (www.bmpdatabase.org).

2.2 Background

2.2.1 Performance of BMP

Many attempts have been made to evaluate BMP performance. Historically, the efficiencies of BMPs have been represented by the percent removal of pollutants. Strecker et al. (2001 and 2004) argued that using percent removal as an indicator of efficiency often gives inaccurate results. They suggested that the efficiency of BMPs might be better characterized by using the effluent EMC and that design standards should consider hydrologic losses that take place with some BMP types.

Particularly, Strecker et al. (2001) and Clary et al. (2002) compared three estimation methods for measuring BMPs efficiency. They found that the effluent quality in any given class of BMPs tend to have a small range. Therefore, they suggested the Effluent Probability Method (EPM), a lognormal probability plot of EMC, as one of the best methods for estimating BMP efficiency and for characterizing the effluent quality. The characterization of EMC using a lognormal distribution is consistent with most stormwater EMC data (US EPA 1983, Driscoll 1986, Van Buren et al. 1997). Brown (2003) developed example EPM plots for TSS, nitrate, and total zinc removal. He concluded that BMP removal of TSS results in different slopes between the influent and effluent lognormal plots.

However, the EPM also has several problems, which have been clearly described by the California Department of Transportation (CalTrans, 2003). One of the downfalls of the EPM is that quantitative assumptions cannot be made without matching data points. Additionally, the method does not account for the hydrologic effect of storm size on BMP efficiency. Finally, EPM does not provide sufficient information regarding proper BMP selection for design. Therefore, the method may not sufficiently describe whether a BMP can satisfy a certain performance standard.

Barrett (2005) compared the pollutant removal of various BMPs and developed a classification of the constituents and BMPs for which the influent EMC, C_{in} , and effluent EMC, C_{out} , were poorly correlated. This is the case for sand filters and wet basins. He found that pollutant-percent removal can be related to C_{in} when C_{out} values are similar to the background concentration for each storm event. He also evaluated the BMP performance in controlling different constituents with estimated pollutant-load reduction rates found from regression analysis. As a result, it was suggested that the percent removal based on concentration reflects the relationship between a BMP and influent-water quality rather than characterizing the BMP itself.

Many mathematical models have been developed to analyze and predict the water treatment of storage ponds (Roesner et al., 1974; Driscoll, 1986; Guo and Adams, 1999; Strecker et al., 2001; Wong et al, 2006). They attempt to represent complex treatment mechanisms through simple mathematical expressions. One of the most popular mathematical models is the $k-C^*$ model which has been widely used to describe pollutant removal in wetlands (Kadlec and Knight, 1996; Kadlec, 2000; Braskerud, 2002; Kadlec, 2003; Rousseau et al, 2004; Lin et al., 2005). The International Water Association (IWA)

(2006) provided the design approach for wetlands using the $k-C^*$ model. It was shown that the model coefficient (k) representing the concentration removal rate is strongly and consistently related to the hydraulic loading rate (q) with a power function (Schierup et al. 1990).

While the $k-C^*$ model has been primarily used for modeling wetland performance, it has also been applied to represent BMP performance. Pack et al. (2005) used the $k-C^*$ model to simulate vegetated infiltration performance on highways, but Pack did not report the comparison of results between simulation and observed values. In addition, Wong et al. (2006) modeled urban stormwater treatment using the $k-C^*$ model in combination with a continuously-stirred tank reactor (CSTR) and tried to simulate the intra-event water quality during a storm. However, what Wong showed was not prediction results but calibration results of the $k-C^*$ model using CSTR numbers with observed data, which did not clearly explain the derivation of the areal removal rate constant, k .

2.2.2 Uncertainty Analysis

Uncertainty analysis is a tool commonly used in all disciplines of civil engineering. Various approaches have been used in uncertainty analysis including analytic methods, approximation methods, and different varieties of the Monte Carlo Simulation (MCS). One of the most well known approximation methods is the first-order second-moment (FOSM) method, also referred to as the first-order error method or the first-order variance estimation method. Since the 1970s, FOSM has been applied in hydrosystem engineering and environmental engineering problems including storm

drainage systems (Yen and Tang 1976), levee systems (Tung and Mays 1981), runoff modeling (Melching 1992), open channel flow (Yeh and Tung 1993), and stream water quality (Burgess and Lettenmaier 1975). In addition, Song and Brown (1990) applied FOSM by including the correlated inputs using the Streeter-Phelps equation. Their study assumed correlation coefficients among nine model inputs and evaluated the uncertainty. Results showed that this method generates similar results to the ones provided when input data were correlated. Alternatively, Melching and Anmangandla (1992) compared the mean-value first-order second-moment (MFOSM) method with the advanced first-order second-moment (AFOSM) method using the Streeter-Phelps equation and found that the AFOSM method produces better results than the MFOSM method. Recently, the FOSM method has been applied to estimate the margin or safety (MOS) in the total daily maximum daily load (TMDL) (Zhang and Yu, 2004).

The derived distribution method (DDM) is the most classical approach in analytical uncertainty analysis (Mays, 1996; Salas et al, 2004; Tung and Yen, 2005). Canter and Knox (1986) applied DDM to the Dupuit-Fochheimer theory to estimate the groundwater table. Kunstmann and Kastens (2006) applied DDM to represent a probability density function (PDF) of output in the case of one or two variables in the Theis equation, the Gauss equation, and the Penman-Monthith equation. They also mentioned that DDM has difficulties in representing the uncertainty of bivariates.

The latin hypercube sampling (LHS) method is a modified stratified sampling of MCS. It can provide accurate estimates of statistical variables of model output at a much smaller computational load than MCS (Melching, 1995). Several studies have applied LHS to estimate sediment transport. Yeh and Tung (1993) compared FOSM, Harr's

probabilistic point estimation (PPE) method, and LHS for uncertainty analysis of erosion and transport and found that FOSM and LHS provide better results than Harr's PPE method. Salas and Shin (1999) applied MCS and LHS to four uncertainty factors—rating curves, incoming sediment type, reservoir efficiency, and annual streamflow—and evaluated the uncertainty of annual reservoir sedimentation volume and accumulated reservoir sedimentation volume of the Kenny Reservoir in Northern Colorado. For water quality, the LHS has been applied to predict streamflow and water quality parameters in the Soil & Water Assessment Tool 2000 (SWAT 2000) and to estimate dissolved oxygen (Sohrabi et al. 2003; Melching and Bauwens 2001). Also, Shirmohammadi et al. (2006) applied LHS with other uncertainty methods, including MCS and the generalized likelihood uncertainty estimation (GLUE), to estimate the uncertainty of sediment estimation in the SWAT model's output. Moreover, they demonstrated the uncertainty of the vegetative filter strip modeling design system, and from this result, suggested that the result represented by the PDF can assist in improving management decisions concerning TMDL allocation and implementation.

The results of this chapter shows that the distribution of effluent EMCs (C_{out}) represents the uncertainty of the variables: influent EMC (C_{in}), areal removal rate constant (k), and combined uncertainty of C_{in} and k . Data uncertainty, such as C_{in} , is evaluated with selected TSS data obtained from a BMP database, and model uncertainty is estimated from a regression relation of q and k .

2.3 Methods

This study uses the prediction interval estimation method, which predicts the distribution of individual data or estimates an interval of a variable, to estimate the areal removal rate constant, and uses three other uncertainty estimation methods to create PDFs of effluent concentration. The DDM was chosen as the analytical method and FOSM was selected as the analytical approximation method. Finally, LHS is used for the numerical estimation method.

2.3.1 Model of Storage BMP Performance

The classical mathematical model for water treatment is the first-order decay model widely used to describe pollutant removal in treatment plants wetlands, swales, etc. (Carleton et al., 2001; Braskerud, 2002; Wong et al., 2006). The performance of volumetric BMPs for stormwater is closely related to water treatment in wetlands; it uses variables such as geometric storage shape, inflow and outflow rates, and influent and effluent concentrations. One of the models used in modeling both systems is the $k-C^*$ model. Many researchers have applied this model to constructed wetland performance and shown good reproducibility of real situations (Kadlec, 2000; Rousseau et al, 2004; Stone et al, 2004; Kadlec, 2003). This model incorporates “irreducible minimum concentration” to the first-decay equation where the observed effluent concentration converges to a constant value. Assumptions of the model are steady and plug flow conditions, valid assumptions used in representing flow hydrodynamics within wetland systems (Kadlec and Knight, 1996).

The $k-C^*$ model is defined by:

$$q \frac{dC}{dy} = k(C - C^*) \quad (2.1)$$

Considering y , the fraction of distance from inlet to outlet, when y equals one, integration of equation (2.1) gives

$$C_{out} = C^* + (C_{in} - C^*)e^{-k/q} \quad (2.2)$$

where:

C_{out} = effluent EMC (mg/L),

C_{in} = influent EMC (mg/L),

C^* = background EMC or “irreducible minimum concentration” EMC (mg/L),

k = areal removal rate constant (m/day), and

q = hydraulic loading rate, defined as the ratio of the inflow discharge divided by

the surface area of the system $\left(\frac{Q}{A}\right)$ (m/day)

Although the model assumes steady-state flow conditions, BMP fills quickly and drains one a long period (24-72 hours) at an essentially constant rate. For that reason, it can be dealt with this assumption for BMPs.

2.3.2 Methods for Uncertainty Analysis

There are two types of uncertainty in this study. One is parameter uncertainty, such as k in the k - C^* model, and the other is data uncertainty, which is mainly represented in C_{in} and C_{out} data. Prediction intervals are used for estimating the uncertainty of the areal-removal-rate constant in the model. DDM, FOSM and LHS are selected for estimating the variance of C_{out} . The variable X represents the independent-random variable q in Section 2.3.2.1 and C_{in} in Section 2.3.2.2-2.3.2.4, while Y represents the dependent variable k in Section 2.3.2.1 and C_{out} in Section 2.3.2.2-2.3.2.4.

2.3.2.1 Prediction Intervals in Estimating k from the Regression Line

k is related to q with a power function in the k - C^* model (Schrierup et al., 1990; Lin et al., 2005). However, the variance of C_{out} , simulated with the k - C^* model changes dramatically depending on k . Therefore, it is necessary to apply a prediction interval in the k and q regression line. A prediction interval is focused on the variance of individual data while a confidence interval is focused on the variance of a regression line. This study works with the prediction interval of k because it is more important to know the performance for an individual event rather than the prediction of the average performance for many similar events (Barrett, 2005). The prediction interval in the regression line relating k and q is calculated by Equation (2.3) (Kutner et al. 2004).

$$Mean \pm t_{0.025} s \sqrt{1 + \frac{1}{n} + \frac{(X - \bar{X})^2}{\sum_{i=1}^n (X_i - \bar{X})^2}} \quad (2.3)$$

where

t = the t distribution for the appropriate degree of freedom (n-2),

n = the number of total data,

s = standard error of the regression,

X = average q at which the confidence interval is calculated,

\bar{X} = mean of observed q from monitoring data, and

X_i = individual observed q from monitoring data.

2.3.2.2 *Derived Distribution Method (DDM)*

In the DDM, the PDF of a variable $y = g(x)$ can be obtained given the PDF of X , $f_x(x)$. The transformation from the PDF of X to that of Y entails the substitution of the inverse function of Y solved for X in the PDF of X . Then, the PDF of Y is (Salas, 2004):

$$f_Y(y) = \left| \frac{dg^{-1}(y)}{dy} \right| f_x[g^{-1}(y)] \quad (2.4)$$

2.3.2.3 *First Order Second Moment Method (FOSM)*

Approximation methods are variations of analytical methods used as approximation techniques. They are used when non-linearity makes DDM nonviable. FOSM is one of these approximation methods that uses a Taylor-series expansion of the performance function and estimates the mean and variance of the performance function. Those are:

$$E(Y) = E[g(X_1, \dots, X_n)] \approx g(\mu_1, \dots, \mu_n) \quad (2.5)$$

$$Var(Y) = Var[g(X_1, \dots, X_n)]$$

$$\approx \sum_{j=1}^n \left(\frac{\partial g}{\partial X_j} \right)_{\mu}^2 Var(X_j) + \sum_{i=1}^n \sum_{j=1}^n \left(\frac{\partial g}{\partial X_i} \right)_{\mu} \left(\frac{\partial g}{\partial X_j} \right)_{\mu} Cov(X_i, X_j), \quad (2.6)$$

in which X indicates random variables and Y specifies a general function $y = g(x)$.

Assuming that the X_i 's are independent variables, $Cov(X_i, X_j) = 0$, then the variance of Y is (Salas, 2004):

$$Var(Y) = Var[g(X_1, \dots, X_n)] \approx \sum_{j=1}^n \left(\frac{\partial g}{\partial X_j} \right)_{\mu}^2 Var(X_j). \quad (2.7)$$

$\hat{\mu}_{\ln x}$ and $\hat{\sigma}_{\ln x}$ can be calculated from the sample mean and standard deviation of logtransformed X . Finally, the inverse of the cumulative distribution function (CDF) is calculated to quantify the percentile of the lognormal distribution using the estimated parameters:

$$X_p = \exp(\mu_{\ln x} \pm Z\sigma_{\ln x}), \quad (2.8)$$

where

Z = the standard normal quantile corresponding to exceedance probability, and

X_p = the X value of p percentile.

The application of FOSM to the k - C^* model in uncertainty both C_{in} and k is represented in Appendix I in detail.

2.3.2.4 Latin Hypercube Sampling (LHS)

The LHS is a stratified sampling method to reduce variance and sampling error.

The steps to apply the methods are (Tung and Yen, 2005):

1. Select the number of subintervals, M , and divide the range $[0, 1]$ into M equal intervals.

2. For each subinterval, define ξ_m as independent-uniform-random numbers from $\xi_m \sim U(0,1/M)$ for $m=1,2,\dots,M$. Then, a sequence of probability values u_m are generated as

$$u_m = \frac{m-1}{M} + \xi_m \quad m = 1, 2, \dots, M$$

3. Compute $z_m = F^{-1}(u_m)$ in which $F(\cdot)$ is the CDF of the random variable of standard normal distribution.

4. Compute mean and standard deviation from log transformed C_{in} or k .

5. Compute generated C_{in} or k assuming lognormal distribution as $x_m = \exp(\mu_{\ln x} + z_m \sigma_{\ln x})$.

6. Apply generated C_{in} or k to the k -C* model

2.4 Data Selection and Model Organization

2.4.1 Data Selection

BMP performance data were collected from the International Stormwater BMP Database (www.bmpdatabase.org) maintained by the American Society of Civil Engineers (ASCE) and the United States Environmental Protection Agency (US EPA). This data is categorized as illustrated in Figure 2.1. For different BMPs, the database includes geometric information, event runoff volumes, water quality data, and other general information. Nine types of BMPs are defined in the database: dry detention basins, wetlands, trenches, media filters, infiltration basins, hydrodynamic devices, porous pavement, grass filters, and wet retention ponds. This chapter addresses only dry detention basins and considers total suspended solid (TSS) as the representative BMP and nonpoint source pollutant. In Chapter 3, BMP geometry and stormwater runoff characteristics will be coupled and their effects on water quality modeled. Results will be compared with field data available in the BMP database.

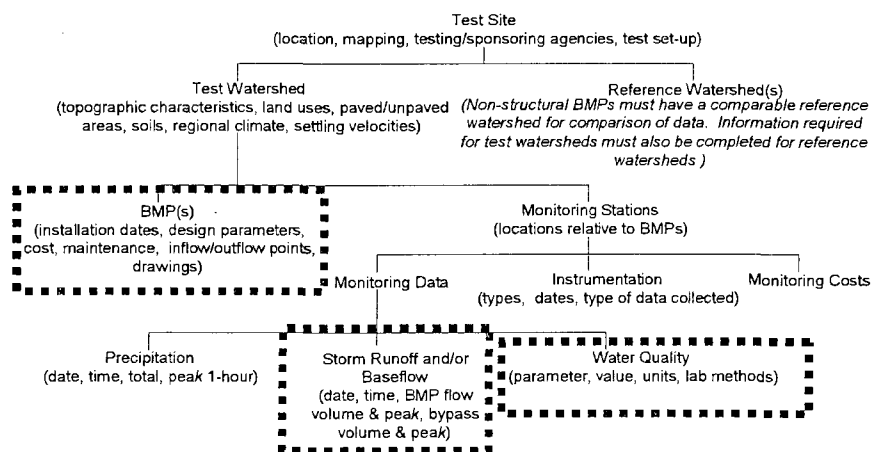


Figure 2.1 Overview of data categories in the International Stormwater BMP Database (www.bmpdatabase.org) (ASCE & US EPA, (2002))

Pre-screening was necessary to select the BMP data to use in the model because some datasets do not make sense based on normal BMP performance. The final BMPs chosen for this study are those in which the average outflow rate is smaller than the average inflow rate and those in which C_{out} is not significantly larger than C_{in} for any event. In the case of the flow rate, the event-based-average inflow rate should be higher than the event-based-average outflow rate because of the performance of BMPs. Regarding the EMCs, it has been observed that C_{out} is sometimes greater than C_{in} . This is because settled pollutants in BMPs can become re-suspended by influent flows. This behavior is not typical of a well designed BMP and is only acceptable when the influent EMC is low compared to the “irreducible minimum effluent EMC”, which indicates that C_{out} values converge to a particular value above zero (Minton (2005) and Schueler (1996)). These criteria were considered in choosing BMPs from the database.

Table 2.1 lists the locations, documented pollutants, and sizes of the four detention BMPs used in this study. All of the chosen detention basins are located in the state of California.

Table 2.1 Selected Best Management Practices in this study

BMP Type	BMP name, Location	BMP size			
		Number of Datasets	Volume (m ³)	Surface area (ha)	Length (m)
Detention Basin	15/78, CA	17	1122.54	0.0977	60.96
	5/605 EDB, CA	2	364.66	0.0598	47.24
	605/91 edb, CA	5	69.57	0.0114	22.86
	Manchester, CA	12	252.79	0.0304	22.86

2.4.2 Statistical Description of Stormwater Constituents

Based on the results obtained by the Nationwide Urban Runoff Program (NURP) study (US EPA 1983) and Van Buren et al. (1997), Strecker et al. (2001) remarked that stormwater constituents can be well represented by a lognormal distribution. The lognormal distribution was adjusted to C_{in} and C_{out} data to verify this statement. Figure 2.2 shows this distribution together with the empirical histogram for sites shown in Table 2.1. It is observed that the lognormal distribution represents the data well. Similar results were obtained for the other locations in this study.

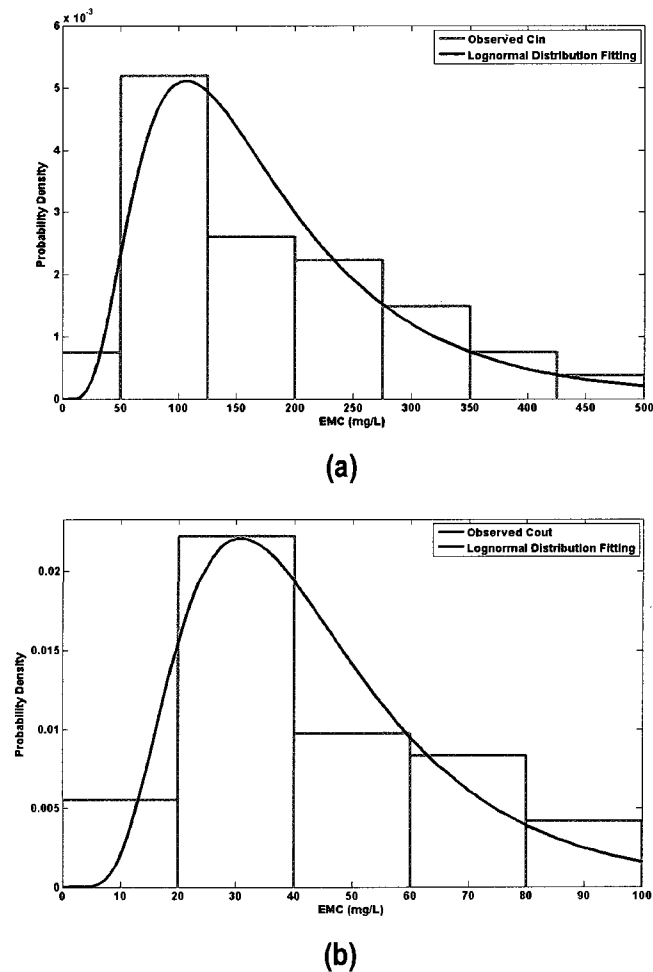


Figure 2.2 Histogram of observed data and lognormal fitting for detention basins; (a) C_{in} and (b) C_{out}

2.4.3 Model Selection and Organization for BMP Performance

The k - C^* model presented in Section 2.3.1 was used for simulating the performance of a BMP. Both parameters of the model, k and C^* , depend on pollutant characteristics such as the particle sizes and higher specific gravity and settling velocity (Wong et al. 2002). Treatment systems receiving large particle concentrations will have a high removal rate and a low C^* since there is more sedimentation. Thus, there is a relationship between the parameter, k , and the settling velocities (or particle size) of suspended particles received from watersheds. Thus, parameter calibration for the k - C^* model should be performed based on local site conditions such as particle size distribution. In addition, C^* depends on temperature and inflow concentration (Kadlec and Knight 1996). Although the areal removal rate constant, k , has a theoretical link to settling velocity, field studies have shown that this theoretical link is not necessarily the case for particles finer than about 40 μm (Wong et al. 2002), which consist of silt, coarse clays, organic fines and phytoplankton (Roesner et al., 2007). Thus, the estimation of k is not straightforward. Scherup et al. (1990) and Lin et al. (2005) suggested that the k -values of the the k - C^* model are strongly dependant on the hydraulic loading rate (HLR). They proposed the following power relationship with coefficients a and b :

$$k = aq^b \quad (2.9)$$

This relationship is used in this study to estimate the value of k . However, k values in the model are very sensitive and must be estimated with more accuracy in order to obtain accurate effluent EMCs. Therefore, the need of high accuracy in the model

results in the need for uncertainty analysis in k . A plot of k versus q based on individual storm events is shown in Figure 2.3 with a 95% prediction interval from Equation (2.3) for TSS in detention basins. k values in Figure 2.3 can be estimated by the inverse of the k - C^* model from observed C_{out} and q values estimated from observed inflow and BMP surface area. Values of the coefficients, a and b , in Equation (2.9) are 1.4841 and 0.9721, respectively. The distance between the median line and the lines of the prediction interval show the uncertainty in k . Thus, the log-transformed k is 0.4370 from Figure 2.3.

The range of C^* suggested in the literature is shown in Table 2.2. This study chooses one constant value, 10 mg/L, for C^* based on Table 2.2 and minimum C_{out} in the dataset. Table 2.3 shows the required given information for input variables for uncertainty analysis of three cases: uncertainty in C_{in} , or k , or both. For example, to analyze uncertainty in C_{in} , the required given information is the log-transformed standard deviation of C_{in} and the log-transformed means of C_{in} and k . The standard deviation of k can be estimated from the distance of the prediction interval between the median k and the 95% prediction interval of k in Figure 2.3.

Table 2.2 Typical background concentration values proposed in literature

Literatures	TSS (mg/L)
Kadlec and Knight (1996)	C_{in} when $0.0 < C_{in} < 290$ mg/L
	$5.1+0.16 C_{in}$ when $0.1 < C_{in} < 807$ mg/L
Barrett (2004)	5~20
Crites et al. (2006)	6
This study	10

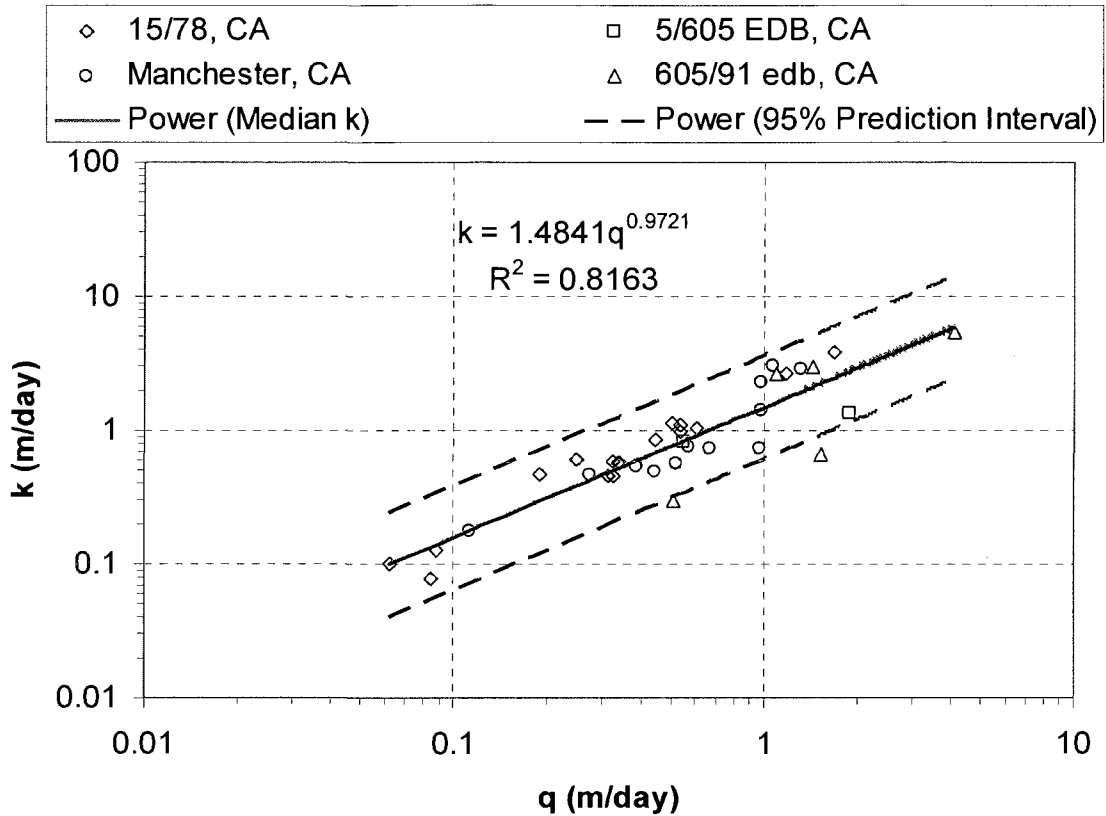


Figure 2.3 Estimated k vs. q using individual storm events for detention basins

Table 2.3 Required parameters information of C_{in} and k for uncertainty analyses

Input Parameters	Log C_{in}		Log k	
Statistical Properties	Mean	Standard Deviation	Mean	Standard Deviation
Value	5.038	0.6083	$\text{Log}(1.4841q^{0.9721})$	0.4370
Cases of Uncertainty Analysis	Uncertainty in C_{in}	*	*	*
	Uncertainty in k	*	*	*
	Uncertainty in C_{in} and k	*	*	*

* : required information

2.5 Results and Discussion

The distribution of C_{out} for the $k-C^*$ model was estimated with two distributed input parameters, C_{in} and k , as shown in Figure 2.4. Results of uncertainty in C_{in} , uncertainty in k , and uncertainty in both C_{in} and k are shown in Section 2.5.1, 2.5.2, and 2.5.3, respectively. These results assume that geometric (A) and hydrological parameters (Q) don't have uncertainty. In addition, the background concentration (C^*) was fixed at 10 mg/L because the minimum value of selected observed data was close to 10 mg/L. C_{in} and k were represented as lognormal distributions because their observed distributions are very close to lognormal as was shown in Figure 2.2 and Figure 2.3.

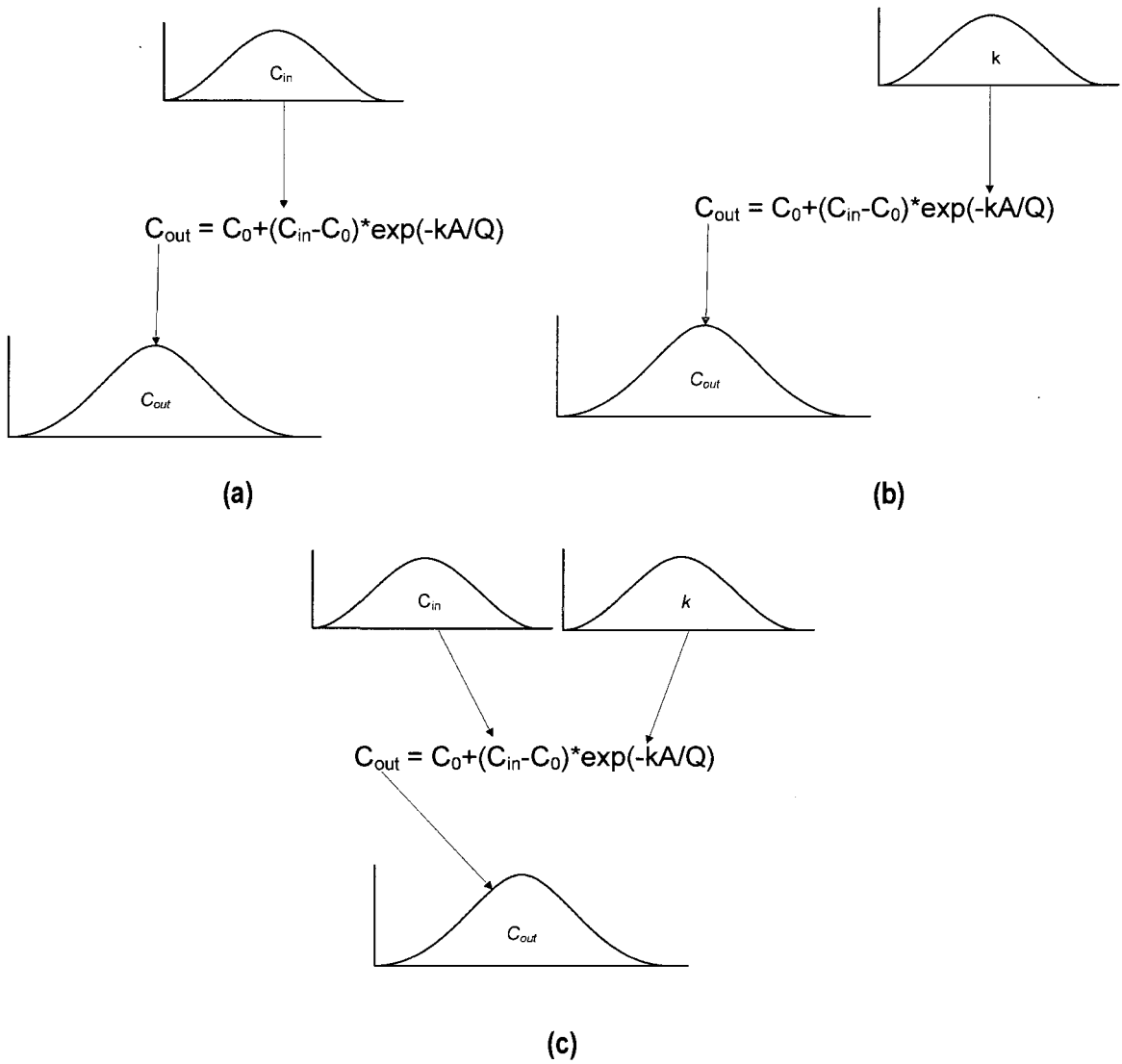


**Figure 2.4 Schematic for generation of probabilistic C_{out} ;
 (a) Uncertainty in C_{in} ; (b) Uncertainty in k ; (c) uncertainty in both C_{in} and k**

2.5.1 Uncertainty in C_{in}

A lognormal distribution $f_{C_{in}}(C_{in})$ for C_{in} is assumed with a mean value $\mu_{\ln C_{in}}$ and standard deviation $\sigma_{\ln C_{in}}$ from the selected TSS of detention basins in the BMP database as shown in Figure 2.1:

$$f_{C_{in}}(C_{in}) = \frac{1}{\sqrt{2\pi}C_{in}\sigma_{\ln C_{in}}} \exp\left[-\frac{1}{2}\left(\frac{\ln(C_{in}) - \mu_{\ln C_{in}}}{\sigma_{\ln C_{in}}}\right)^2\right] \quad (2.10)$$

According to Equation (2.4), The PDF for C_{out} , $f(C_{out})$ is given by

$$f_{C_{out}}(C_{out}) = \left| \frac{dg^{-1}(C_{out})}{dC_{out}} \right| f_{C_{in}}[g^{-1}(C_{out})] \quad (2.11)$$

where,

$$g^{-1}(C_{out}) = C^* + (C_{out} - C^*) \exp(k/q) = C_{in} \quad \text{and} \quad (2.12)$$

$$\left| \frac{dg^{-1}(C_{out})}{dC_{out}} \right| = |\exp(k/q)| = \exp(k/q) \quad (2.13)$$

Substituting Equation (2.12) and (2.13) into Equation (2.11), the resulting PDF for the effluent EMC, $f_{C_{out}}(C_{out})$ is

$$f(C_{out}) = \frac{1}{\sqrt{2\pi}[C_{out} - C^*\{1 - 1/\exp(k/q)\}]\sigma_{\ln C_{in}}} \exp\left[-0.5\left(\frac{\ln[C_{out} - C^*\{1 - 1/\exp(k/q)\}] - (\mu_{\ln C_{in}} - (k/q))}{\sigma_{\ln C_{in}}}\right)^2\right] \quad (2.14)$$

k can be estimated using $1.4841q^{0.9721}$ for detention basins from Figure 2.3. Then,

$$f(C_{out}) = \frac{1}{\sqrt{2\pi} [C_{out} - C^* \{-1/\exp(1.4841q^{-0.0279})\}] \sigma_{\ln C_{in}}} \exp \left[-0.5 \left(\frac{\ln \left[\frac{C_{out} - C^* \{-1/\exp(1.4841q^{-0.0279})\}}{\sigma_{\ln C_{in}}} \right] - (\mu_{\ln C_{in}} - 1.4841q^{-0.0279})}{\sigma_{\ln C_{in}}} \right)^2 \right]$$

(2.15)

Equation (2.15) shows that $f(C_{out})$ is a three-parameter lognormal distribution. Depending on q , the scale parameter $(1.4841q^{-0.0279})$ and location parameter $(C^* \{-1/\exp(1.4841q^{-0.0279})\})$ are changed. $f(C_{out})$ is very sensitive to the value of $\exp(1.4841q^{-0.0279})$, when k is a function of q . k becomes closer to the two-parameter-lognormal distribution when the value of $\exp(1.4841q^{-0.0279})$ is close to 1. However, $f(C_{out})$ changes to the three-parameter-lognormal distribution for values of $\exp(1.4841q^{-0.0279})$ much greater than 1. Plots of $f_{C_{out}}(C_{out})$ as a function of q are shown in Figure 2.5. Figure 2.5 (a),(b), and (c) show the PDFs of C_{out} found with DDM, LHS, and FOSM, respectively. FOSM is applied to the two-parameter-lognormal distribution instead of the three-parameter-lognormal distribution because the latter distribution needs an extra statistical value, the skewness coefficient, to estimate parameters. Mean value of C_{out} ranges were between 30~60 mg/L for all three cases.

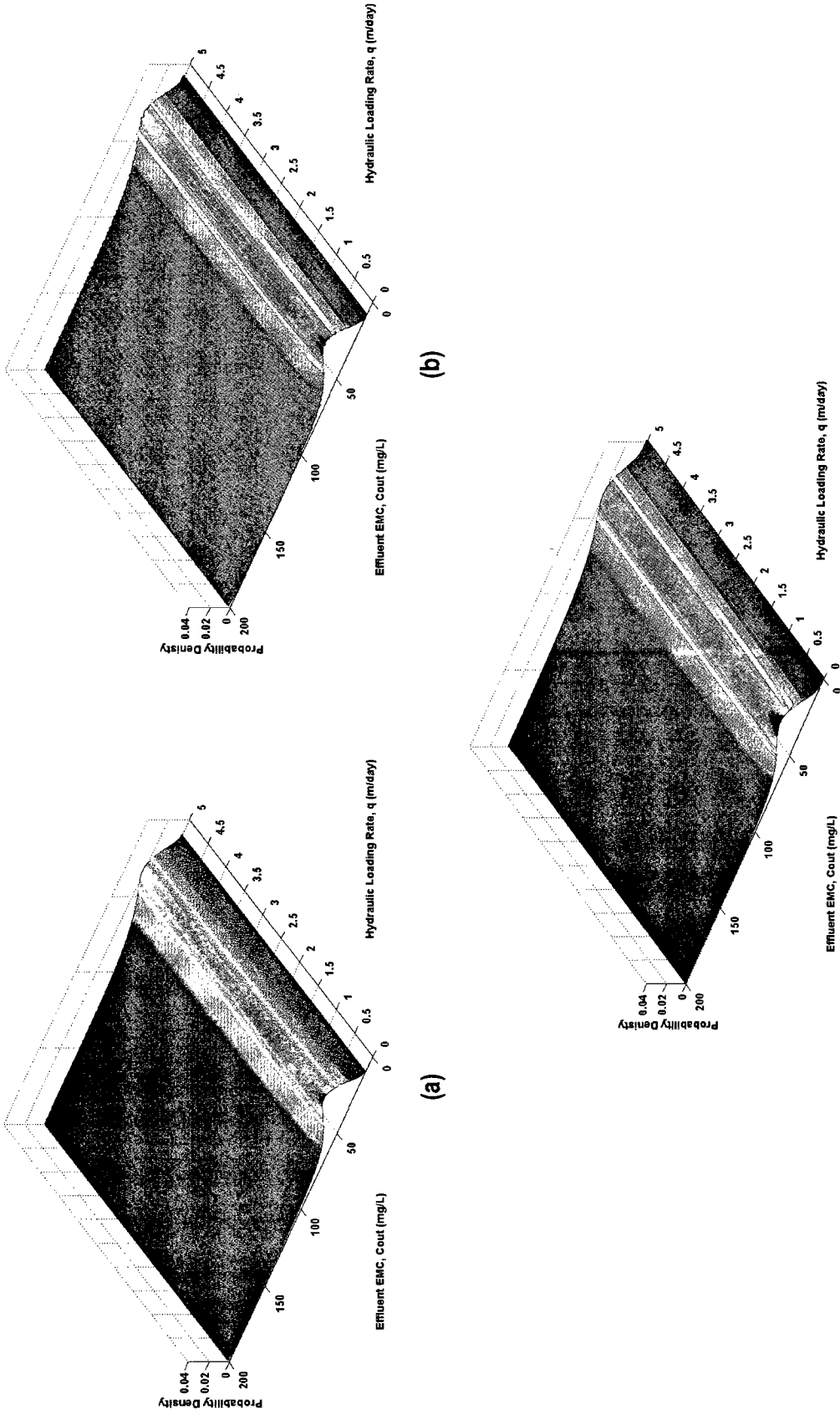


Figure 2.5 Probability density functions for C_{out} as function of q for detention basins; (a) DDM; (b) LHS; (c) FOSM

Comparisons of the PDFs for the three methods, DDM, LHS and FOSM, are shown in Figure 2.6. The PDF obtained using FOSM differs from the DDM and the LHS when q is both 0.01 and 5 m/day. This discrepancy is explained by conceptual differences among the three methods. No assumptions regarding the distribution of C_{out} are required by DDM and LHS methods. On the contrary, it is necessary to assume a known PDF for C_{out} when the FOSM method is used. This assumption makes the method simpler but introduces error. DDM is the most accurate method, but it is difficult to define the exact value corresponding to a specific percentile because it needs an extra computation to estimate percentile from PDF matched with C_{out} . With LHS, it is relatively easy to estimate the precise value of a specific percentile, but a lot of sampling is required.

For $q = 0.01$ and 5 m/day, $\exp(1.4841q^{-0.0279})$ is 5.41 and 4.13, respectively, which are much greater than 1, and the PDF in equation (2.14) differs from the lognormal distribution to a large extent. This creates the differences observed between the DDM and LHS PDFs and the lognormal PDF obtained using FOSM. As a result, it can be indicated that LHS is correct representation rather than FOSM since LHS PDFs coincide with DDM PDFs.

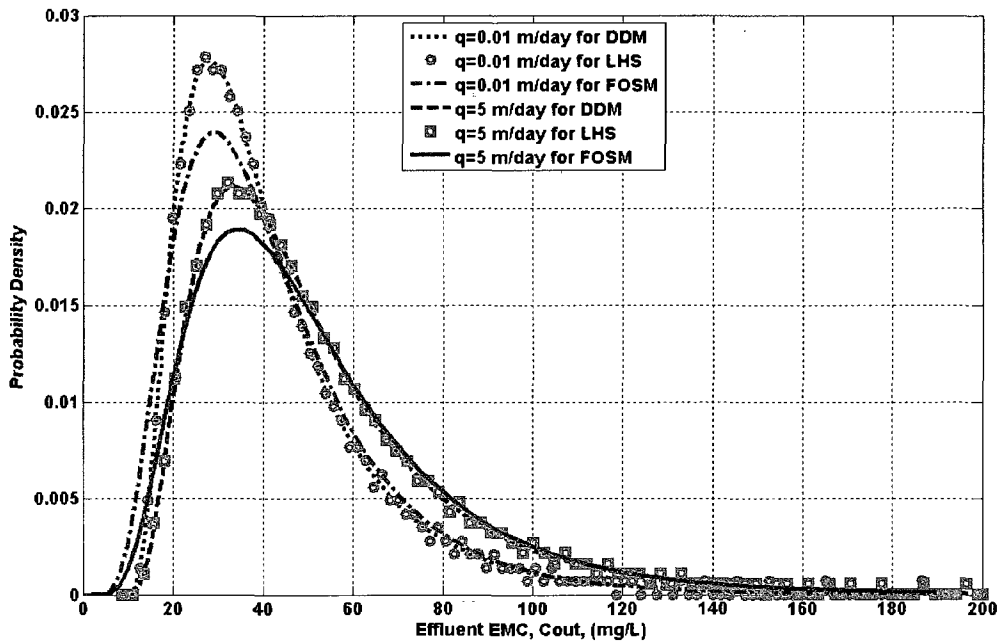


Figure 2.6 Comparison of $f(C_{out})$ considering uncertainty in C_{in} among DDM, LHS and FOSM for detention basins

Figure 2.7 shows the PDFs of C_{out} which represent the observed data well. This figure shows the PDF computed using LHS, but similar results are obtained with the other PDFs shown in Figure 2.5. The 95% and 50% confidence intervals are plotted as well. These intervals represent the variability of the data very well, with C_{out} values being higher and more scattered for large values of q . Most of the observed data are low q values. As expected, about half of the observed data are placed out of the 50% confidence interval and two points (5% of the total data) are located outside of the 95% confidence interval.

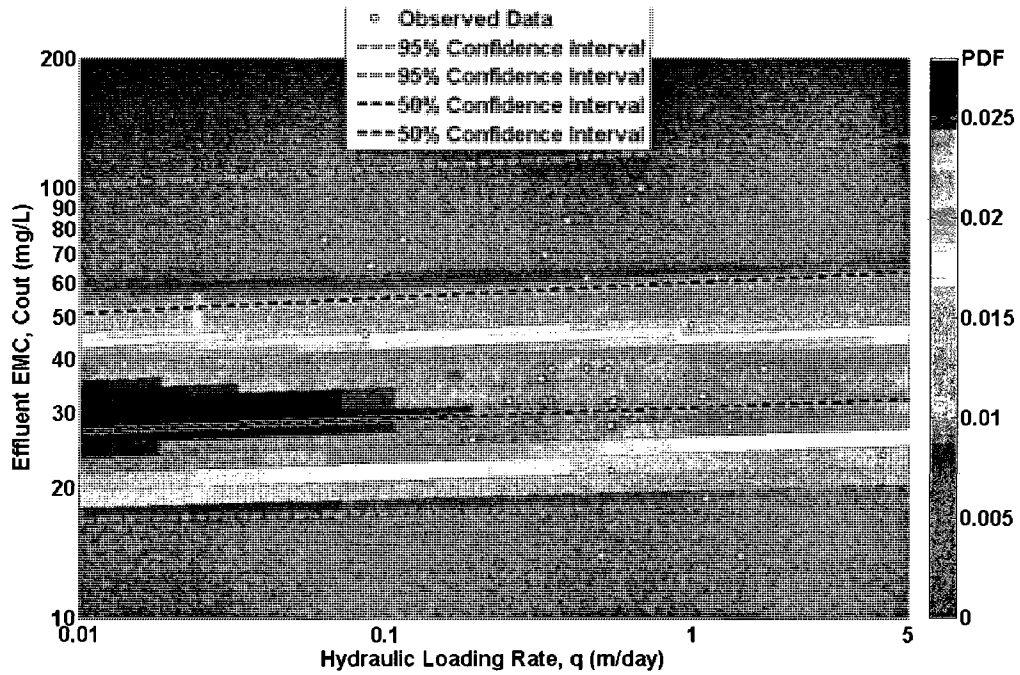


Figure 2.7 Uncertainty in C_{in} : probability density functions of LHS including confidence intervals and observed data for detention basins

Figure 2.8 compares the 50% and 95% upper and lower confidence intervals obtained using LHS and FOSM. With the exemption of the lower 95% confidence limits, the rest of the limits are very similar. It can be concluded that the distributed C_{out} is essentially identical for LHS and FOSM.

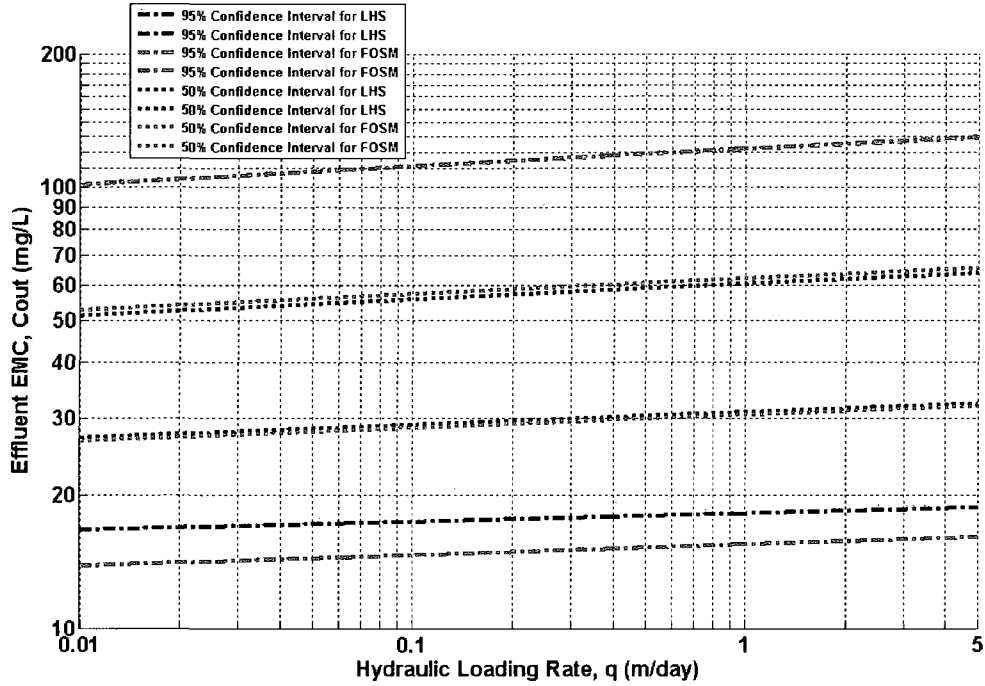


Figure 2.8 The comparison of confidence intervals between LHS and FOSM on considering uncertainties in C_{in} for detention basins

2.5.2 Uncertainty in k

What follows is the uncertainty analysis for C_{out} assuming k is lognormally distributed with a certain mean and standard deviation. $f(C_{out})$ can then be derived using the DDM method defined in equation (2.4)

$$f(C_{out}) = \frac{1}{\sqrt{2\pi} \ln\left(\frac{C_{in} - C^*}{C_{out} - C^*}\right) \sigma_{\ln k} |(C_{out} - C^*)|} \exp\left[-\frac{1}{2} \left(\frac{\ln\left[q \ln\left(\frac{C_{in} - C^*}{C_{out} - C^*}\right)\right] - \mu_{\ln k}}{\sigma_{\ln k}} \right)^2\right] \quad (2.16)$$

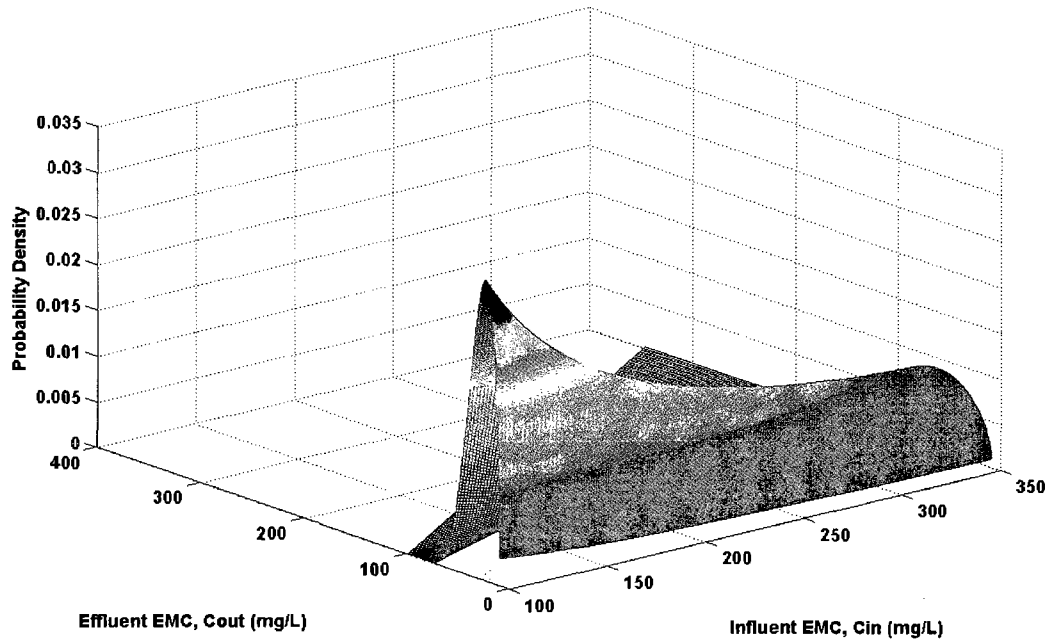
In equation (2.16), the independent variables are q and C_{in} . Log-transformed mean and standard deviation of k , which are required for estimating the uncertainty in k ,

are listed in Table 3. What follows is a sensitivity of uncertainty analysis of equation (2.16) to C_{in} (Section 2.5.2.1) and q (Section 2.5.2.2).

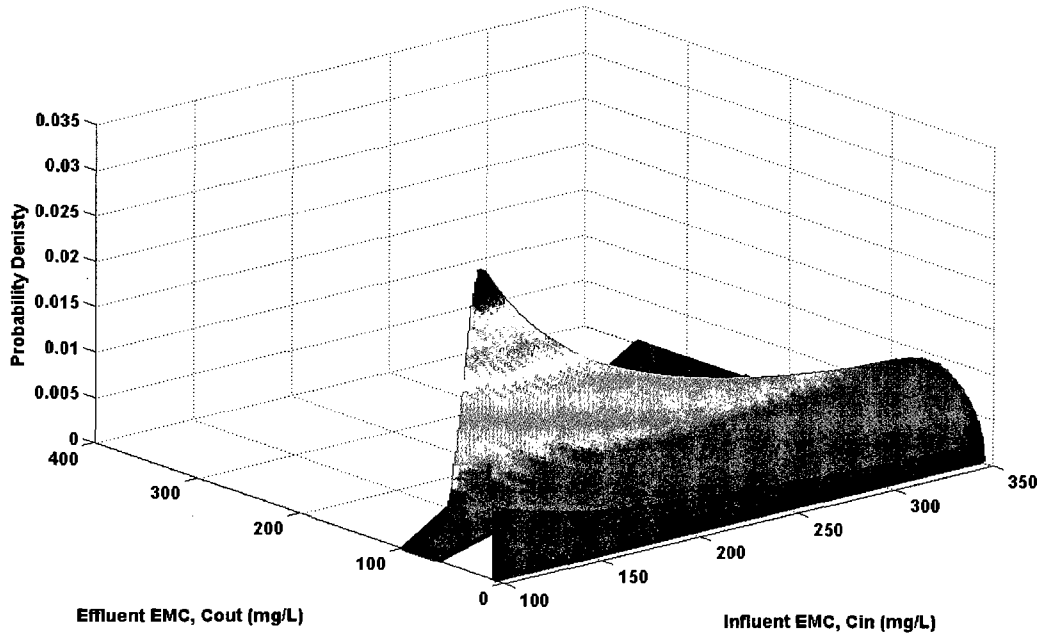
2.5.2.1 Sensitivity of Uncertainty in k to C_{in}

A constant value of $q=0.1\text{m/day}$ is assumed to determine the effect of C_{in} on the uncertainty of C_{out} with respect to k . Figure 2.9 shows $f(C_{out})$ for different values of C_{in} . Figure 2.9(a) shows $f(C_{out})$ obtained using DDM and Figure 2.9(b) shows $f(C_{out})$ obtained using LHS. In both cases, the variance of C_{out} decreases as C_{in} decreases. For low C_{in} , C^* limits the variance of C_{out} .

Figure 2.10 shows both PDFs for values of $C_{in}=100\text{mg/L}$ and 350mg/L . Both methods produce very similar distributions and represent a higher variability in C_{out} as C_{in} increases. In other words, it is more difficult to predict C_{out} for a high C_{in} at a constant q . Figure 2.11 shows the PDFs of C_{out} for the observed data when q is restricted to 0.1m/day . This figure shows the PDF computed using LHS, but almost identical results are obtained with the PDFs using DDM, as illustrated in Figure 2.9(a). The 95% and 50% confidence intervals become wider as q increases. For this analysis, only three data points were available; two of the three points lie within the 50% confidence interval and the third is within the 95% confidence interval.



(a)



(b)

Figure 2.9 $f(C_{out})$ as a function of C_{in} using $q=0.1\text{m/day}$ when considering uncertainty in k for detention basins (a) DDM; (b) LHS

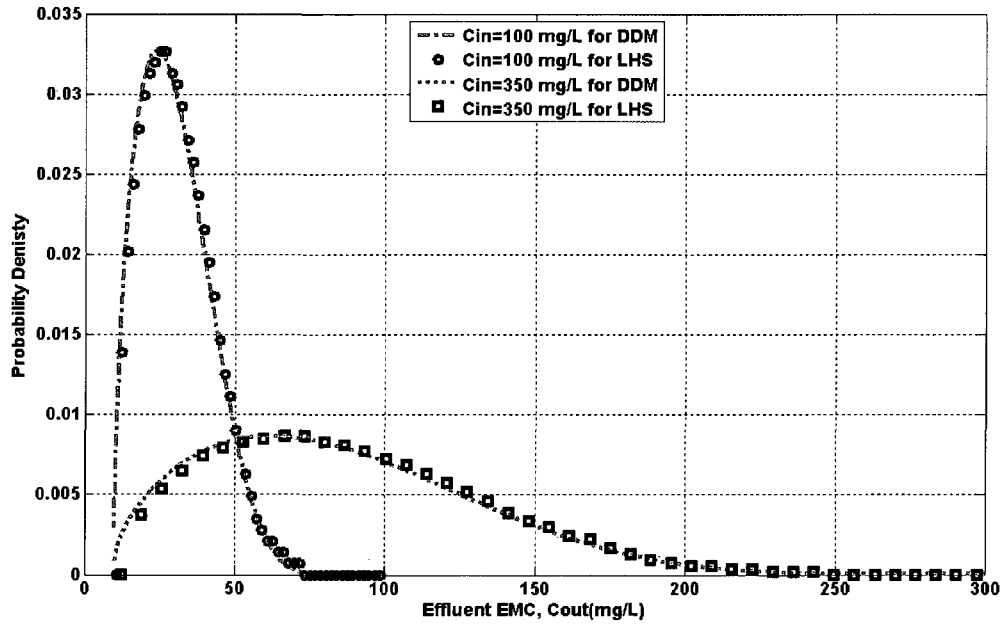


Figure 2.10 Comparison of $f(C_{out})$ as a function of C_{in} using $q=0.1\text{m/day}$ on considering uncertainty in k for detention basins between DDM and LHS

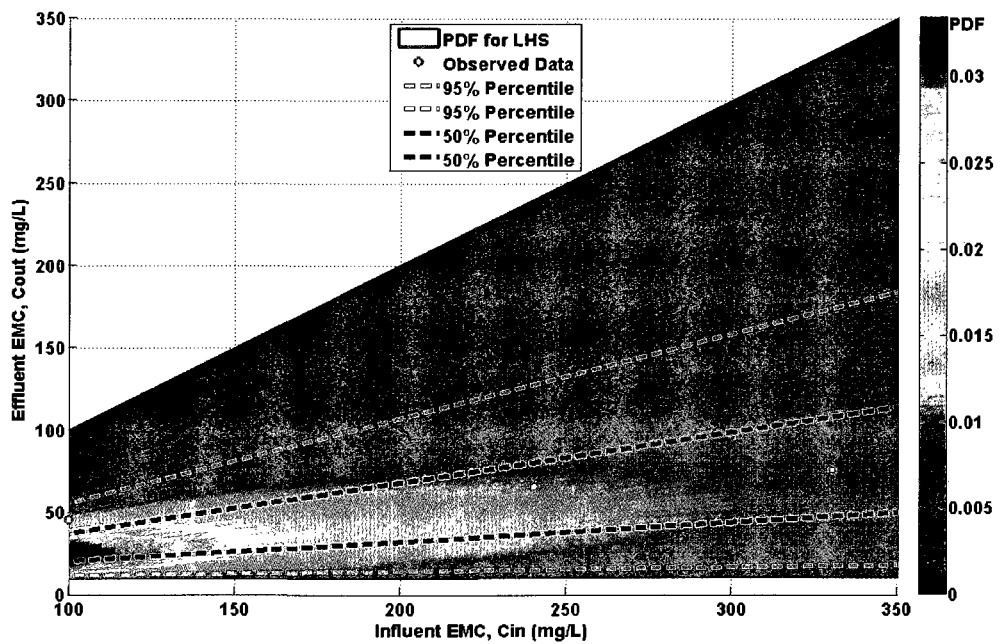
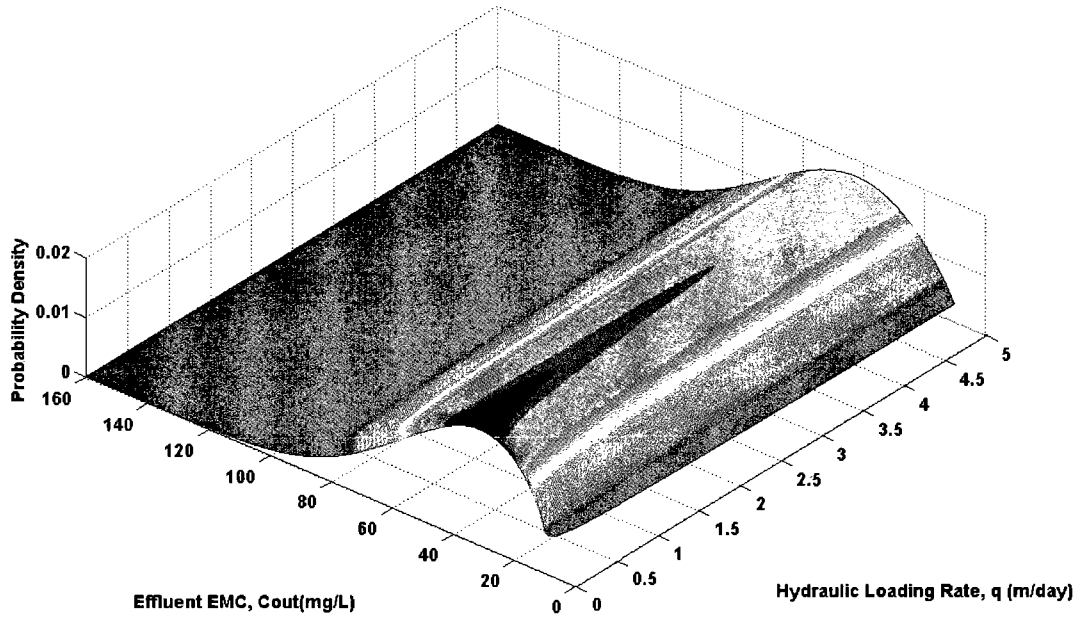


Figure 2.11 Uncertainty in k to C_{in} : probability density functions from LHS including confidence intervals and observed data for detention basins

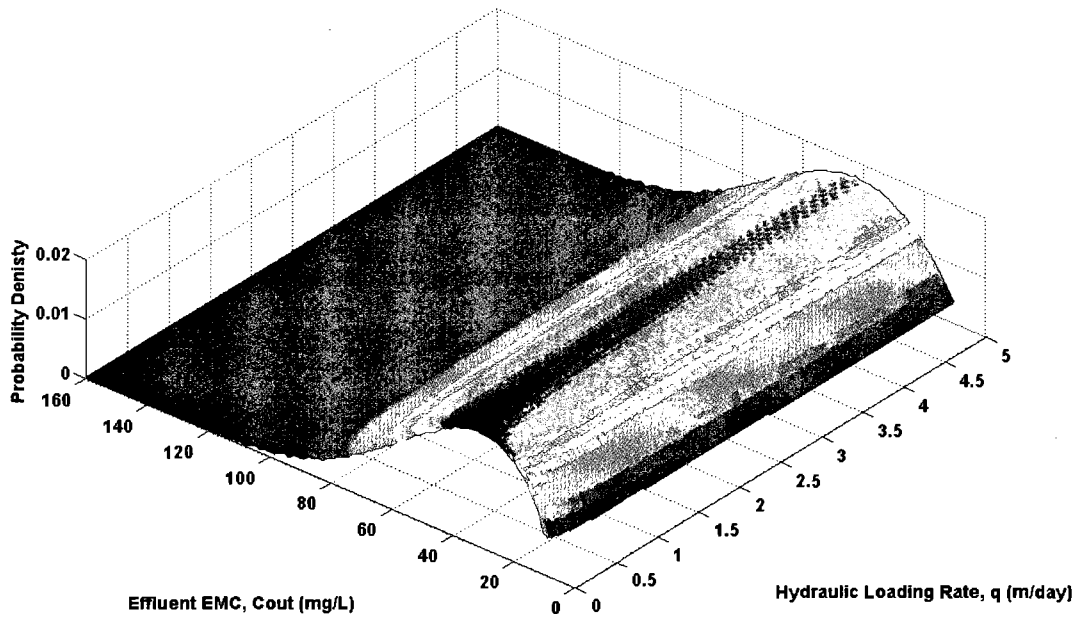
2.5.2.2 Sensitivity of Uncertainty in k to q

A constant value of $C_{in} = 170$ mg/L is assumed in order to determine the effect of q on the uncertainty of k . Figure 2.12 shows $f(C_{out})$ for different values of C_{in} using DDM and LHS, respectively. In both cases, the shapes of the PDFs of C_{out} demonstrate a more positive skew with decreasing q . FOSM is difficult to apply because the shape of the PDF is difficult to define with well-known types of distributions as shown in equation (2.16). Thus, it can be concluded that LHS is the better method to represent the uncertainty in k to C_{in} and q .

Figure 2.13 shows PDFs for values of $q=0.01$ m/day and 5m/day. Both the DDM and LHS methods produce very similar distributions and represent higher variability in C_{out} as q increases. In other words, it can be represented that C_{out} is higher probability to lower C_{out} with decreasing q . As a result, it is more difficult to predict C_{out} for high q at a constant C_{in} .



(a)



(b)

Figure 2.12 $f(C_{out})$ as a function of q using $C_{in} = 170 \text{ mg/L}$ on considering uncertainty in k for detention basins (a) DDM; (b) LHS

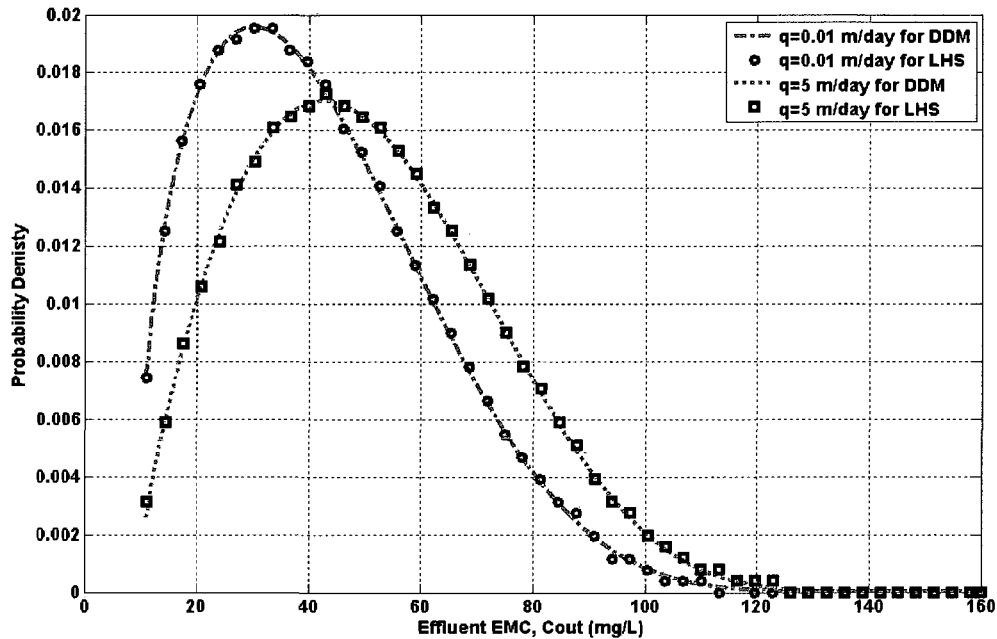


Figure 2.13 Comparison of $f(C_{out})$ as a function of q using $C_{in} = 170$ mg/L and considering uncertainty in k for detention basins between DDM and LHS

Figure 2.14 shows PDFs of C_{out} for the observed data when C_{in} is restricted to 170 mg/L. This figure shows the PDF computed using LHS, but similar results are obtained with the PDF for DDM, as illustrated in Figure 2.13. The 95% and 50% confidence intervals are plotted as well. These intervals represent that C_{out} values are higher and a little more scattered for larger values of q . Two of the three observed data are scatter within the 50% confidence interval, and third point is located within the 95% confidence interval. While only having three the data using for comparison, they do validate that this PDF shows that the results of the k - C^* model describe the behavior of observed data. Based on the results shown above, it is found that the shape of the PDF as a function of C_{in} shows more change of variance than as a function of q . It can be

concluded that C_{in} is a more sensitive variable than q for the uncertainty in k when the k - C^* model is considered with TSS the pollutant in detention basins.

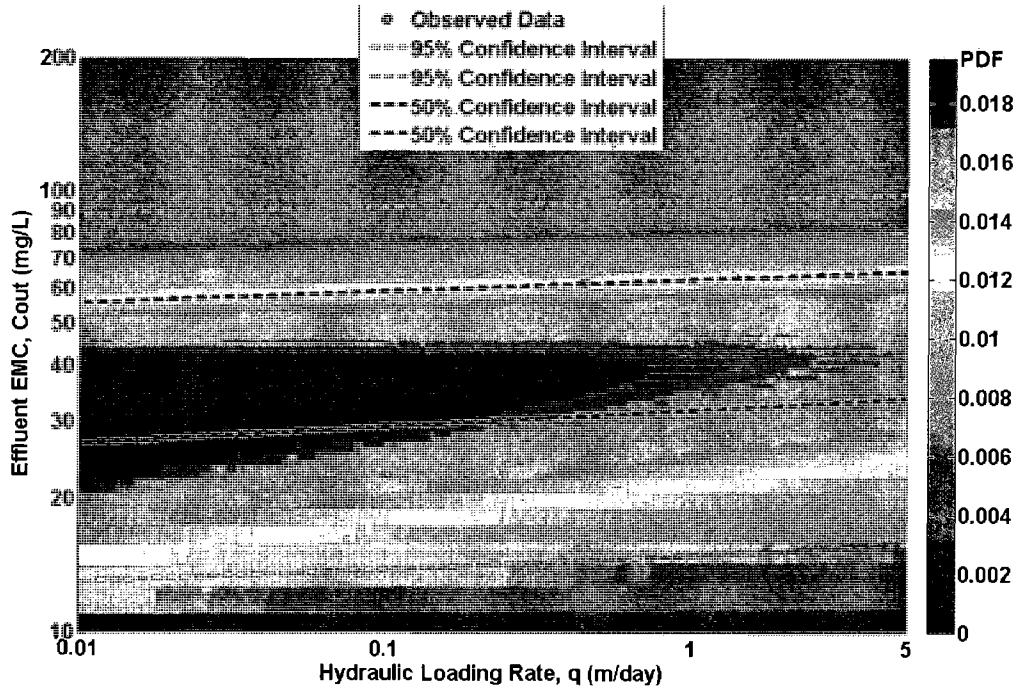
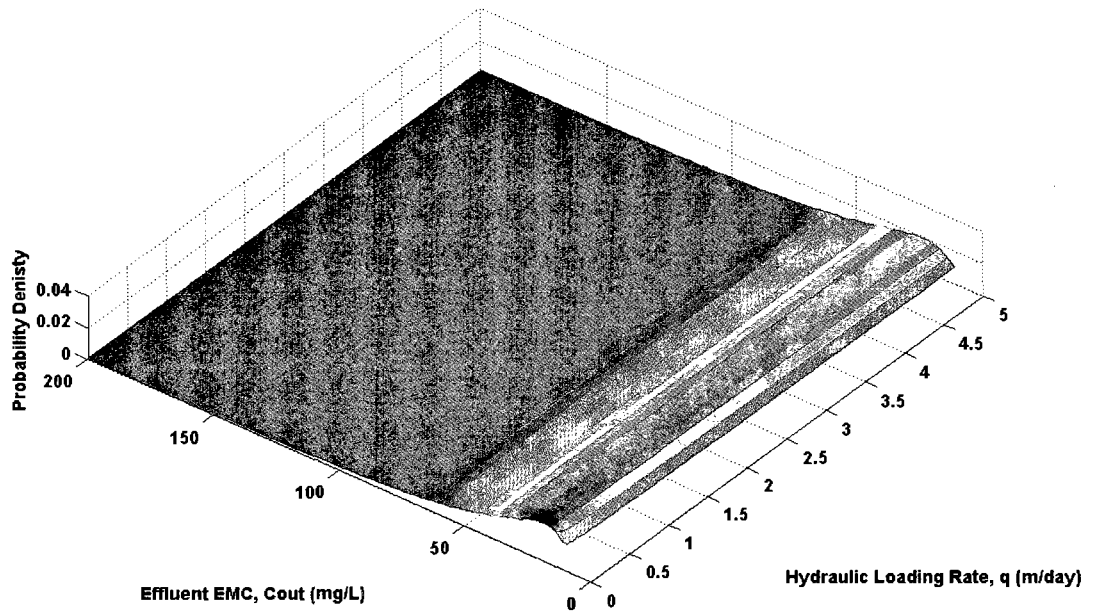


Figure 2.14 Uncertainty in k to q : probability density functions from LHS including confidence intervals and observed data for detention basins

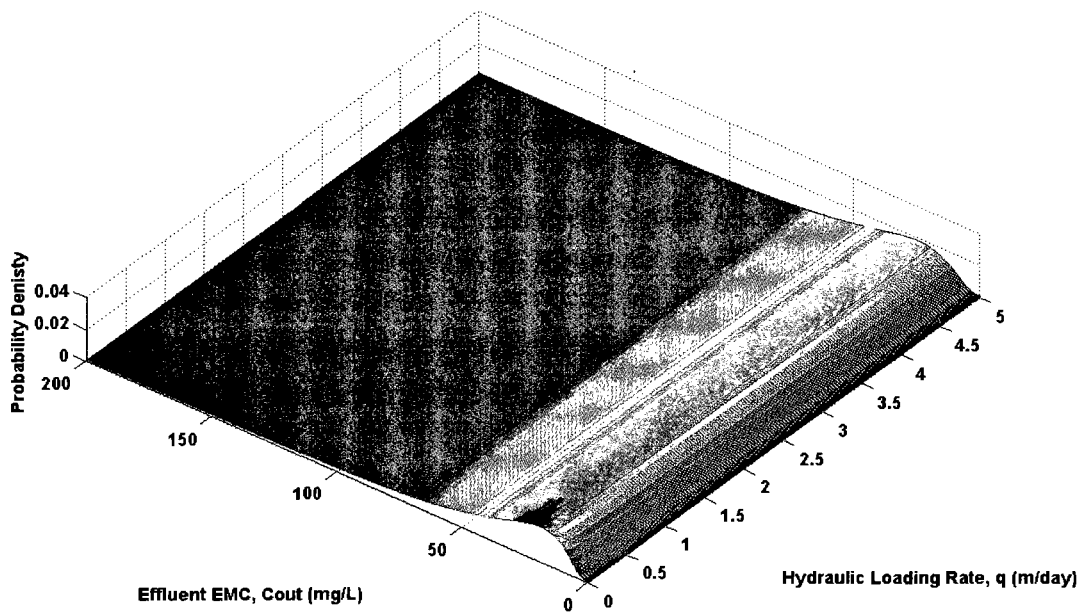
2.5.3 Uncertainty in Both C_{in} and k

This chapter assumes that there is no correlation between C_{in} and k in order to simplify calculations. Because of mathematical complexities, the DDM cannot be applied to derive $f(C_{out})$ when uncertainties in both C_{in} and k are simultaneously applied to the k - C^* model. The analysis in the previous chapter showed that the LHS and DDM methods generate very similar distributions. Thus, the LHS method is used in this

chapter to evaluate the FOSM method as shown in Figure 2.15(a). To apply the FOSM method, it is assumed that C_{out} is lognormally distributed as shown in Figure 2.15(b).



(a)



(b)

Figure 2.15 $f(C_{out})$ as a function of q on considering uncertainty in both C_{in} and k for detention basins ;(a) LHS, (b) FOSM

Figure 2.16 shows a comparison of both PDFs for $q=0.01$ and $q=5$ m/day. Both distributions are relatively similar for $q=5$ m/day, but differences are observed in the peak value of the different methods for $q=0.01$ m/day. The distribution of C_{out} is skewed to the right (positive side) when q is both 0.01 and 5 m/day. LHS does not require identification of the output distribution. In other words, it can be represented by any type of distribution. However, FOSM assumes the distribution of output as a lognormal distribution. Thus, the shapes of the PDFs generated by the LHS and FOSM methods differ.

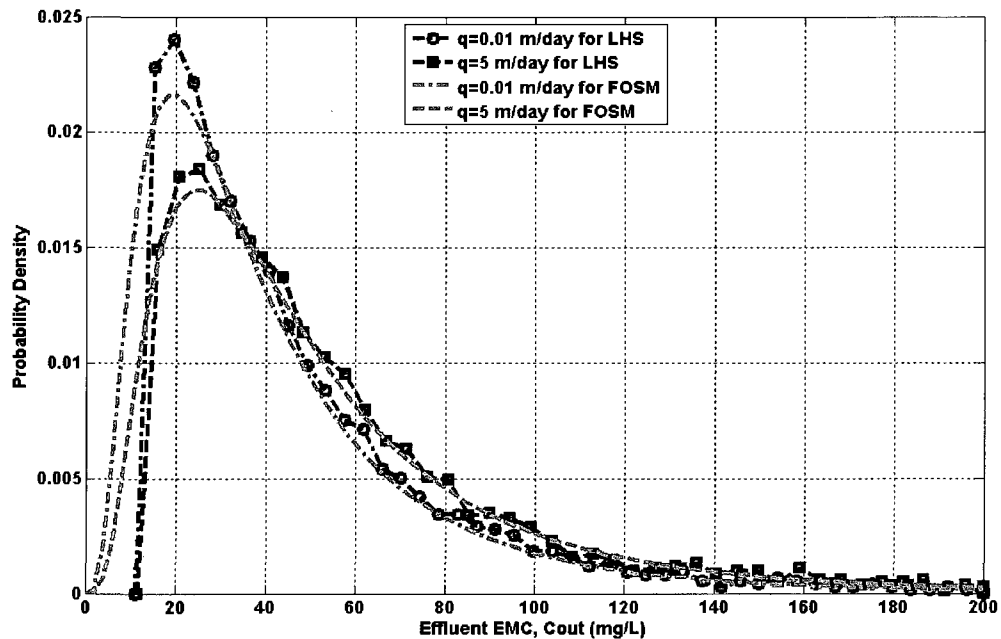


Figure 2.16 Comparison of $f(C_{out})$ as a function of q on considering uncertainty in k for detention basins between LHS and FOSM

Figure 2.17 shows the PDFs obtained with LHS, their confidence intervals of 50% and 95%, and the observed data. About two-thirds of the total data are located within the 50% confidence interval, and all observed data are located within the placed 95% confidence interval. A comparison of Figure 2.6 with Figure 2.17 shows none of the data fell outside the 95% confidence interval. Therefore, TSS treatment in detention basins is better explained by an uncertainty analysis when variability is considered in both C_m and k .

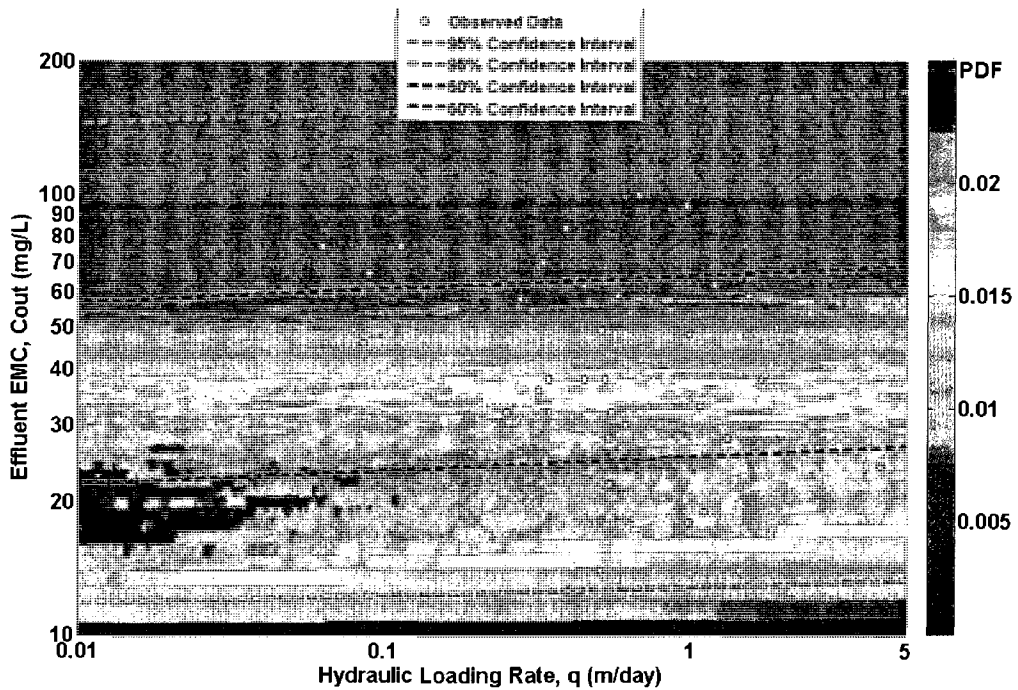


Figure 2.17 Uncertainty in both C_m and q : probability density functions of LHS including confidence intervals and observed data for detention basins

Figure 2.18 compares the 50% and 95% confidence intervals obtained using LHS and FOSM when uncertainties in C_{in} and k are considered. These methods produce different distributions because the FOSM analysis assures a lognormal distribution for C_{out} while the LHS method does not. Nevertheless, confidence intervals between LHS and FOSM are not different substantially different. Thus, the assumption of a lognormal distribution for C_{out} seems to be practical for estimating the variance of C_{out} .

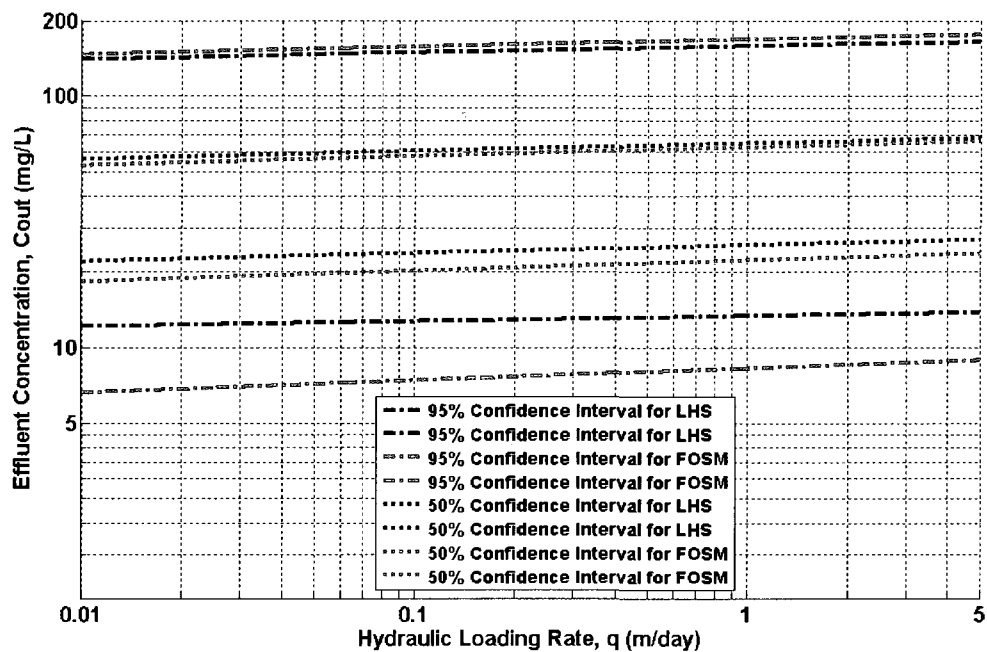


Figure 2.18 The comparison of confidence intervals between LHS and FOSM on considering uncertainties in C_{in} and k for detention basins

2.6 Conclusions

This chapter has investigated the application of several uncertainty-analysis methods when using the k - C^* model to characterize the variability of C_{out} at the outlet of stormwater detention basins. Three methods were studied:

- DDM, an analytic method to estimate the PDF of a dependent variable based on the PDF of an independent variable. It generates the most accurate PDF for a univariate case, but it is not as effective in obtaining results in the multivariable case due to the mathematical complexity of numerical solutions. An unknown distribution of the independent variable makes the applicability of this method difficult.
- FOSM, a simple analytic method for uncertainty analysis. However, this method requires the distribution of the results to be a known continuous distribution. Thus, the applicability of this method is reduced in the case where the output distribution is not known.
- LHS, a special case of the stratified sampling method on MCS. It generates results through an appropriate sampling of the input variables and provides very accurate results, even when the distribution of the input variables is unknown and not unique.

It is concluded that LHS is the most efficient method to characterize the uncertainty of C_{out} when there is variability in more than one parameter of independent variables in the k - C^* model.

With respect to the k - C^* model and its performance under uncertainty in input variables, the following is concluded:

- The observed variance of C_{in} is very large. This variance significantly affects the computation of effluent EMC when using the model. For small values of q , the peak-probability density of C_{out} for the DDM and LHS methods are greater than the peak-probability density of C_{out} for FOSM because the PDF for DDM and LHS are lognormal 3-parameter distributions and the PDF for FOSM applies to the lognormal 2-parameter distribution.
- Two input variables are defined when the uncertainty in k is incorporated in the analysis. Therefore, one of the variables has to be fixed in order to determine the PDF of C_{out} . This study shows significant differences in the PDF of C_{out} when each of k and C_{in} variables is fixed independently.
- If C_{in} is known, the uncertainty of C_{out} is explained entirely by the uncertainty in the parameter k . In this case, uncertainty conditions are obtained by an independent analysis of the functions relating the uncertainty in C_{in} to C_{out} and the uncertainty in q to C_{out} .
- The uncertainty in k as a function of C_{in} generates greater variance of C_{out} for larger C_{in} . As C_{in} decreases, C_{out} decreases and converges to C^* .
- The uncertainty in k as a function of q generates increasing variance in C_{out} as q increases. However, sensitivity of the variance to a change in q is not sensitive to a change in C_{in} .

- The incorporation of uncertainty in both C_{in} and k generates a variance in C_{out} slightly larger than that obtained if only uncertainty in C_{in} is considered. Thus, it is concluded that the effect of uncertainty in C_{in} is much more significant than that of uncertainty in k . However, 95% of the observed C_{out} data is contained in the 95% confidence interval when only the variability of C_{in} is considered. On the other hand, 100% of the observed C_{out} is contained in that confidence interval when uncertainty in k is also incorporated in the analysis.

To summarize, the LHS is the most efficient method among all of the three methods tested to characterize the uncertainty of C_{out} in both univariate or bivariate cases in the k - C^* model. With respect to the k - C^* model itself, the computed value of C_{out} is much more sensitive to C_{in} than to k ; thus, for practical purposes, uncertainty in C_{out} can be adequately estimated using only the uncertainty associated with C_{in} .

2.7 References

- American Society of Civil Engineers (ASCE). (1992). "Design and construction of urban stormwater management systems", American Society of Civil Engineers, New York, N. Y.
- American Society of Civil Engineers and US Environment Protection Agency (ASCE & US EPA) (2002). "Urban stormwater best management practice (BMP) performance monitoring: A guidance manual for meeting the national stormwater BMP database requirements.", Report prepared by GeoSyntec Consultants and the Urban Water Resources Research Council of ASCE in cooperation with the Office of Water, US EPA.
- Barrett, M. E. (2004). "Retention pond performance: examples from the International Stormwater BMP Database" Proceedings of the 2004 World Water and Environmental Resources Congress: Critical Transitions in Water and Environmental Resources Management, Salt Lake City, Utah, 439-448.
- Barrett, M. E. (2005). "Performance comparison of structural stormwater best management practices." *Water Environment Research*, 77(1), 78-86.
- Braskerud, B. C. (2002). "Factors affecting phosphorus retention in small constructed wetlands treating agricultural non-point source pollution." *Ecological Engineering*, 19(1), 41-61.
- Brown, A. (2003). "Development of a BMP evaluation methodology for highway applications." M.S. Thesis, Department of Civil, Construction, and Environmental Engineering, Oregon State University, Corvallis, OR.
- Burgers, S. J., and Lettenmaier, D. P. (1975). "Probabilistic methods in stream quality management." *Water Resources Bulletin*, 11(1), 115-130.
- California Department of Transportation (CalTrans) (2003). "Storm water BMP handbook - new development and redevelopment, appendix B: general applicability of effluent probability method", January. Available at <http://www.cabmphandbooks.com>.
- Canter, L. W., and Knox, R. C. (1986). *Ground Water Pollution Control*, Lewis Publishers, Chelsea, Michigan.
- Carleton, J. N., Grizzard, T. J., Godrej, A. N., and Post, H. E. (2001). "Factors affecting the performance of stormwater treatment wetlands", *Water Research*, 35(6), 1552-1562.
- Clary, J., Urbonas, B., Jones, J., Strecker, E., Quigley, M., and O'Brien, J. (2002). "Developing, evaluating and maintaining a standardized stormwater BMP effectiveness database." *Water Science and Technology*, 45(7), 65-73.

- Crites, R. W., Reed, S. C., and Middlebrooks, E. J. (2006). Natural wastewater treatment systems, CRC/Taylor & Francis, Boca Raton, FL.
- Driscoll, E. D. (1986). "Methodology for analysis of detention basins for control of urban runoff quality." United States Environmental Protection Agency, Office of Water, Nonpoint Source Branch, [Washington, D.C.].
- Guo, J. C. Y., and Urbonas, B. (1996). "Maximized detention volume determined by runoff capture ratio." *Journal of Water Resources Planning and Management-ASCE*, 122(1), 33-39.
- Guo, J. C. Y., and Urbonas, B. (2002). "Runoff capture and delivery curves for storm-water quality control designs." *Journal of Water Resources Planning and Management-ASCE*, 128(3), 208-215.
- Guo, Y. P., and Adams, B. J. (1999). "Analysis of detention ponds for storm water quality control." *Water Resources Research*, 35(8), 2447-2456.
- International Water Association (IWA) (2006). *Constructed wetlands for pollution control : processes, performance, design and operation*, IWA Pub., London.
- Kadlec, R. H. (2000). "The inadequacy of first-order treatment wetland models." *Ecological Engineering*, 15(1-2), 105-119.
- Kadlec, R. H. (2003). "Effects of pollutant speciation in treatment wetlands design." *Ecological Engineering*, 20(1), 1-16.
- Kadlec, R. H., and Knight, R. L. (1996). *Treatment Wetlands*, Lewis Publishers, Boca Raton.
- Kunstmann, H., and Kastens, M. (2006). "Direct propagation of probability density functions in hydrological equations." *Journal of Hydrology*, 325(1-4), 82-95.
- Kutner, M. H., Nachtsheim, C. J., and Neter, J. (2004). *Applied Linear Regression Models*, Irwin, Homewood, Ill.
- Lettenmaier, D. P., and Burges, S. J. (1975). "Dynamic water-quality management strategies." *Journal Water Pollution Control Federation*, 47(12), 2809-2819.
- Lin, Y. F., Jing, S. R., Lee, D. Y., Chang, Y. F., Chen, Y. M., and Shih, K. C. (2005). "Performance of a constructed wetland treating intensive shrimp aquaculture wastewater under high hydraulic loading rate." *Environmental Pollution*, 134(3), 411-421.
- Mays, L. W. (1996). *Water Resources Handbook*, Chapter 7, McGraw-Hill, New York.
- Mays, L. W., and Tung, Y.-K. (1992). *Hydrosystems Engineering and Management*, Chapter 8, McGraw-Hill, Boston.
- Melching, C. S. (1992). "An improved 1st-order reliability approach for assessing uncertainties in hydrologic modeling." *Journal of Hydrology*, 132(1-4), 157-177.

- Melching, C. S. (1995). "Reliability estimation." *Computer models of watershed hydrology*, V. P. Singh, ed., Water Resources Publications, Littleton, Colo., 69–118.
- Melching, C. S., and Anmangandla, S. (1992). "Improved 1st-order uncertainty method for water-quality modeling." *Journal of Environmental Engineering-ASCE*, 118(5), 791-805.
- Melching, C. S., and Bauwens, W. (2001). "Uncertainty in coupled nonpoint source and stream water-quality models." *Journal of Water Resources Planning and Management-ASCE*, 127(6), 403-413.
- Minton, G. R. (2005). *Stormwater treatment : biological, chemical, and engineering principles*, Resource Planning Associates, Seattle, Washington, U.S.A.
- Pack, C.A., Heaney, J.P., and Lee, J. G. (2005). "Long-term performance modeling of vegetative/infiltration BMPs for highways". Proceedings of the 2005 World Water and Environmental Resources Congress, May 15-19, Anchorage, Alaska.
- Roesner, L. A., Nichandros, H. M., Shubinski, R. P., Feldman, A. D., Abbott, J. W., and Friedland, A. O. (1974). "A model for evaluating runoff-quality in metropolitan master planning." Technical Memorandum No.23 (NTIS PB-234312), ASCE Urban Water Resources Research Program, New York, NY.
- Roesner, L. A., Pruden, A., and Kidner, E. M.; (2007). "Improved protocol for classification and analysis of stormwater-borne solids", WERF Project No. 04-SW-4; Water Environment Research Foundation, Alexandria, Virginia.
- Rousseau, D. P. L., Vanrolleghem, P. A., and De Pauw, N. (2004). "Model-based design of horizontal subsurface flow constructed treatment wetlands: a review." *Water Research*, 38(6), 1484-1493.
- Salas, J. D., and Shin, H. S. (1999). "Uncertainty analysis of reservoir sedimentation." *Journal of Hydraulic Engineering-ASCE*, 125(4), 339-350.
- Salas, J. D., Smith, R. A., Tabious, G. Q. and Heo, J.-H. (2004). *Statistical Techniques in Water Resources and Environmental Engineering*. Colorado State University.
- Schierup, H.H., Brix,H., and Lorenzen,B. 1990. "Wastewater treatment in constructed reed beds in Denmark – state of the art", In: Cooper,P.F. & Findlater,B.C., Editors: *Constructed Wetlands in Water Pollution Control Advances in Water Pollution Control* , page 495-504. Pergamon Press, London.
- Schueler, T. R. (1996). "Irreducible pollutant concentrations discharged from urban BMPs." *Watershed Protection Techniques*, 2(2), 369-372.
- Shirmohammadi, A., Chaubey, I., Harmel, R. D., Bosch, D. D., Munoz-Carpena, R., Dharmasri, C., Sexton, A., Arabi, M., Wolfe, M. L., Frankenberger, J., Graff, C., and Sohrabi, T. M. (2006). "Uncertainty in TMDL models." *Transactions of the Asabe*, 49(4), 1033-1049.

- Sohrabi, T. M., Shirmohammadi, A., Chu, T. W., Montas, H., and Nejadhashemi, A. P. (2003). "Uncertainty analysis of hydrologic and water quality predictions for a small watershed using SWAT2000." *Environmental Forensics*, 4(4), 229-238.
- Song, Q., and Brown, L. C. (1990). "DO model uncertainty with correlated inputs." *Journal of Environmental Engineering-ASCE*, 116(6), 1164-1180.
- Stone, K. C., Poach, M. E., Hunt, P. G., and Reddy, G. B. (2004). "Marsh-pond-marsh constructed wetland design analysis for swine lagoon wastewater treatment." *Ecological Engineering*, 23(2), 127-133.
- Strecker, E. W., Quigley, M. M., Urbonas, B., and Jones, J. "Analyses of the expanded EPA/ASCE international BMP database and potential implications for BMP design." Proceedings of the 2004 World Water and Environmental Resources Congress: Critical Transitions in Water and Environmental Resources Management, 363-372.
- Strecker, E. W., Quigley, M. M., Urbonas, B. R., Jones, J. E., and Clary, J. K. (2001). "Determining urban storm water BMP effectiveness." *Journal of Water Resources Planning and Management-ASCE*, 127(3), 144-149.
- Tung, Y. K., and Mays, L. W. (1981). "Risk models for flood levee design." *Water Resources Research*, 17(4), 833-841.
- Tung, Y.-K., and Yen, B. C. (2005). *Hydrosystems Engineering Uncertainty Analysis*, McGraw-Hill, New York.
- U.S. EPA (1983). "Results of the nationwide urban runoff program. volume 1. final report." Water Planning Division, Washington, DC.
- Urbonas, B. R., and Roesner, L. A. (1993). "Hydrologic design for urban drainage and flood control " *Chap. 28 in Handbook of Hydrology*, D. R. Maidment, ed., McGraw-Hill, New York.
- Van Buren, M. A., Watt, W. E., and Marsalek, J. (1997). "Application of the log-normal and normal distributions to stormwater quality parameters." *Water Research*, 31(1), 95-104.
- Wong, T. H. F., Fletcher, T.D., Duncan, H.P., Coleman, J.R., and Jenkins, G.A. (2002). "A model for urban stormwater improvement conceptualization." the Ninth International Conference on Urban Drainage, Portland, Oregon.
- Wong, T. H. F., Fletcher, T. D., Duncan, H. P., and Jenkins, G. A. (2006). "Modelling urban stormwater treatment - A unified approach." *Ecological Engineering*, 27(1), 58-70.
- Yeh, K. C., and Tung, Y. K. (1993). "Uncertainty and sensitivity analyses of pit-migration model." *Journal of Hydraulic Engineering-ASCE*, 119(2), 262-283.

- Yen, B. C., and Tang, W. H. (1976). "Risk-safety factor relation for storm sewer design." *Journal of the Environmental Engineering Division-ASCE*, 102(2), 509-516.
- Zhang, H. X., and Yu, S. L. (2004). "Applying the first-order error analysis in determining the margin of safety for total maximum daily load computations." *Journal of Environmental Engineering-ASCE*, 130(6), 664-673.

2.8 Appendix I. FOSM Application

The effluent pollutant concentration in the BMP is calculated as the estimated pollutant concentration using the k - C^* model through Equations (2.2).

$$\mu_{\ln out} = \ln(C_{out,median}) = \ln\{C^* + (C_{in,median} - C^*) \cdot \exp(-k_{median}/q)\} \quad (2.17)$$

If $C_{out,median}$ is log-transformed, it is the mean of log transformed values and marked $\mu_{\ln out}$. Standard deviation of k can be calculated as log transformed mean and standard deviation from Equation (2.18a) as shown in Equation (2.18b).

$$\sigma_x^2 = \{\exp(\sigma_{\ln x}^2) - 1\} \cdot \exp\{2\mu_{\ln x} + \sigma_{\ln x}^2\} \quad (2.18a)$$

$$\sigma_k = \sqrt{\{\exp(\sigma_{\ln k}^2) - 1\} \cdot \exp\{2\mu_{\ln k} + \sigma_{\ln k}^2\}} \quad (2.18b)$$

It is assumed that C_{in} and k are independent. Therefore, the standard deviation of the C_{out} can be evaluated using Equation (2.7) in Chapter 2 from Equation (2.18b) as shown in Equation (2.19):

$$\sigma_{C_{out}} = \left[\exp(-k_{median}/q)^2 \cdot \sigma_{C_{in}}^2 + \left\{ \frac{(C_{in,median} - C^*)}{q} \exp(-k_{median}/q) \right\}^2 \cdot \sigma_k^2 \right]^{1/2} \quad (2.19)$$

Using Equation (2.19), the mean value of C_{out} ($\mu_{C_{out}}$) can be estimated as shown in Equation (2.20c):

$$\mu_{\ln x} = \frac{1}{2} \ln \left\{ \frac{\mu_x^2}{1 + \left(\frac{\sigma_x}{\mu_x} \right)^2} \right\} \quad (2.20a)$$

$$\mu_{\ln C_{out}} = \frac{1}{2} \ln \left\{ \frac{\mu_{C_{out}}^2}{1 + \left(\frac{\sigma_{C_{out}}}{\mu_{C_{out}}} \right)^2} \right\} \quad (2.20b)$$

$$\mu_{C_{out}} = \sqrt{\frac{\exp(2\mu_{\ln C_{out}}) + \sqrt{(\exp(4\mu_{\ln C_{out}}) + 4\sigma_{C_{out}}^2 \exp(2\mu_{\ln C_{out}}))}}{2}} \quad (2.20c)$$

The log-transformed standard deviation of C_{out} can be determined using Equation (2.21a) from Equations (2.19) and (2.20c) as shown in Equation (2.21b).

$$\sigma_{\ln x} = \left[\ln \left\{ 1 + \left(\frac{\sigma_x}{\mu_x} \right)^2 \right\} \right]^{1/2} \quad (2.21a)$$

$$\sigma_{\ln C_{out}} = \left[\ln \left\{ 1 + \left(\frac{\sigma_{C_{out}}}{\mu_{C_{out}}} \right)^2 \right\} \right]^{1/2} \quad (2.21b)$$

The confidence intervals of C_{out} can be estimated using Equation (2.17) and (2.21b) through Equations (2.22) and (2.23).

$$C_{out,95\%UCL} = \exp(\mu_{\ln C_{out}} + 1.96\sigma_{\ln C_{out}}) \quad (2.22)$$

$$C_{out,95\%LCL} = \exp(\mu_{\ln C_{out}} - 1.96\sigma_{\ln C_{out}}) \quad (2.23)$$

3 EFFECT OF BMP SIZE AND RUNOFF ON THE PERFORMANCE OF BEST MANAGEMENT PRACTICES WITH UNCERTAINTY ANALYSIS

3.1 Introduction

Best Management Practices (BMPs) are widely used to control stormwater runoff and nonpoint source pollutants. Although hydrologic performance of BMPs and their design methodology are well developed, the level of pollutant removal and treatment performance is difficult to assess. The main reason for this difficulty is there are significant uncertainties in the variables believed to affect pollutant removal in BMPs. In addition, the influent concentration to the BMP differs depending on rainfall characteristics, land use, seasons, and other conditions, which makes it difficult to evaluate pollutant concentrations in the runoff. Therefore, it is necessary to consider uncertainty in assessing the effectiveness of functions related to BMP performance. Particularly, more detailed study is necessary on the effects of BMP geometry and inflow since these are the most significant factors of BMP design (Urbonas, 1995).

The object of this study is to examine the effect of BMP size and BMP inflow on BMP performance. The BMPs chosen for this study were detention basins and retention ponds. Total suspended solids (TSS) is the pollutant of interest because it is the most used water quality parameter in stormwater BMPs. This study applied the k - C^* model as the BMP performance model. Uncertainty was included in the model parameters k , q , and C_{in} as discussed in Chapter II to produce a probabilistic outflow concentration from the BMP

performance model. Observed data of BMP geometry, hydrologic information, and pollutant concentration obtained from the International Stormwater BMP Database (www.bmpdatabase.org) were used to build the model.

3.2 Background

3.2.1 Performance Effects of BMP Geometry and Inflow

Carleton et al. (2001) investigated the relationship between percent pollutant removal and factors affecting performance in wetlands. They applied volume and areal based 1st order models and found that the volume-based 1st order model is more appropriate for TP removal in wetlands. Shammaa et al. (2002) investigated factors affecting TSS removal in stormwater detentions basins. They showed that detention time and detention volume are the major factors effecting TSS removal. Also, geometric considerations, such as detention basin length to width ratio, pond depth, bottom grading, and side slope, are also related to TSS removal. Finally, they concluded that the most important factor affecting TSS removal is detention time.

Barrett (2004) investigated the factors affecting the pollutant-removal performance of retention ponds. He investigated the correlation of retention pond performance, represented as percent removal or effluent EMC, with permanent pool volume size, pond surface area, and climate variation. He concluded that the effluent concentration of TSS is independent of permanent-pool volume and that the percent removal of TSS is not correlated with pond surface area. Starzec et al. (2005) collected metal contents in sediment data from Swedish wet detention basins to determine the

relationship between BMP geometric functions and pollutant removal efficiency. They found that metal removal efficiency is stable over 250m²/ha (surface area relative to its catchment area), which implies that only a smaller surface area than 250m²/ha has an effect on the removal efficiency of metals. Barrett (2008) represents several BMP performances using the linear regression method of influent and effluent EMCs for data from the International Stormwater BMP Database. He suggested that plotting the influent and effluent EMCs is a good approach to represent BMP performance because influent EMC is one of the dominant variables in BMP performance.

Kadlec (2000) and Lin et al. (2005) suggested that there is a strong relationship between k and q in the k - C^* model. Moreover, Lin et al. (2005) found that k is related to q with a power function and that q is related to BMP surface area in TSS and total ammonium nitrogen (TAN) removal in the free-surface wetland. They suggest that wetland surface area would tend to be overestimated because low values of q would tend to underestimate the areal removal rate constant.

3.2.2 Latin Hypercube Sampling

Influent and effluent EMCs as well as the rate k all contain uncertainty. To evaluate the sensitivity of these uncertainties, it is necessary to apply various uncertainty analysis methods. This study applies the latin hypercube sampling (LHS) method for the uncertainty of influent EMC and k .

LHS is a special method of stratified sampling. It is a strategy of efficient sampling that can reduce the variance of results to a meaningful uncertainty assessment.

This method also provides an efficient and practical sampling methodology in the case of large Monte Carlo simulations (MCS) (Murphy et al. 2006).

LHS can provide accurate estimates of statistical variables of model output with much smaller computational work than MCS (Melching, 1995). Several studies have applied LHS to estimate sediment transport. Yeh and Tung (1993) compared the first-order second-moment (FOSM) method, Harr's probabilistic point estimation (PPE) method, and LHS for the uncertainty analysis of erosion and transport. It was found that FOSM and LHS provide better results than Harr's PPE method. Salas and Shin (1999) applied MCS and LHS to evaluate uncertainties of annual and accumulated reservoir sedimentation volumes of the Kenny Reservoir in Northern Colorado. They found that annual-stream flow and annual-suspended-sediment load are the most sensitive factors in the evaluation of uncertainty in annual-reservoir-sedimentation volume and that the annual-sediment load and the annual streamflow are the most significant parameters in the evaluation of uncertainty in accumulated-reservoir-sedimentation volume in the case considered. For water quality, the LHS method has been applied to predict streamflow and water quality parameters in order to evaluate the uncertainty of dissolved oxygen concentration in the Soil & Water Assessment Tool 2000 (SWAT 2000) (Sohrabi et al., 2003), in SALMON-Q, in KOSIM models (Melching and Bauwens, 2001), and in the DUFLOW model (Manache and Melching, 2004). Also, Shirmohammadi et al. (2006) applied LHS with other uncertainty methods, including MCS and generalized likelihood uncertainty estimation (GLUE), to estimate uncertainty of sediment estimation in the SWAT model's output. LHS was applied to estimate the parameters of the distributed hydrologic runoff models such as the Hydrological Simulation Model (HYSIM) (Murphy

et al. 2006), SWAT (Muleta and Nicklow, 2005) and MIKE SHE (Christiaens and Jeyen, 2002). The most significant feature of these hydrologic and environmental models is that they have many input parameters which make it difficult to evaluate the uncertainties of the model outputs with general MCS. LHS resolves this problem with fewer sampling numbers and shows more accurate uncertainty output values as a result in models.

3.3 Method

3.3.1 Data Selection

There are many factors that affect BMP effluent concentration such as influent concentration, the size of the permanent pool, pond geometry, temperature, area of the pond, and the inflow rate for a storm event. However, it is very difficult to consider all factors simultaneously in a BMP performance model (Barrett, 2008). This study uses data for each of these factors from the International Stormwater BMP Database (www.bmpdatabase.org). The dataset applied to this study includes stormwater inflow and outflow data, BMP geometry data, and water quality data categories assembled together as shown in Figure 3.1. This study uses TSS as the pollutant because only the TSS dataset in detention basins and retention ponds had a large enough number of data to analyze their performance; other pollutants in detention basins and retention ponds and TSS data in other BMPs were too few in number to be used. Data assembled from the BMP database were pre-screened for application in the BMP performance model. This pre-screening had two conditions: 1) the average-event inflow rate (Q_{in}) had to be equal

or greater than the outflow rate (Q_{out}) and 2) the influent EMC (C_{in}) had to be greater than the effluent EMC (C_{out}).

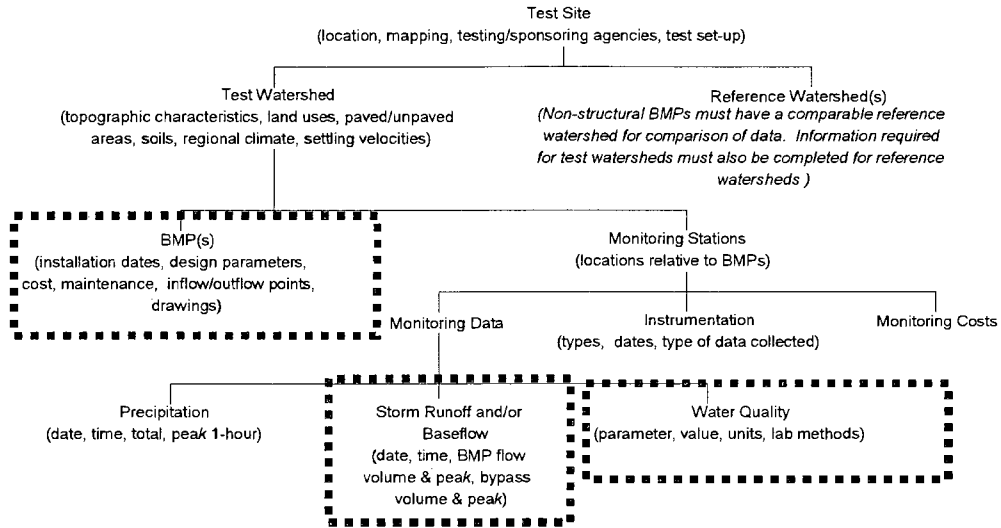


Figure 3.1 Outline of the international stormwater BMP database and data collection of this study (www.bmpdatabase.org)

Table 3.1 lists the geometric information and location of detention basins and retention ponds and the number of data sets assembled for each BMP in this study. All of the chosen detention basins are located in the state of California, but the locations of the retention basins are located in both California and Colorado.

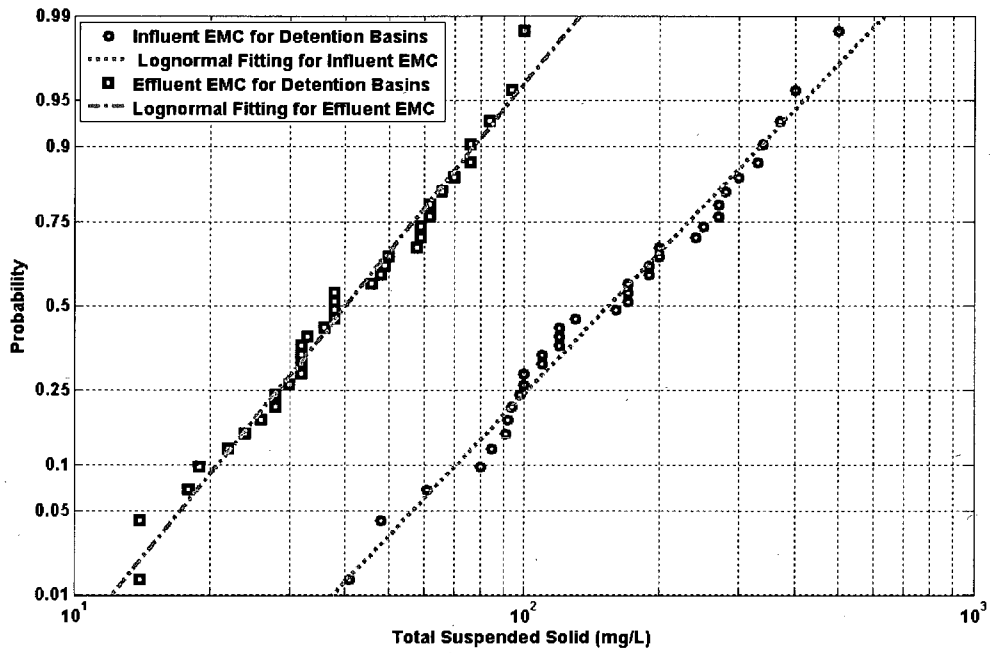
Table 3.1 Geometric information of BMPs and assembled number of dataset in this study

BMP Type	BMP Name and Location	Number of Dataset	BMP size				
			Volume (m ³)	Surface Area (m ²)	Length (m)	Width (m)	Depth (m)
Detention Basins	15/78, CA	17	1122.54	977	60.96	16.02	1.15
	5/605 EDB, CA	2	364.66	598	47.24	12.66	0.61
	605/91 edb, CA	5	69.57	114	22.86	13.29	0.83
	Manchester, CA	12	252.79	304	22.86	4.99	0.61
Retention Ponds	La Costa WB, CA	6	259.10	1,115	60.96	18.29	0.93
	Lakewood RP (96), CO	5	19.82	16	8.84	1.77	1.90
	Lakewood RP (97-98), CO	16	18.96	85	16.97	5.01	0.42

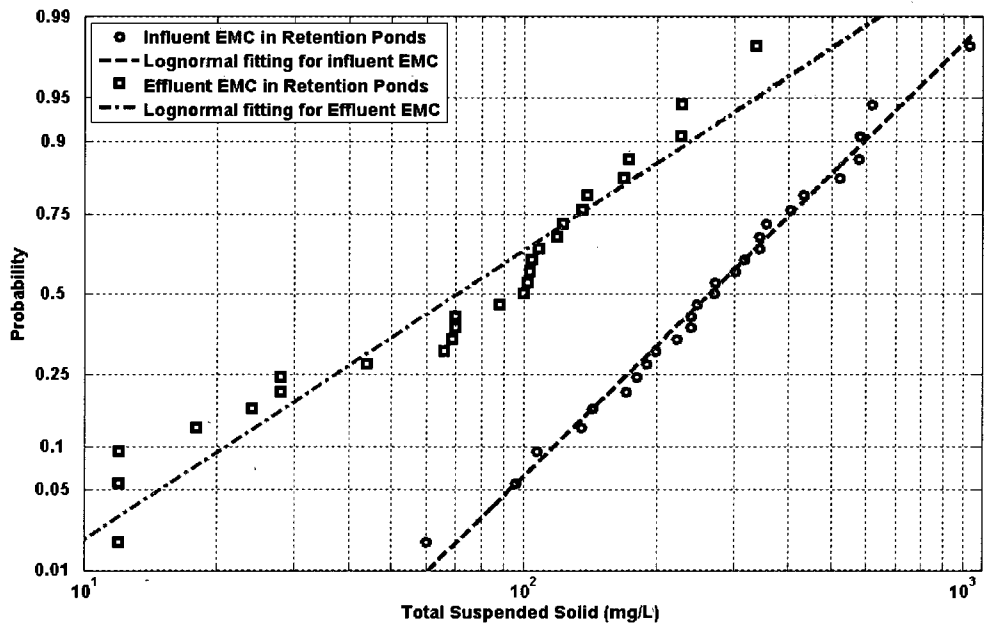
Figure 3.2 and Table 3.2 show lognormal (base e) probability plots and the log-transformed statistical variables of observed EMCs of TSS in detention basins and retention ponds for the sites listed in Table 3.1. Figure 3.2(a) shows how both influent and effluent TSS in detention basins are closely represented by lognormal probability plots. However, effluent TSS in retention ponds is quite scattered, as seen in Figure 3.2(b). Moreover, the slopes of the probability plots between the influent EMCs and effluent EMCs in Figure 3.2(a) are very similar, but the slopes in Figure 3.2(b) are quite different, which indicates that influent and effluent EMCs in detention basins represent relatively similar standard deviations while influent and effluent EMCs in retention ponds represent different standard deviations (GeoSyntec et al., 2000).

Table 3.2 Statistical variables of influent and effluent EMCs in detention basins and retention ponds

TSS	Log transformed Influent EMC		Log transformed Effluent EMC	
	Mean	Standard Deviation	Mean	Standard Deviation
Detention Basins	5.0380	0.6083	3.6903	0.5147
Retention Ponds	5.5292	0.6660	3.8990	1.4435



(a) Detention Basins



(b) Retention Ponds

Figure 3.2 Lognormal probability plots of observed EMCs;
(a) detention basins; (b) retention ponds

3.3.2 Model of Storage BMP Performance

The k - C^* model combined with uncertainty analyses was selected to represent the BMP performance in this study as described by Chapter 2.3.1.

3.3.3 Relating Hydraulic Loading Rate and Areal Removal Rate Constant

The areal removal rate constant, k , is related to the hydraulic loading rate, q , through a power function as shown in Figure 3.3. However, the variance of effluent EMC in the k - C^* model is very sensitive to k . Therefore, it is necessary to apply a prediction interval in the k and q regression line. k values in Figure 3 are estimated from the observed data with the k - C^* model. A prediction interval is focused on the variance of individual data while a confidence interval is focused on the variance of a regression line (Kutner et al. 2004). This study chose the prediction interval of k because it is essential to know the performance for an individual event rather than the prediction of the average performance for many similar events (Barrett, 2005). The prediction interval in the regression line relating k and q is calculated as (Kutner et al. 2004)

$$Mean \pm t_{0.025} s \sqrt{1 + \frac{1}{n} + \frac{(X - \bar{X})^2}{\sum_{i=1}^n (X_i - \bar{X})^2}} \quad (3.1)$$

where

$t_{0.025}$ = 95% t statistics value for the appropriate degree of freedom (n-2),

n = the number of total data,

s = standard error of the regression,

X = average q at which the confidence interval calculated,

\bar{X} = mean of observed q from monitoring data, and

X_i = individual observed q from monitoring data.

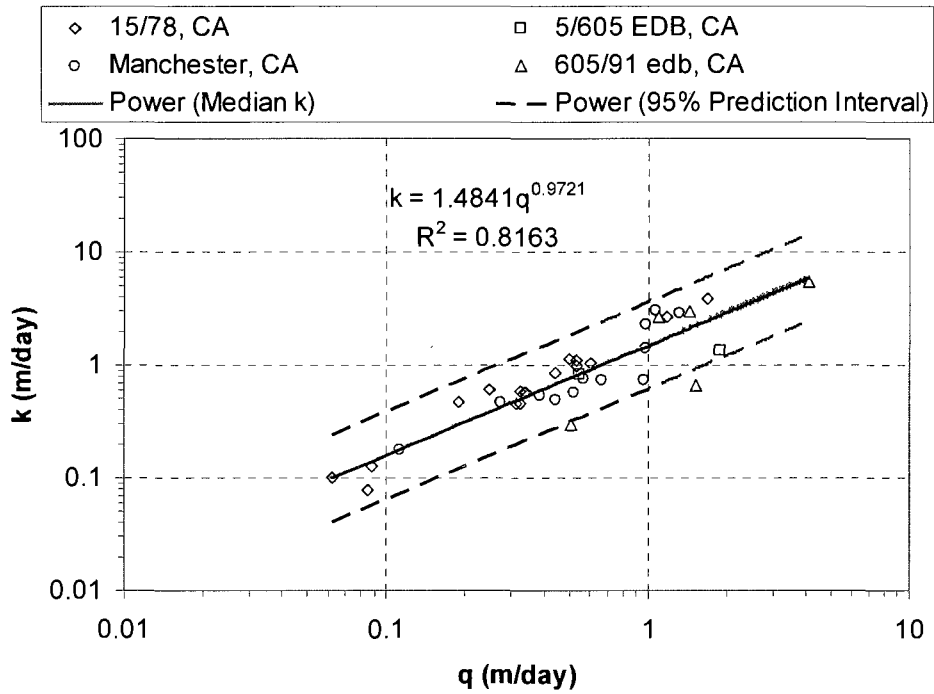
This study applies TSS data sets from detention basins and retention ponds to compare the characteristics of BMP performance. The k - C^* model is used for simulating the performance of the BMP. Both parameters of the model, k and C^* , depend on pollutant characteristics such as the particle size and settling velocity (Wong et al. 2002). Treatment systems receiving large particle concentrations will have a high decay rate, k , and low C^* since there is more sedimentation. Thus, there is a relationship between the parameter k and the settling velocities (or particle size) of suspended particles in the watershed. Parameter k calibration for the k - C^* model can be performed based on local conditions such as settling velocity (Kadlec and Knight 1996). Although the areal removal rate constant, k , has a theoretical link to settling velocity, field studies have shown that this theoretical link is not necessarily the case for particles finer than about 40 μm (Wong et al. 2002). Thus, the estimation of k is not straightforward. Previous research found that the k -values of the k - C^* model are strongly dependant on the HLR (q) (Scherup et al. (1990); Kadlec (2000); Lin et al. (2005)). The following power relationship was proposed with coefficients a and b

$$k = aq^b \quad (3.2)$$

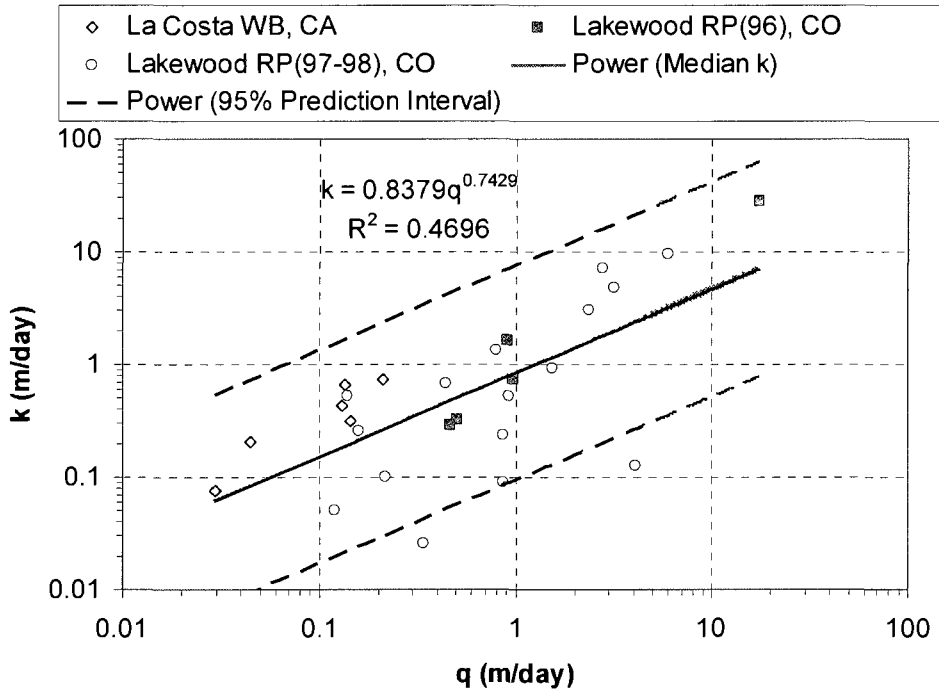
This relationship can be used to estimate the value of k in order to build the k - C^* model for prediction (Lin et al. 2005). This study also applies Equation (3.2) to the model.

However, k -values in the model are very sensitive to effluent EMC and must be estimated with more accuracy in order to obtain accurate effluent EMCs. Therefore, the need of high accuracy in the model results in the need for an uncertainty analysis of k . A plot of k versus q based on storm event is shown in Figure 3.3 with a 95% prediction interval from Equation (3.1) for TSS in detention basins. k values in Figure 3.3 can be estimated by an inverse of the k - C^* model using observed C_{out} and q values estimated from observed inflow and BMP surface area. Data are categorized by BMP and location. Values of the coefficients a and b in Equation (3.2) are 1.4841 and 0.9721 for detention basins and 0.8379 and 0.7429 for retention ponds. From Figure 3.3, k values depending q in retention pond represents smaller than k in detention basins. Size of retention ponds is greater than that of detention basins and it also has a permanent pool. These factors make that retention ponds are easily mixed with multiple events unlikely detention basins and these mixing of multiple events in retention ponds may cause low k values.

If parameter b in Equation (3.2) is close to 1, the power term of q in the equation finally goes to 0. This means that the HLR does not have a large effect on the effluent EMC calculation. Therefore, the BMP surface area and inflow, which is obtained with the HLR, cannot produce a large change in effluent EMC. On the other hand, if parameter b is less than 1, then the power term of HLR is greater than 0. Thus, the effluent EMC will be affected by changes in BMP surface area and inflow.



(a)



(b)

Figure 3.3 q vs. k with 95% prediction interval;
 (a) TSS in detention basins; (b) TSS in retention ponds

The distance between the median line and the prediction interval lines shows the uncertainty in k . Thus, the standard deviation of log-transformed k is 0.4370 for detention basins and 1.0624 for retention ponds from Figure 3.3. The standard deviations of the log-transformed k are slightly different for each point, but this difference is very small. Thus, this study uses the average value for the standard deviation of k .

Table 3.3 shows the required input variables for uncertainty analysis incorporating uncertainty in both C_{in} and k . The standard deviation of k can be estimated from the distance of the prediction interval between the median k and the 95% prediction interval of k from Equation (3.1). The standard deviation of the log-transformed k for retention ponds is more than twice the value for detention ponds because k values depending on q in retention ponds are scattered wider than in detention basins as shown in Figure 3.3. This means that the variance of C_{out} for retention ponds would be significantly greater than for detention basins. The range of C^* is suggested in the literature as shown in Table 3.4. This study chose one constant value, 10mg/L, for C^* in both detention basins and retention ponds because most observed data in detention basins and retention ponds have 10 mg/L as the minimum C_{out} .

Table 3.3 Required parameters information of k for detention basins and retention ponds

Input Parameters	Detention Basins		Retention Ponds	
Log-transformed Statistical Properties	mean	standard deviation	mean	standard deviation
C_{in}	5.038	0.6083	5.5292	0.6660
K	$\text{Log}(1.4841q^{0.9721})$	0.4370	$\text{Log}(0.8379q^{0.7429})$	1.0624

Table 3.4 Typical background concentration values proposed in literatures

Literatures	TSS (mg/L)
Kadlec and Knight (1996)	C_m when $0.0 < C_m < 290$ mg/L $5.1+0.16 C_m$ when $0.1 < C_m < 807$ mg/L
Barrett (2004)	5~20
Crites et al. (2006)	6
This Study	10

3.3.4 Uncertainty Analysis and LHS

The LHS method was selected for estimating the variance of k and C_{out} . The LHS method is described as Section 2.3.2.4.

3.4 Results

This chapter estimated the distribution of C_{out} using the k - C^* model with two distributed input parameters, C_m and k , as shown in Figure 4. This model assumed that geometric (A) and hydrological parameters (Q) did not have uncertainty. Moreover, the background concentration (C^*) was fixed at 10 mg/L because the minimum value of selected observed data was close to 10 mg/L. Also, this study assumed that C_m and k were represented as lognormal distributions because the distributions of their observed data are very close to lognormal distribution as shown in Figure 3.2 and Figure 3.3.

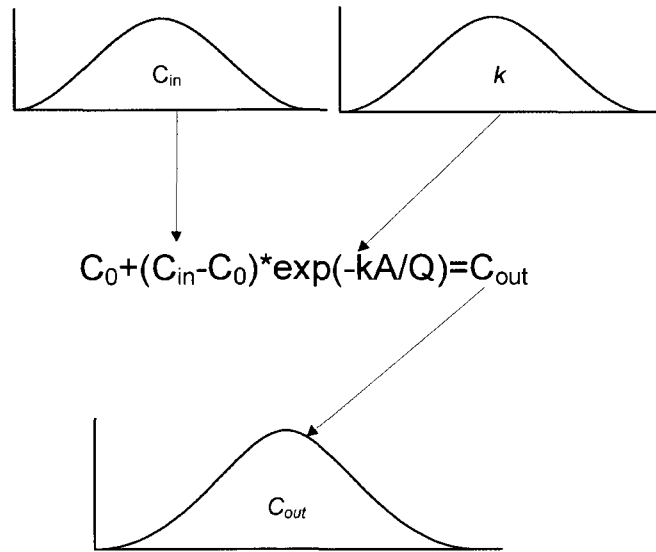


Figure 3.4 Schematic for generation of probabilistic C_{out}

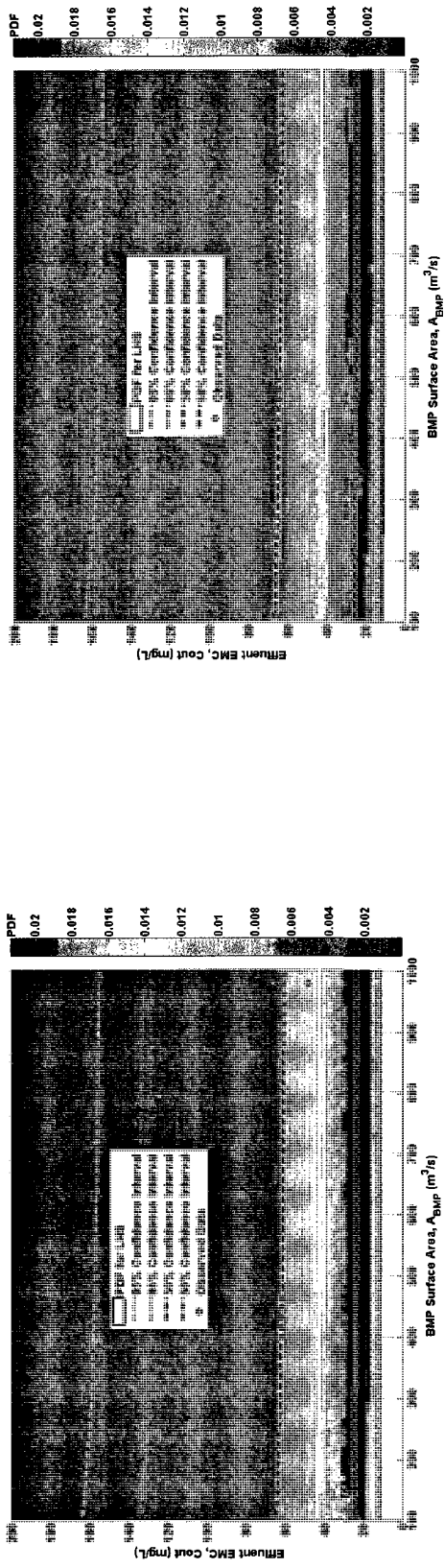
3.4.1 Effect of BMP Surface Area

Figure 3.5 shows the distribution of TSS effluent EMC and the Probability Density Function (PDF) of TSS depending as a function of the surface area of a detention basin with constant inflow. The figure shows 50% and 95% confidence intervals for effluent EMC. The observed data selected from the BMP database fell between 25-65 mg/L and 13-160 mg/L, respectively; all the observed data are located within the 95% confidence interval.

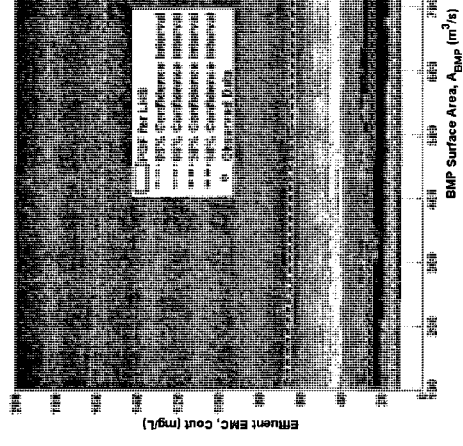
From Figure 3.5, it is observed that the confidence intervals of effluent EMC do not change much as the BMP surface area changes. Figure 3.6 also shows the distribution of TSS effluent EMC depending on the surface area of a retention pond with constant inflow runoff. Confidence intervals of effluent EMC decrease as surface area increases. This implies that the surface area of a retention pond does have an effect on TSS removal. Therefore, it can be concluded that BMP surface area affects retention pond efficiency

but has little effect on detention basin efficiency. Nevertheless, the confidence intervals of effluent EMC in Figure 3.5 and Figure 3.6 decrease as the BMP surface area increases. This indicates that TSS effluent concentration decreases as the BMP surface area increases in both detention basins and retention ponds.

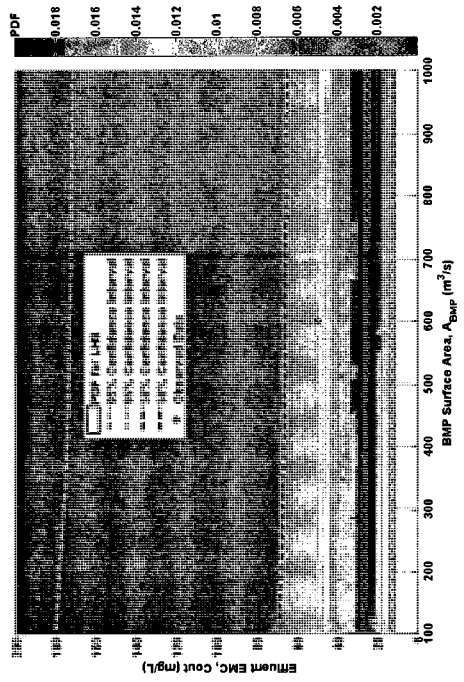
On the other hand, the 50% confidence intervals of effluent EMC in retention ponds shown in Figure 3.6 range from 10-50 mg/L to 100-200 mg/L, depending on average flow, and the 95% confidence interval of effluent EMC ranges between 10 mg/L to 350-650 mg/L, depending on average flow. Particularly, the 95% upper confidence interval decreases as the BMP surface area increases. This implies that the surface area has an effect on retention pond performance. Finally, it is concluded that the confidence intervals of retention ponds are wider and more variable than the confidence intervals of detention basins because the variation of input variables, such as C_{in} and k , in retention ponds are greater than the variation of input variables in detention basins.



(a)



(b)



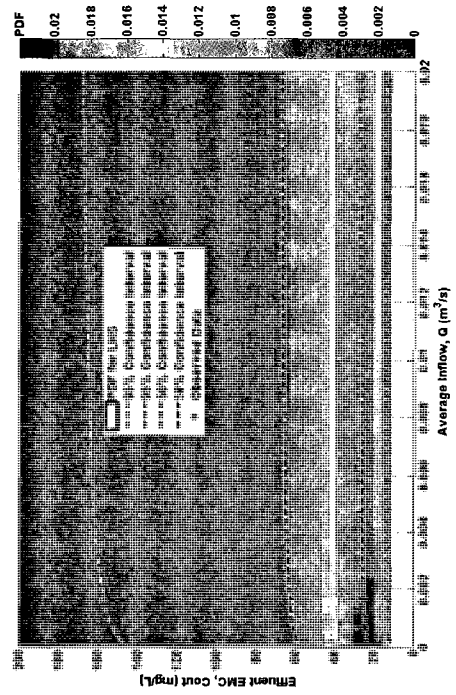
(c)

Figure 3.5 Probability density functions for TSS effluent EMCs in detention basins as a function of BMP Surface area ; (a) average $Q=0.001\text{m}^3/\text{s}$; (b) average $Q=0.0037\text{m}^3/\text{s}$; (c) average $Q=0.013\text{m}^3/\text{s}$

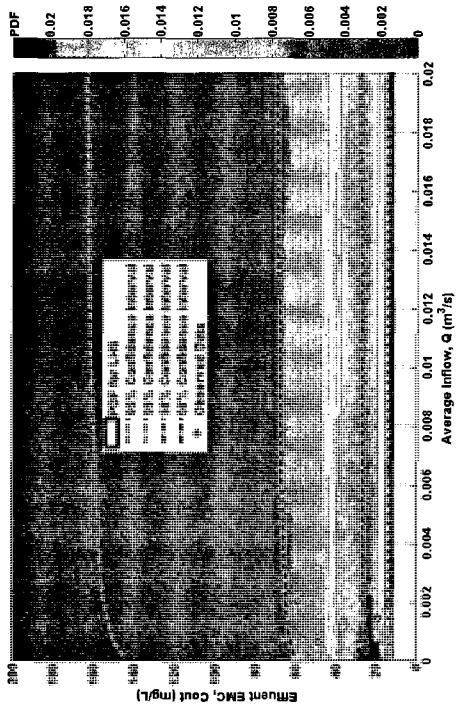
3.4.2 Effect of Inflow

Figure 3.7 shows the distribution of TSS effluent EMC depending on the average inflow of detention basins with a constant BMP surface area. Widths of 50 % and 95% confidence intervals are very similar (Figure 4), ranging between 25-60 mg/L and 15-160 mg/L. Observed data was used to verify results. All observed data are located within the 95% confidence interval.

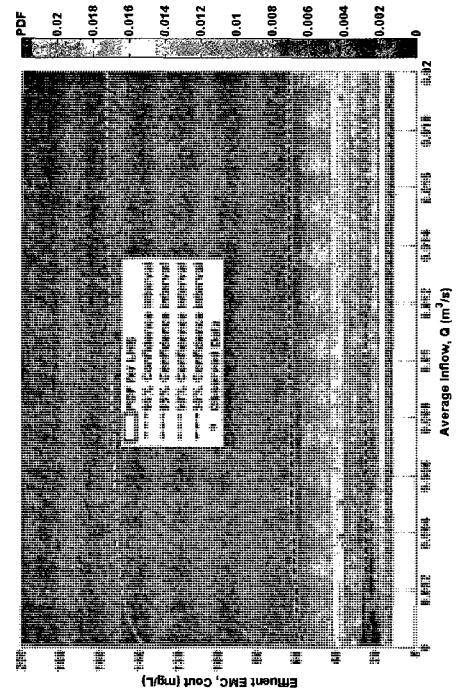
Figure 3.8 represents the distribution of TSS effluent EMC depending on the average inflow of retention ponds with a constant BMP surface area. Confidence intervals of TSS effluent EMC in Figure 3.7 and Figure 3.8 increase as the average inflow increases. This indicates that TSS effluent concentration decreases as the average inflow increases in both detention basins and retention ponds.



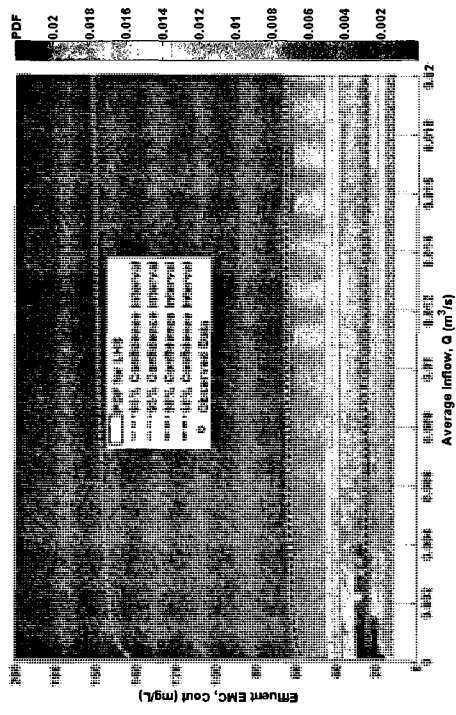
(a)



(b)



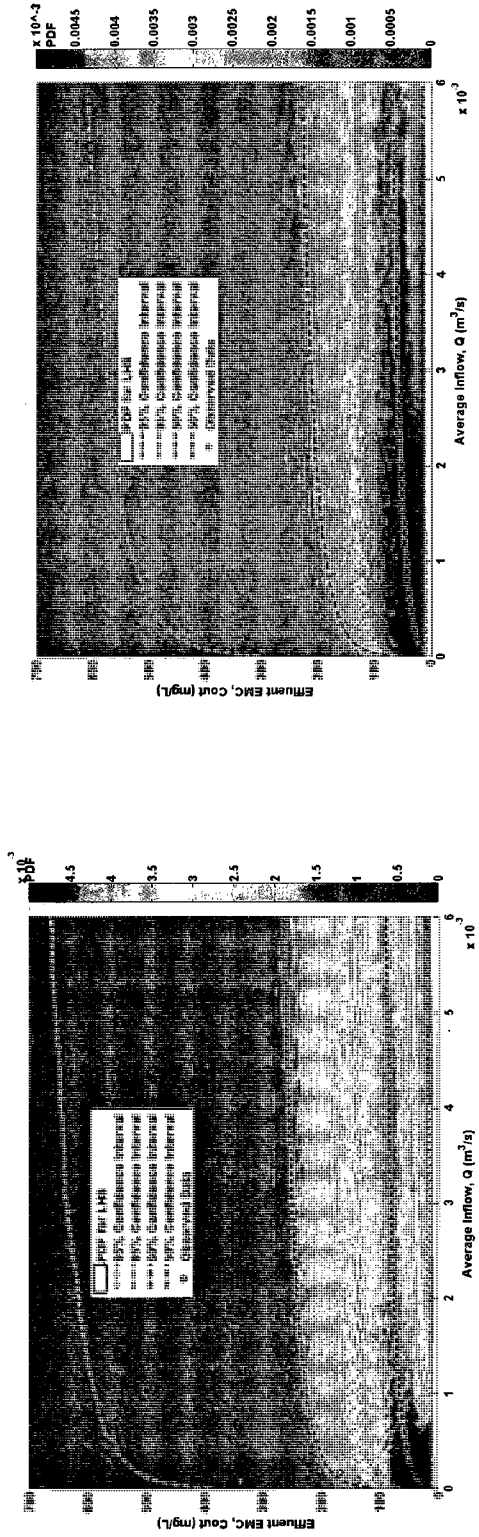
(c)



(d)

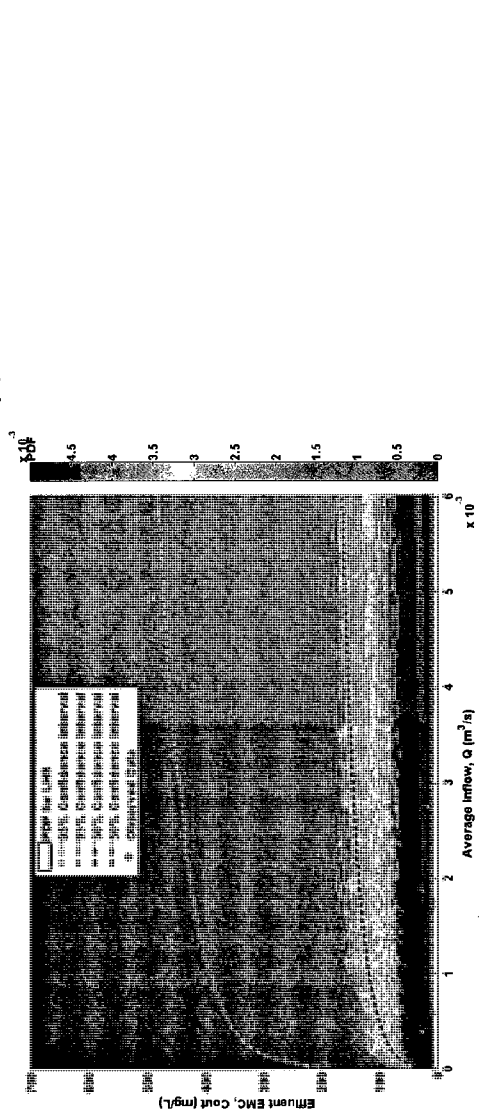
Figure 3.7 Probability density functions for TSS effluent EMCs in detention basins as a function of average inflow ;(a) $A_{BMP}=110 \text{ m}^2$; (b) $A_{BMP}=300 \text{ m}^2$; (c) $A_{BMP}=600 \text{ m}^2$; (d) $A_{BMP}=1000 \text{ m}^2$

The confidence intervals of effluent EMC in Figure 3.8 increase greatly as the average inflow increases. This indicates that the average inflow in a retention pond has an effect on TSS removal. Therefore, it can be concluded that the average inflow affects TSS removal in retention ponds but has less effect in detention basins. In addition, the confidence intervals become wider as the average inflow increases as shown in Figure 3.7 and Figure 3.8. The change in the confidence intervals is small depending on the inflow discharge in Figure 3.7 (a),(b),(c) and (d), but the confidence intervals in Figure 3.8(a),(b) and (c) become much wider as the inflow-flow rate increases. According to the $k-C^*$ model, it is shown that the modeled detention basin effluent EMCs have fairly consistent variances when changes in average inflow and surface area are made in the model, but that the effluent EMCs in retention ponds sensitive to average inflow and surface area. This occurs because of parameter b in the regression relationship of q to k shown in Figure 3.3.



(a)

(b)



(c)

Figure 3.8 Probability density functions for TSS effluent EMCs in retention ponds as a function of average inflow ; (a) $A_{BMP}=16 \text{ m}^2$; (b) $A_{BMP}=85 \text{ m}^2$; (c) $A_{BMP}=1110 \text{ m}^2$

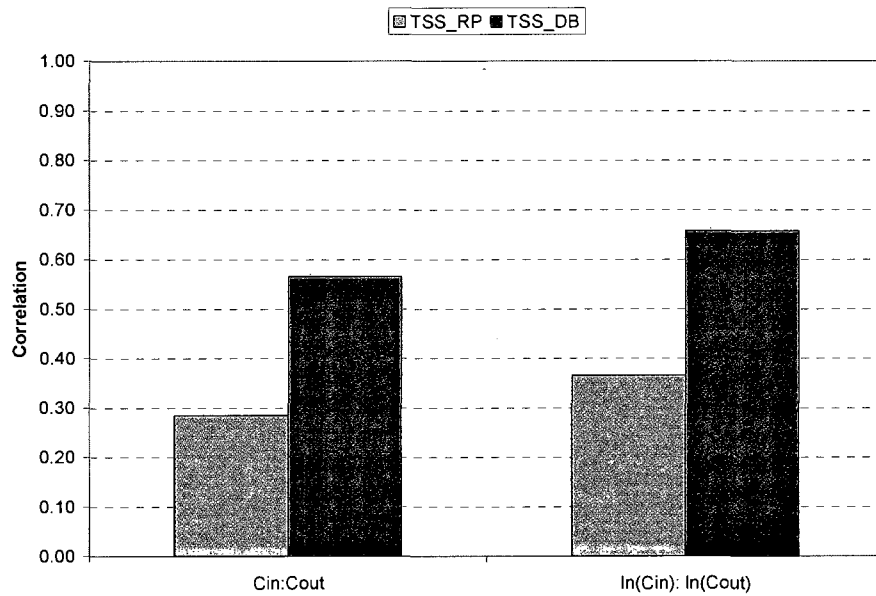
3.4.3 Analysis of BMP Performance between Detention Basins and Retention Ponds

3.4.3.1 Correlation of Concentration, BMP Geometry and Inflow

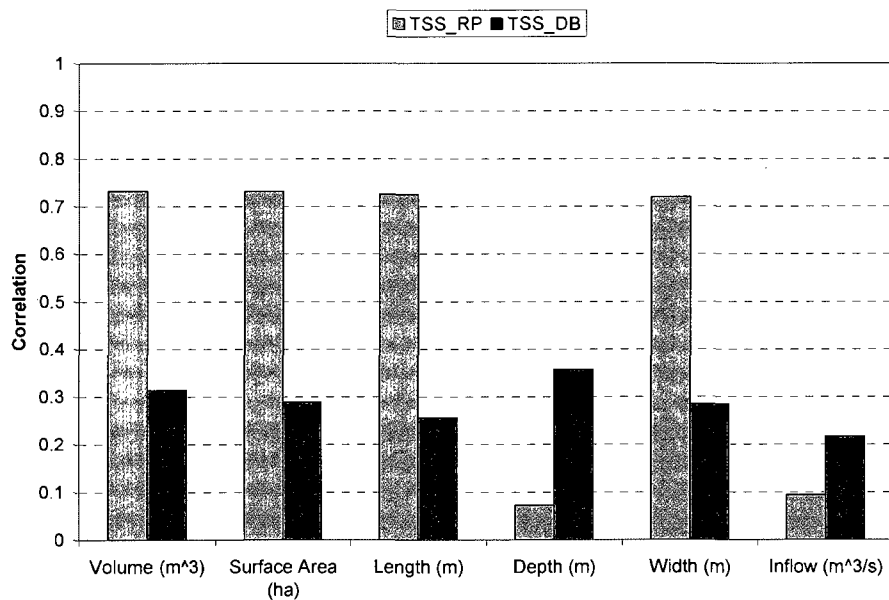
Figure 3.9(a) shows the correlation coefficients between C_{in} and C_{out} of TSS in detention basins and retention ponds. Log-transformed C_{in} and C_{out} represent a greater correlation coefficient than the original data set. The correlation coefficients of the original C_{in} and C_{out} and log-transformed C_{in} and C_{out} in detention basins are greater than correlations in retention ponds.

Figure 3.9(b) shows the correlation coefficients based on observed data of $\log\left(\frac{C_{in} - C^*}{C_{out} - C^*}\right)$ for BMP geometric functions and inflow in both detention basins and retention ponds. Concentration efficiency has a low correlation with BMP geometry in detention basins and a high correlation with BMP geometry in retention ponds. This indicates that the concentration efficiencies determined from Equation (2.2) show the distinctive magnitudes of correlation coefficients between detention basins and retention ponds. On the other hand, correlation coefficients of inflow with concentration efficiencies are very low, as seen in Figure 3.9(b). The correlation coefficients of retention ponds are higher than those of detention basins for all geometric properties except depth. This indicates that surface area is the most significant variable among BMP geometric functions with concentration efficiency based on the $k-C^*$ model in retention ponds. On the contrary, the correlation coefficient of depth for detention basins in Figure

3.9(b) is higher than other BMP geometric functions. This implies that depth is the most significant parameter among BMP geometric parameters in detention basins.



(a)



(b)

Figure 3.9 Correlations in detention basins and retention ponds

(a) Influent EMC: Effluent EMC; (b) $\log\left(\frac{C_m - C^*}{C_{out} - C^*}\right)$: BMP geometric functions and inflow

3.4.3.2 Analysis from the k - C^* Model

The k - C^* model is finally represented as the following

$$C_{out} = C^* + (C_{in} - C^*) \exp(-aq^{b-1}) \quad (3.3)$$

The parameter a indicates the removal efficiency of BMPs. If a is large, C_{out} increases, but if a is small, C_{out} decreases. Parameter b represents the importance of q on the estimation of C_{out} . According to the correlation analysis of this BMP data set, C_{in} is the most sensitive parameter to C_{out} in comparison to other variables like BMP geometry and inflow in detention basins. In other words, the effect of BMP geometry and inflow on C_{out} in detention basins is small. Therefore, BMP surface area and inflow have little effect on the estimation of C_{out} . In retention ponds, however, the BMP surface area, more than C_{in} , inflow, and the geometric variables studied, is the most important parameter in the estimation of C_{out} .

3.4.3.3 Analysis of Probability Plots

The slopes in Figure 3.2 represent the standard deviations of the C_{in} and C_{out} datasets in detention basins and retention ponds. These slopes are almost parallel in detention basins (Figure 3.2(a)). This means that the standard deviation of C_{in} and C_{out} is very similar, even though the mean of the two datasets are different. This indicates that the C_{in} data can be converted to C_{out} by multiplying by a certain constant value and, therefore, the power term q^b in the k - C^* model should be a constant.

However, the slopes of C_{in} and C_{out} in retention ponds (Figure 3.2(b)) are not parallel. This indicates that the standard deviation of C_{in} and C_{out} is different and that C_{out} cannot be evaluated simply by multiplying a certain constant value to C_{in} .

3.5 Conclusions

This study investigated the effect of BMP surface area and inflow on TSS removal in detention basins and retention ponds using the $k-C^*$ model incorporating uncertainty analysis. According to the results in Section 3.4.1 and 3.4.2, effluent EMC increases with the increase of the inflow in both detention basins and retention ponds. Also, effluent EMC decreases with the increase of BMP surface area in both BMP types. These conditions rationally coincide with natural BMP behaviors.

Confidence intervals of C_{out} for detention basins and retention ponds are very different due to statistical characteristics of the dataset and parameter b in Equation (3.2). In addition, the results of detention ponds suggest that surface area and inflow do not have a noticeable effect on C_{out} . It is believed that C_{in} is more significantly associated than BMP surface area and inflow for the performance of the $k-C^*$ model of detention basins. The results for the retention ponds, however, suggest that surface area and inflow influence the change of effluent EMC. According to the results, it can be concluded that the sensitive factors for the performance of the $k-C^*$ model are C_{in} for detention basins and BMP surface area, inflow, and C_{in} for retention ponds. As described above, it is necessary to get more data to verify the performance of detention basins and retention ponds and to investigate regional effects such as elevation, weather, geomorphology, etc to BMP performance.

3.6 References

- Barrett, M. E. (2004). "Retention pond performance: Examples from the international stormwater BMP database" Proceedings of the 2004 World Water and Environmental Resources Congress: Critical Transitions in Water and Environmental Resources Management, ASCE, Salt Lake City, Utah, 439-448.
- Barrett, M. E. (2005). "Performance comparison of structural stormwater best management practices." *Water Environment Research*, 77(1), 78-86.
- Barrett, M. E. (2008). "Comparison of BMP performance using the international BMP database." *Journal of Irrigation and Drainage Engineering-ASCE*, 134(5), 556-561.
- Carleton, J. N., Grizzard, T. J., Godrej, A. N., and Post, H. E. (2001). "Factors affecting the performance of stormwater treatment wetlands." *Water Research*, 35(6), 1552-1562.
- Christiaens, K., and Feyen, J. (2002). "Constraining soil hydraulic parameter and output uncertainty of the distributed hydrological MIKE SHE model using the GLUE framework." *Hydrological Processes*, 16(2), 373-391.
- Crites, R. W., Middlebrooks, E. J., and Reed, S. C. (2006). *Natural Wastewater Treatment Systems*, CRC Press.
- GeoSyntec Consultants, U. D. a. F. C. D., URS Greiner Woodward Clyde and Urban Water Resources Research Council of the American Society of Civil Engineers. (2000). "Determining urban stormwater best management practice (BMP) removal efficiencies, task 3.4, final data exploration and evaluation report." Prepared in cooperation with Office of Water, US Environmental Protection Agency, Washington, D.C.
- Kadlec, R. H. (2000). "The inadequacy of first-order treatment wetland models." *Ecological Engineering*, 15(1-2), 105-119.
- Kadlec, R. H., and Knight, R. L. (1996). *Treatment wetlands*, Lewis Publishers, Boca Raton.
- Kutner, M. H., Nachtsheim, C. J., and Neter, J. (2004). *Applied linear Regression Models*, Irwin, Homewood, Ill.
- Lin, Y. F., Jing, S. R., Lee, D. Y., Chang, Y. F., Chen, Y. M., and Shih, K. C. (2005). "Performance of a constructed wetland treating intensive shrimp aquaculture wastewater under high hydraulic loading rate." *Environmental Pollution*, 134(3), 411-421.

- Manache, G., and Melching, C. S. (2004). "Sensitivity analysis of a water-quality model using Latin hypercube sampling." *Journal of Water Resources Planning and Management-ASCE*, 130(3), 232-242.
- Melching, C. S. (1995). "Chapter 3: Reliability Estimation." *Computer Models of Watershed Hydrology*, V. P. Singh, ed., Water Resources Publication, Littleton, CO, 69-118.
- Melching, C. S., and Bauwens, W. (2001). "Uncertainty in coupled nonpoint source and stream water-quality models." *Journal of Water Resources Planning and Management-ASCE*, 127(6), 403-413.
- Muleta, M. K., and Nicklow, J. W. (2005). "Sensitivity and uncertainty analysis coupled with automatic calibration for a distributed watershed model." *Journal of Hydrology*, 306(1-4), 127-145.
- Murphy, C., Fealy, R., Charlton, R., and Sweeney, J. (2006). "The reliability of an 'off-the-shelf' conceptual rainfall runoff model for use in climate impact assessment: uncertainty quantification using Latin hypercube sampling." *Area*, 38(1), 65-78.
- Salas, J. D., and Shin, H. S. (1999). "Uncertainty analysis of reservoir sedimentation." *Journal of Hydraulic Engineering-ASCE*, 125(4), 339-350.
- Schierup, H., Brix, H., and Lorenzen, B. (1990). "Wastewater treatment in constructed reed beds in Denmark: state of the art." *Constructed Wetlands in Water Pollution Control: Advances in Water Pollution Control No 11*, P. F. Cooper and B. C. Findlater, eds., Pergamon Press, London, U.K.
- Shammaa, Y., Zhu, D. Z., Gyurek, L. L., and Labatiuk, C. W. (2002). "Effectiveness of dry ponds for stormwater total suspended solids removal." *Canadian Journal of Civil Engineering*, 29(2), 316-324.
- Shirmohammadi, A., Chaubey, I., Harmel, R. D., Bosch, D. D., Munoz-Carpena, R., Dharmasri, C., Sexton, A., Arabi, M., Wolfe, M. L., Frankenberger, J., Graff, C., and Sohrabi, T. M. (2006). "Uncertainty in TMDL models." *Transactions of the ASABE*, 49(4), 1033-1049.
- Sohrabi, T. M., Shirmohammadi, A., Chu, T. W., Montas, H., and Nejadhashemi, A. P. (2003). "Uncertainty analysis of hydrologic and water quality predictions for a small watershed using SWAT2000." *Environmental Forensics*, 4(4), 229-238.
- Starzec, P., Lind, B. O. B., Lanngren, A., Lindgren, A., and Svenson, T. (2005). "Technical and environmental functioning of detention ponds for the treatment of highway and road runoff." *Water Air and Soil Pollution*, 163(1-4), 153-167.
- Stone, K. C., Hunt, P. G., Novak, J. M., and Johnson, M. H. (2003). "In-stream wetland design for non-point source pollution abatement." *Applied Engineering in Agriculture*, 19(2), 171-175.

- Urbonas, B. R. (1995). "Recommended parameters to report with BMP monitoring data." *Journal of Water Resources Planning and Management-ASCE*, 121(1), 23-34.
- Wong, T. H. F., Fletcher, T.D., Duncan, H.P., Coleman, J.R., and Jenkins, G.A. (2002). "A model for urban stormwater improvement conceptualization." the Ninth International Conference on Urban Drainage, E. W. Strecker and W. C. Huber, eds., ASCE, Portland, Oregon.
- Wong, T. H. F., Fletcher, T. D., Duncan, H. P., and Jenkins, G. A. (2006). "Modelling urban stormwater treatment - A unified approach." *Ecological Engineering*, 27(1), 58-70.
- Yeh, K. C., and Tung, Y. K. (1993). "Uncertainty and sensitivity analyses of pit-migration model." *Journal of Hydraulic Engineering-ASCE*, 119(2), 262-283.

4 PROBABILISTIC ESTIMATION OF POLLUTANT LOAD TO RECEIVING WATER FROM BMPS USING UNCERTAINTY ANALYSIS

4.1 Introduction

Stormwater runoff contains significant concentrations of a number of pollutants. It is one of the main sources of water quality deterioration for receiving waters in urban areas. Therefore, the control of nonpoint pollution should be considered to the same extent as the control of stormwater flooding in stormwater management. In order to reduce nonpoint pollutions, structural best management practices (BMPs) are widely applied. However, models for BMP performance are not reliable in their simulation of nonpoint-pollution removal because of the many uncertainties associated with nonpoint source pollutant removal in the BMPs. Thus incorporation of uncertainty in estimation of pollutant loading would assist stormwater managers in determining the degree of compliance with the Total Maximum Daily Load (TMDL) requirements that could be expected from a given BMP placed in a watershed. The objective of this study is to estimate the pollutant loading released to receiving water by BMPs using a BMP performance model that includes uncertainty. This BMP performance model will relate the BMP surface area and the imperviousness of the study watershed to the effectiveness of two BMPs (extended detention and retention ponds) in removing stormwater pollutants. Total suspended solids (TSS) is chosen as the representative stormwater pollutant. An additional objective of this study is to illustrate an evaluation method to

determine the effectiveness of BMPs in meeting a TMDL using Load Frequency Curves (LFCs).

4.2 Background

4.2.1 Stormwater Storage-Release Systems

Many researchers have studied storage-release stormwater management systems to control stormwater runoff and nonpoint source pollutants. Storage-release models for pollutant removal used in much of the literature are a first-order loading model, which directly computes pollutant loading but not concentration (Roesner 1982; Nix and Heaney, 1988; Patry and Kennedy, 1989; Segarra-Garcia and Loganathan, 1992; Segarra-Garcia and Basha-Rivera, 1996). Lee et al. (2005) modified the continuous rainfall-runoff model Storage, Treatment, Overflow, Runoff Model (STORM; Hydrologic Engineering Center 1977) to compute the removal of pollutants using a first-order plug flow concentration model driven by the flow results of the modified STORM.

Results from these studies have been expressed as plots of the percentage of pollutant removed as a function of BMP storage depth in watershed area (acre-inches/acre, or ha-mm/ha) and release rate. However, these results did not use inflow to the BMP as an input parameter. When the first order kinetic model is applied, the drain time is the most important input variable and the drain time is dependent on basin volume. However, hydraulic loading rate (HLR) is strongly correlated with pollutant removal and is a function of inflow rate and surface area in wetland (Kadlec, 2000). In addition, the ratio of BMP surface area to watershed area is as important in determining pollutant load

removal as is BMP volume (Driscoll, 1983). Background concentration (C^*) of outflow from the BMP can be held constant as verified by many researchers (Schueler, 1996; Wong and Geiger, 1997; Minton, 2005). This chapter uses these important parameters such as inflow rate, BMP surface area to watershed area ratio, and BMP volume to estimate pollutant load removal; C^* is held constant. But the largest variation in the modeling done here is that uncertainty is applied to the inflow concentration (C_{in}) and the areal removal rate constant (k) to the BMP.

4.2.2 The Storage-Treatment-Overflow-Runoff Model

In the 1970s, the US Army Corps of Engineers developed a model capable of computing stormwater runoff to a storage-treatment control structure. This model is the Storage-Treatment-Overflow-Runoff Model (STORM). STORM is practical and easily understood and has been used to estimate the quantity and quality of watershed runoff based on watershed land use. STORM and its underlying algorithm have been applied to the estimation of runoff quantity and quality, and the model depends on different land use in the watershed (Roesner et al., 1974). STORM, or at least its methodology, is still used to estimate the quantity and quality of runoff because it is simple to run and capable of long-term continuous simulation while many other models are only capable of single event simulation and are very complicate. Its algorithm has been applied to both explicit processes using spreadsheets (Lee et al., 2005) and to analytical methods (Adams and Papa, 2000). Additionally, STORM can be used to design BMP volume. For instance, the California Stormwater Best Management Practice Handbook (California Stormwater

Quality Association, 2003) uses the STORM for sizing stormwater detention basins. But the known volume is dependent on the drawdown rate.

The algorithm of STORM is based on the rational method and is easy to incorporate with other models such as NetSTORM. NetSTORM combines several computational methods related to rainfall analysis such as the rainfall disaggregation method, the Intensity-Duration-Frequency (IDF) analysis method, and the STORM (Heineman, 2004). This study uses QuickSTORM in Rainmaster, the DOS version of NetSTORM. QuickSTORM contains the same algorithm as STORM in NetSTORM.

4.2.3 BMP Performance Model

Many approaches have been suggested to evaluate BMP performance. The most traditional of these approaches is the percent removal of pollutants. Strecker et al. (2001) compared three pollutant removal estimation techniques; statistical concentration, loading removals and percent removal by event based TSS and found that percent removal was not a suitable method to represent the performance of general BMPs. He suggested that effluent quality may be a better representative of BMP performance. A few years later, Barrett (2005) also represented BMP performance using observed BMP performance data. He reached a similar conclusion as Strecker et al. (2001), that percent removal is not appropriate to describe BMP performance. Additionally, he found BMP types and influent event mean concentration (EMC) have a strong correlation to BMP performance.

The U.S. Environmental Protection Agency (US EPA) (2002) recommends the effluent probability method (EPM) as the most useful method for quantifying BMP efficiency. The EPM shows normal probability plots of log transformed influent and

effluent EMC data in one figure. As a result, it provides a direct comparison of influent and effluent EMCs and BMP effectiveness (US EPA, 2002). However, the EPM is limited in applicability because it cannot represent BMP performance associated with each storm event, and it cannot provide a particular value for characterizing BMP performance (Caltrans 2003).

Due to the limitations of the recommended EPM, this study will use the $k-C^*$ model to characterize BMP performance. The $k-C^*$ model has already been applied in the modeling of wetland performance, and many references have verified that this model characterizes the removal of wetland pollutants very well (Kadlec and Knight, 1996; Kadlec, 2000; Braskerud, 2002; Kadlec, 2003; Rousseau et al, 2004; Lin et al., 2005). Recently, the $k-C^*$ model has been applied to the simulation of stormwater BMPs by Wong et al. (2002) and Huber (2006) because wetland characteristics are similar to the characteristics of detention basins and retention ponds. However, the $k-C^*$ model is difficult to obtain a reliable prediction of pollutant removal because the determination of its parameter values is not straightforward (Wong et al. 2006). Hence, it is necessary to develop a more sophisticated model to predict pollutant removal.

4.2.4 Uncertainty Analysis

Uncertainty analysis has been applied to various problems in the engineering field to quantify the reliability or probabilistic risk of systems. One of the most general and simple uncertainty analysis is the first order second moment (FOSM). It is also known as the first order error (FOE) method or the first order variance estimation (FOVE) method.

This method is the first order approximation method because it only considers the first order of the Taylor series. FOSM has been applied to various hydrosystem problems such as storm drainage (Yen and Tang 1976) and levee systems (Tung and Mays 1981). In environmental engineering, several researches have applied FOSM to the Streeter-Phelps equation used to estimate dissolved oxygen in streamflow (Burgess and Lettenmaier 1975; Tung and Hathhorn, 1988; Song and Brown, 1990; Melching and Anmangandla 1992).

The FOSM is used to estimate the margin of safety (MOS) with respect to the TMDL (Zhang and Yu, 2004; Franceschini and Tsai, 2008). Shirmohammadi et al. (2006) applied several uncertainty analysis methods such as the Monte Carlo simulation (MCS), the first order error (FOE) analysis, the latin hypercube sampling (LHS), and the generalized likelihood uncertainty estimation (GLUE) to the soil and water assessment tool (SWAT) in order to represent the cumulative density function (CDF) of monthly sediment reduction as a measure of BMP effectiveness. They suggested uncertainty analysis be used to improve the estimation of Margin of Safety (MOS) and TMDL. Arabi et al. (2006) characterized the effectiveness of BMPs in terms of estimated monthly reductions in sediment, total phosphorus (TP), and total nitrogen (TN) with two types of uncertainty analysis methods: the One-factor-At-a-Time (OAT) sensitivity analysis and GLUE using SWAT. In addition, they suggested the probabilistic estimation of the MOS for TMDL development.

4.2.5 Load Duration Curve

Load duration curves (LDC) have been developed to quantify total daily maximum load (TMDL). The use of LDC in quantifying TMDL is known as the “Kansas

approach” because Stiles (2001) applied this approach to bacteria TMDLs in the state of Kansas. This method has been well documented in the literature and has been modified for use in EPA Region IV. Using flow duration curves (FDCs), the Kansas approach relates the pollutant concentration to streamflow to establish the existing loading of the pollutant and the allowable pollutant load (TMDL). Four steps are taken in this method to determine TMDL and establish the required load reduction (O’Donnell et al. (2005)).

Several researchers (Stiles (2001), Cleland (2002 and 2003), Bonta and Cleland (2003) and O’Donnell et al. (2005)) utilized the LDC for TMDL estimation because it provides a technical approach for identifying “daily loads” in TMDL development, which accounts for the variable nature of water quality through time. In this method, a maximum concentration standard can be used with a hydrologic flow duration curve (FDC) to identify a TMDL that contains the full range of stream flow conditions. Using the LDC for TMDL approach, the maximum daily load can be verified for any given day (EPA, (2007)). While load duration curves have become more widely used and persuasive in TMDL estimation, they have not been expanded satisfactorily to BMP applications for TMDL. Zhang and Yu (2004) and Franceschini and Tsai (2008) estimated MOS with uncertainty and reliability methods based on statistical methods.

4.3 Methods

4.3.1 Outline of Urban Stormwater System

This study assumes urban runoff is routed through a BMP or a bypass overflow, if required, as shown in Figure 4.1. Additionally, EMC data are assumed to have a log-normal distribution based on empirical observation, and it is also assumed the runoff

volumes considered in the model (V_{in} , V_o , V_{out} , and V_{TOT}) are not uncertain. V_{in} is runoff volume from the study watershed, V_o is the overflow volume through the bypass overflow, V_{out} is the outflow volume from the BMP and V_{TOT} is the total flow volume which combines overflow and outflow volume from the BMP. The influent and effluent concentrations of the BMP are also assumed to have a lognormal distribution.

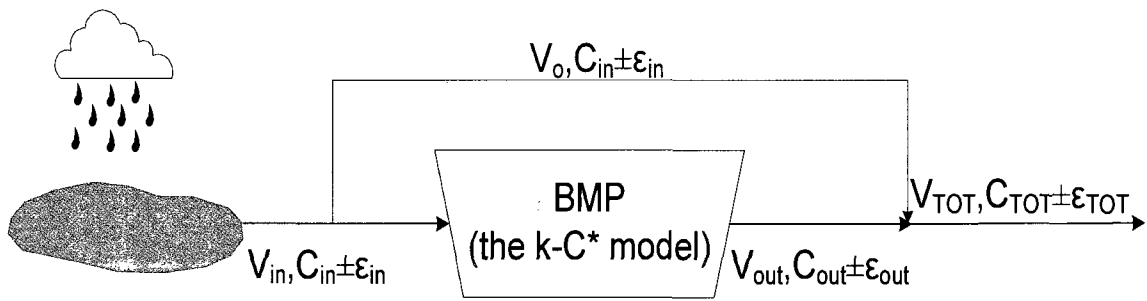


Figure 4.1 Schematic process of urban runoff through the BMP

4.3.2 Precipitation Data

Sixty years of continuous hourly precipitation data are used to simulate V_{in} , V_o , and V_{out} in Figure 4.1 with STORM. Continuous precipitation data for Fort Collins are obtained from the National Climate Data Center (NCDC, 2008). This rain gauge NCDC COOP ID number is 090451 and record ranges are from January 1, 1948 to December 31, 2007. According to Roher (2004), there is an error in the dataset on September 20, 1980. A value of 6.5 inches (165mm) is recorded in hour 2400. This value changed to 0.65 inches (16.5 mm) to be consistent with work conducted with Fort Collins precipitation data in a previous study (Nehrke and Roesner, 2004; Roher, 2004).

4.3.3 BMP Performance Data

BMP performance data were assembled from the International BMP database (ASCE & US EPA, (2002)) managed by the American Society of Civil Engineers (ASCE) and the United States Environmental Protection Agency (US EPA) as described in Section 3.3.1.

4.3.4 BMP Performance Model

The $k-C^*$ model combined with uncertainty analyses was selected to represent the BMP performance in this study as described by Section 2.3.1.

4.3.5 Relationship between Hydraulic Loading Rate and Areal Removal Coefficient

A prediction interval is used to TSS data in detention basins and in retention ponds as described by Section 3.3.3.

4.3.6 Generation of Probabilistic Outcomes

This study estimated the distribution of C_{out} using the $k-C^*$ model with two distributed input parameters C_{in} and k as shown in Figure 4.2. It assumes that the geometric (A) and hydrological parameters (Q) of the BMP have no uncertainty. Moreover, the background concentration (C^*) was fixed to 10 mg/L because the minimum value of selected observed data was close to 10 mg/L. In addition, this study

assumed that C_{in} and k were lognormally distributed because their distributions are very close to lognormal as shown in Section 3.3.3.

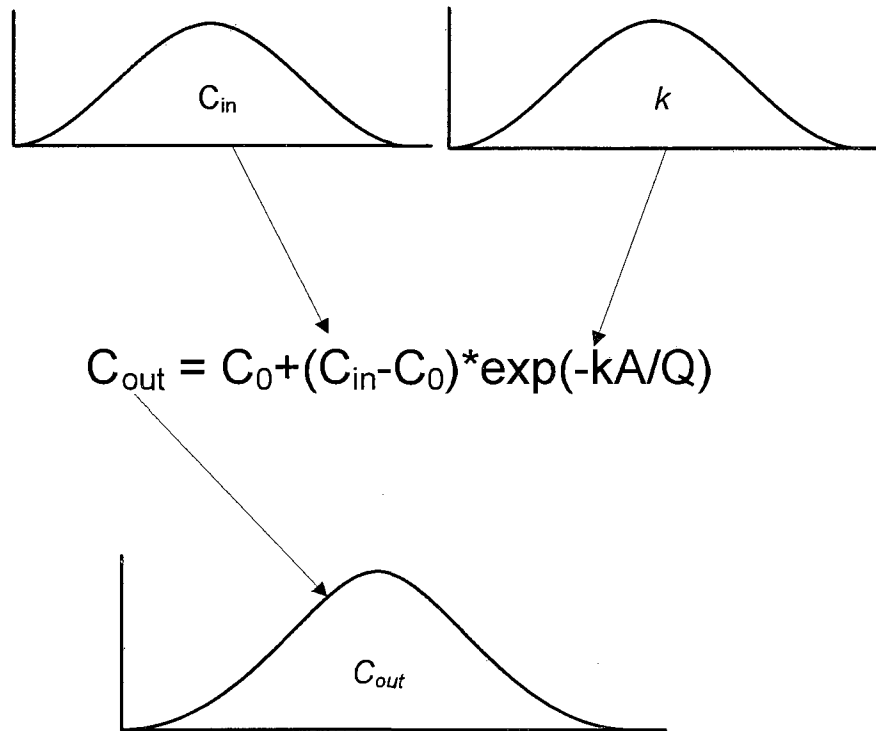


Figure 4.2 Schematic for generation of probabilistic C_{out}

4.3.7 First Order Second Moment (FOSM) Method

Theory of FOSM is described as Section 2.3.2.3.

4.3.8 Steps for Pollutant Load Estimation with Uncertainty

The following four steps demonstrate how to estimate pollutant mass balance with uncertainty. Ninety-five percent confidence intervals are used and the $k-C^*$ model was

employed to model BMP performance. Chapter 2 incorporates the $k-C^*$ model with uncertainty analysis to determine TSS removal in stormwater BMPs. The basic steps in the procedure are: 1) log transformation of the original EMC data, 2) estimation of the mean and standard deviation of the log-transformed EMC data, and 3) computation of pollutant load.

4.3.8.1 Log Transformation of Original EMC Data

In the following steps, x is the original EMC data and y is the log transformed EMC data. The log transformed data, y , is assumed to be normally distributed. Equation (4.1) log transforms the original EMC data

$$y = \log(x) \quad (4.1)$$

4.3.8.2 Estimation of Mean and Standard Deviation of Log Transformed EMC data

The mean (μ_x) and standard deviation (σ_x) of the lognormal EMC distribution are estimated using Equations (4.2) through (4.4) using the method of moments.

$$\hat{\mu}_y = \frac{1}{2} \ln \left(\frac{\hat{\mu}_x^2}{1 + \hat{\eta}_x^2} \right) \quad (4.2)$$

$$\hat{\sigma}_y^2 = \ln(1 + \hat{\eta}_x^2) \quad (4.3)$$

$$\hat{\mu}_{x,median} = \exp(\hat{\mu}_y) \quad (4.4)$$

where,

$\hat{\mu}_x$ is the mean of EMC data.

$\hat{\mu}_{x,median}$ is the median of EMC data. ($= C_{in}, C_{out}$ and C_{TOT})

$\hat{\eta}_x$ is the coefficient of variation for EMC data $\left(= \frac{\sigma_x}{\mu_x} \right)$.

μ_y is the mean of log transformed EMC data, and

σ_y is the standard deviation of log transformed EMC.

4.3.8.3 Computation of Pollutant Load

The inflow pollutant mass and its uncertainty are computed as the product of total runoff and EMC as shown in Equations (4.5) through (4.7).

$$M_{in,median} = M_R = C_{in,median} \cdot V_R \quad (4.5)$$

$$M_{in,95\%UCL} = C_{in,95\%UCL} \cdot V_R \quad (4.6)$$

$$M_{in,95\%LCL} = C_{in,95\%LCL} \cdot V_R \quad (4.7)$$

The bypass pollutant mass and its uncertainty can be determined through similar equations (Equations (4.8) through (4.10)).

$$M_{O,median} = C_{in,median} \cdot V_O \quad (4.8)$$

$$M_{O,95\%UCL} = C_{in,95\%UCL} \cdot V_O \quad (4.9)$$

$$M_{O,95\%LCL} = C_{in,95\%LCL} \cdot V_O \quad (4.10)$$

Only the bypass-overflow volume is needed because the pollutant concentration is assumed to be the same as C_{in} . The effluent pollutant concentration in the BMP is calculated as the estimated pollutant concentration using the k - C^* model through Equations (4.11).

$$\mu_{in\ out} = \ln(C_{out,median}) = \ln\{C^* + (C_{in,median} - C^*) \cdot \exp(-k_{median} / q)\} \quad (4.11)$$

If $C_{out,median}$ is log-transformed, it is the mean of log transformed values and marked $\mu_{\ln out}$. Standard deviation of k can be calculated as log transformed mean and standard deviation from Equation (2.18b) in Appendix I as shown in Equation (4.12).

$$\sigma_k = \sqrt{\{\exp(\sigma_{\ln k}^2) - 1\} \cdot \exp(2\mu_{\ln k} + \sigma_{\ln k}^2)} \quad (4.12)$$

It is assumed that C_{in} and k are independent. Therefore, the standard deviation of the C_{out} can be evaluated using Equation (2.7) in Chapter 2 from Equation (4.12) as shown in Equation (4.13):

$$\sigma_{C_{out}} = \left[\exp(-k_{median} / q)^2 \cdot \sigma_{C_{in}}^2 + \left\{ \frac{(C_{in,median} - C^*)}{q} \exp(-k_{median} / q) \right\}^2 \cdot \sigma_k^2 \right]^{1/2} \quad (4.13)$$

Using Equation (4.13), the mean value of C_{out} ($\mu_{C_{out}}$) can be estimated as shown in Equation (4.14):

$$\mu_{C_{out}} = \sqrt{\frac{\exp(2\mu_{\ln C_{out}}) + \sqrt{(\exp(4\mu_{\ln C_{out}}) + 4\sigma_{C_{out}}^2 \exp(2\mu_{\ln C_{out}}))}}{2}} \quad (4.14)$$

The log-transformed standard deviation of C_{out} can be determined using Equation (4.3) from Equations (4.13) and (4.14) as shown in Equation (4.15).

$$\sigma_{\ln C_{out}} = \left[\ln \left\{ 1 + \left(\frac{\sigma_{C_{out}}}{\mu_{C_{out}}} \right)^2 \right\} \right]^{1/2} \quad (4.15)$$

The confidence intervals of C_{out} can be estimated using Equation (4.11) and (4.15) through Equations (4.16) and (4.17).

$$C_{out,95\%UCL} = \exp(\mu_{\ln C_{out}} + 1.96\sigma_{\ln C_{out}}) \quad (4.16)$$

$$C_{out,95\%LCL} = \exp(\mu_{\ln C_{out}} - 1.96\sigma_{\ln C_{out}}) \quad (4.17)$$

The pollutant loading, M_{BMP} , and its confidence intervals are determined through Equations (4.18) and (4.20).

$$M_{out,median} = C_{out,median} \cdot V_{out} \quad (4.18)$$

$$M_{out,95\%UCL} = C_{out,95\%UCL} \cdot V_{out} \quad (4.19)$$

$$M_{out,95\%LCL} = C_{out,95\%LCL} \cdot V_{out} \quad (4.20)$$

Finally, the pollutant mass and its uncertainty at the receiving water can be estimated as the summation of outflow mass in the BMP and the bypass flow. M_{TOT} combines M_O and M_{out} as shown in Figure 4.1. To estimate the median and 95% confidence intervals for M_{TOT} , the calculated M_O and M_{out} from one thousand generated samples for each C_{in} and k by Monte Carlo Simulation (MCS) combines and calculates the median and 95% confidence intervals for M_{TOT} from one thousand results depending on each storm event.

4.3.9 Computation of the Event-Based Pollutant Load Frequency Curve

The following steps demonstrate how to compute a pollutant-load frequency curve on an event basis. The general steps are: 1) separation of flows into the BMP and the overflow bypass, 2) development of the load-frequency curve, and 3) calculation of the probable removal rate.

4.3.9.1 Separation of Flows into BMP and Overflow Bypass

QuickSTORM in Rainmaster was used to separate inflows between the BMP and the overflow bypass. The input values for the QuickSTORM model are shown in Table 4.1. The drawdown time in a BMP is assumed as 24 hrs in this study.

Table 4.1 QuickSTORM Input Parameters

Area (acres)	1
Depression Storage (in)	0.1
Evaporation Rate (in/day)	0.18
Interevent Time (hours)	6
Runoff Coefficient	0.28
	(40% imperviousness)
Treatment rate where bypass activate (mgd)	0
First flush depth (in)	0
Time of concentration	0.15

4.3.9.2 Development of Load Frequency Curve (LFC)

The LFC is developed using an approach similar to that used to develop the flow frequency curve. The main difference between the curves is flow frequencies are in terms of flows while load frequencies are in terms of loads. This study used 60-years of individual events to examine the frequency of pollutant loading.

Pollutant load frequency exceedance curves were developed by multiplying flow rates generated by STORM by estimated pollutant concentration found using the $k-C^*$ model. This approach used the descending order of average pollutant loading per individual event. A 24-hour inter-event time and minimum threshold of 0.01 inch runoff depth were specified to separate the flow data into individual events. The frequency and event pollutant loading can be estimated by the Cunnane (1978) formula (Equation (4.25)).

$$T = \frac{N + 1 - 2A}{M - A} \quad (4.25)$$

where,

T=return interval (years),

N=number of years of record,

M=rank of the event (in descending order of magnitude),

A=plotting position parameters (0.4).

E=exceedances per year

Exceedances per year can be converted from return interval using Equation (4.26) (Rohrer, 2004).

$$E = \frac{1}{T} \quad (4.26)$$

Figure 4.3 shows the schematic of LFC with 95% confidence intervals. Scattered dots indicate event pollutant loads.

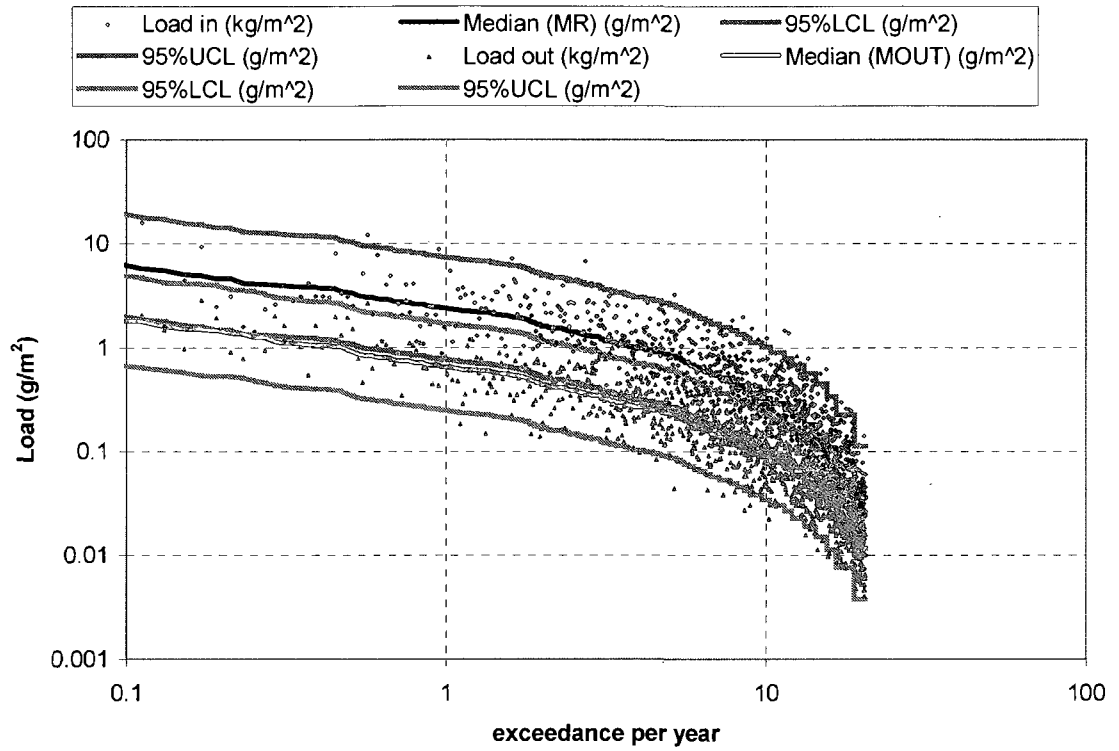


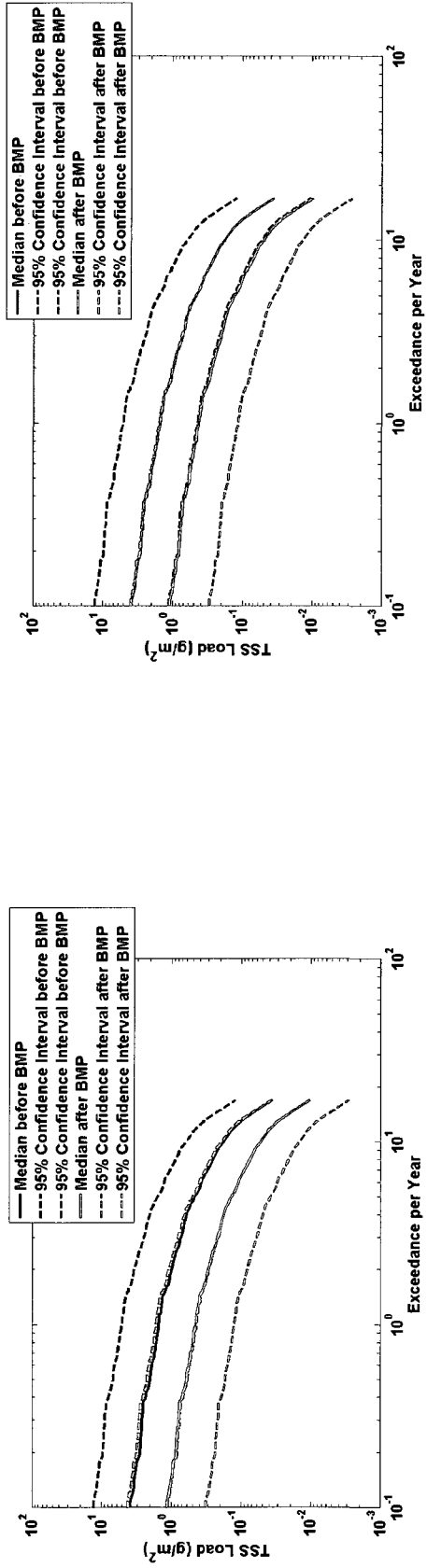
Figure 4.3 Schematic of Load Frequency Curve and 95% Confidence Intervals

4.4 Results

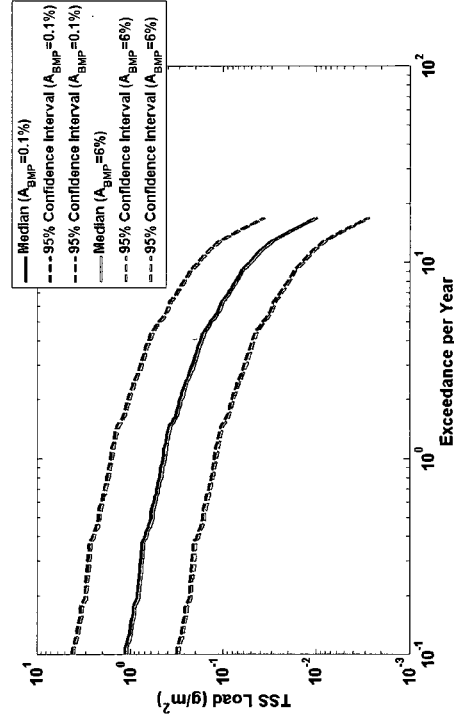
4.4.1 Load Frequency Curves (LFCs)

Figure 4.4 shows detention basin results in terms of LFCs comparing conditions without and with treatment in detention basin BMPs of different surface area ratios with different smoothing techniques applied. Figure 4.4(a) compares the pollutant load expected with no BMP treatment and the load expected when a BMP with a surface-area ratio of 0.1% is applied. Figure 4.4(b) compares the pollutant load expected with no BMP treatment and the load expected when a BMP with a surface-area ratio of 6% is applied. Figure 4.4(c) compares the two BMP treatments with surface-area ratios of 0.1 and 6% shown in Figure 4.4 (a) and (b).

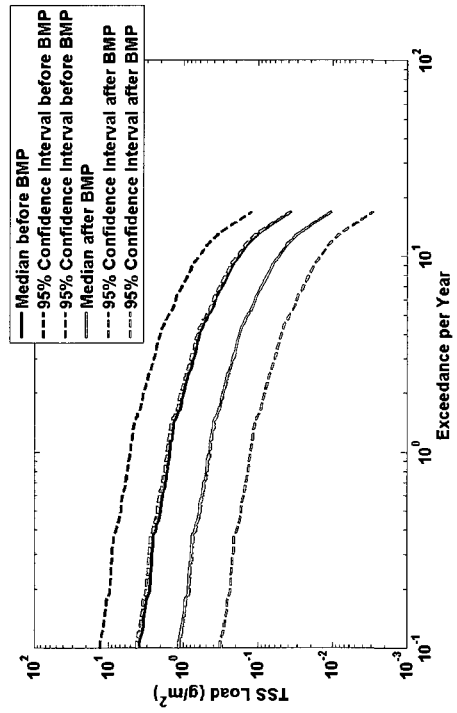
Figure 4.4 (a) and (b) illustrate the confidence interval of LFCs for detention basins are very similar in their confidence intervals to those of the LFCs of detention basins without treatment. Figure 4.4(c) shows the surface-area ratios of BMP detention basins have little effect on their treatment of pollutant loads. This indicates the BMP surface-area ratio of detention basins has negligible affect on detention basin performance. Therefore, it can be concluded that: 1) pollutant loads (illustrated through LFCs) in stormwater storage systems have similar variances to pollutant loadings without detention basin BMP treatment and 2) the surface-area ratios of detention basins have little effect on pollutant removal.



(a)



(b)



(c)

Figure 4.4. Comparison of LFCs as function of BMP volume (=2.03 cm) and imperviousness (=40%) and with median and 95% confidence intervals in detention basins ; (a) without BMP as BMP surface-area ratio=0.1%; (b) without BMP vs. with BMP as BMP surface-area ratio=6%; (c) with BMP as BMP surface-area ratio=0.1% vs. with BMP as BMP surface-area ratio=6%.

Figure 4.5 shows retention pond results in terms of LFCs comparing conditions without and with treatment in retention pond BMPs of different surface area ratios. Figure 4.5(a) compares the pollutant load expected with no BMP treatment and the load expected when a BMP with a surface-area ratio of 0.1% is applied. Figure 4.5(b) compares the pollutant load expected with no BMP treatment and the load expected when a BMP with a surface-area ratio of 6% is applied. Figure 4.5(c) compares the two BMP treatments with surface-area ratios of 0.1 and 6% shown in Figure 4.5 (a) and (b).

Figure 4.5 (a) and (b) illustrate the confidence interval of LFCs for retention ponds are greater than when no BMP treatment is applied. Figure 4.5(c) shows the surface-area ratios of BMP detention basins do effect their treatment of pollutant loads. This indicates the BMP surface-area ratio of retention ponds do affect treatment performance. Therefore, it can be concluded that: 1) pollutant loads (illustrated through LFCs) in stormwater storage systems have higher standard deviations when treatment is done with retentions ponds opposed to no BMP treatment and 2) the surface-area ratios of retention ponds do effect pollutant removal.

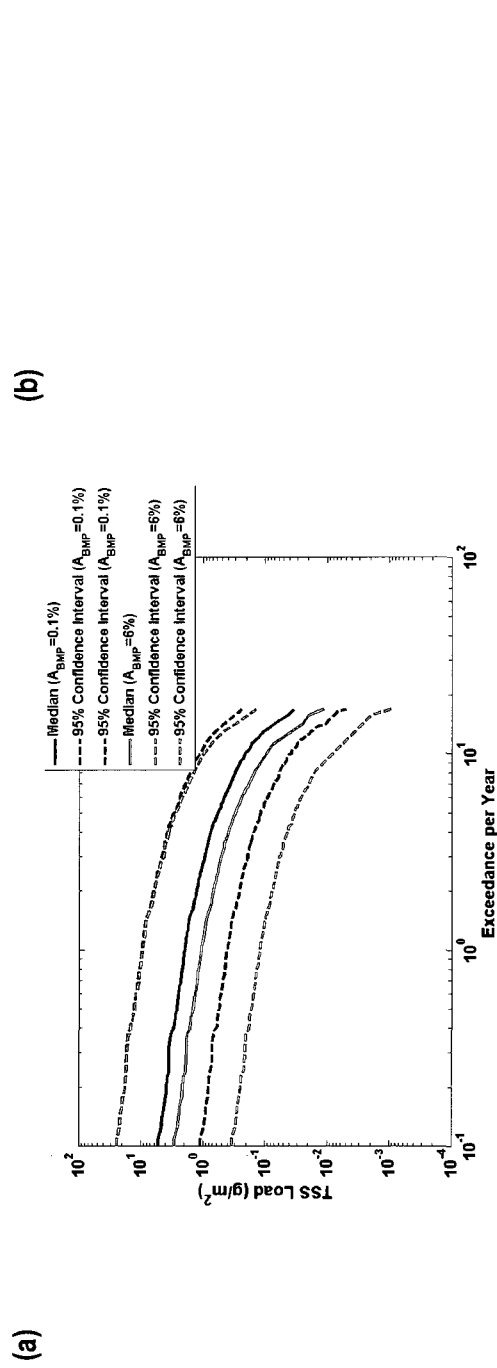
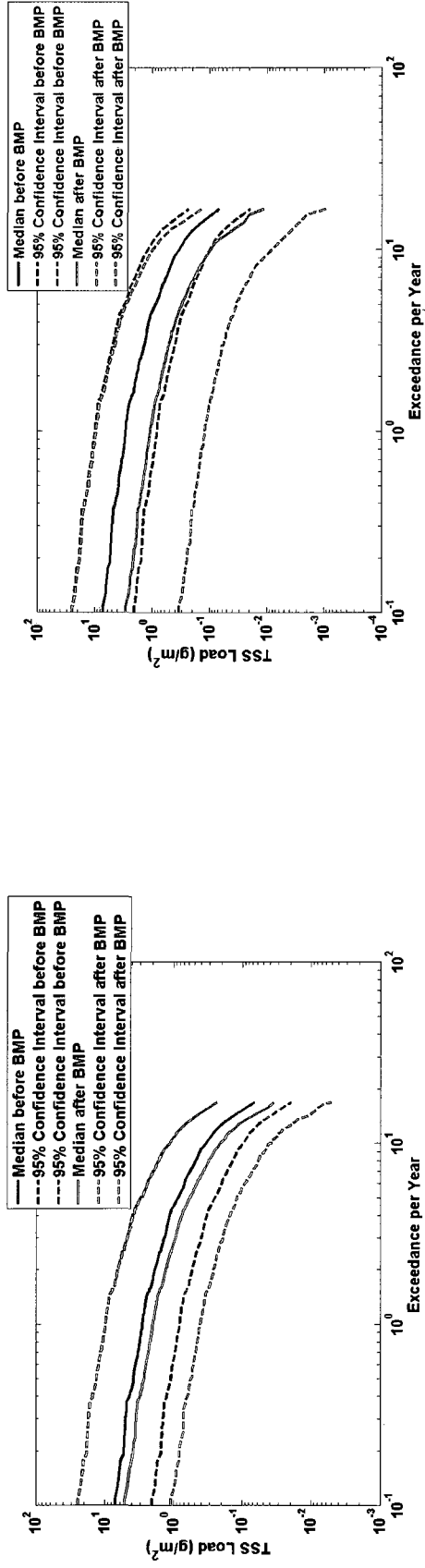


Figure 4.5 Comparison of LFCs as function of BMP volume (=2.03 cm times watershed) and imperviousness (=40%) and with median and 95% confidence intervals in retention ponds; (a) without BMP vs. with BMP as BMP surface area ratio=0.1%; (b) without BMP vs. with BMP as BMP surface area ratio=6%; (c) with BMP as BMP area ratio=0.1% vs. with BMP as BMP area ratio=6%.

4.4.2 Generic Procedure for BMP Design

This chapter is for the BMP design approach using previous results from Chapters 2 to 4. The objective of the following example is to show how a BMP can be sized to various target conditions; an example is given and a BMP design procedure focused on water quality performance is suggested. Table 4.2 shows STORM input parameters for the postdevelopment and postdevelopment plus BMP scenarios.

Table 4.2 STORM parameters depending on conditions for no target pollutant values

Parameters	Postdevelopment	Postdev.+BMP
Area (acre)	1	1
Depression storage (in)	0.1	0.1
Evaporation (in/day)	0.18	0.18
Intervent time (hours)	6	6
Runoff coefficient	0.279 (40% imp.)	0.279 (40% imp.)
Treatment rate (mgd)	0	0.011 (0.4 in)
Treatment rate where bypass activates (mgd)	0	0
Storage (mg)	0	0.011 (0.4 in)
First flush depth (in)	0	0
Time of concentration (hours)	0.1	0.1

This example is considered when there are target load values for the stormwater discharge expressed as an allowable load exceedance frequency. It is assumed here that target TSS load is 0.7 g/m^2 and storm exceedance is 4 exceedances per year. This criterium or target is shown in Figure 4.6. Figure 4.6 shows LFCs for postdevelopment without runoff controls and postdevelopment plus BMP including 95% confidence intervals. To evaluate the performance of the BMP with respect to this criterium, loads based on storm event are computed for both postdevelopment and postdevelopment plus BMP conditions. If a “target area” is defined at the quadrant below and to the right of the target load-frequency, the LFC for postdevelopment shows that about 49.0% of total

storm events are located in this target performance area and LFC for postdevelopment plus BMP shows that about 57.0% of total storm events are located in this target performance area. For this approach, BMP size can be adjusted depending on target pollutant load amount and regulated storm exceedance.

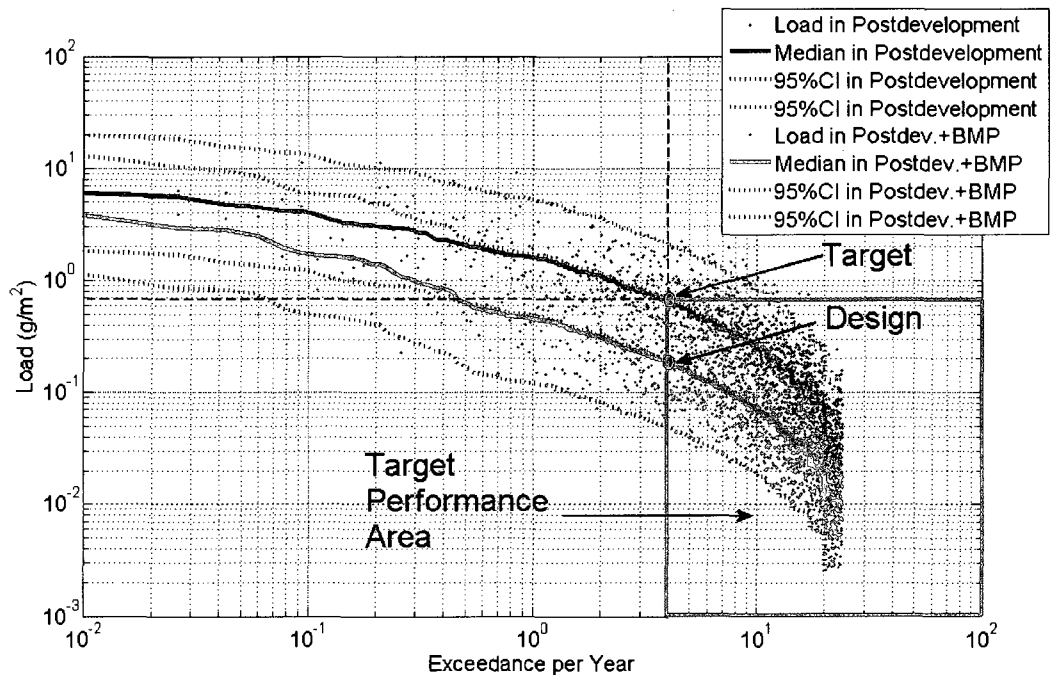


Figure 4.6 Load frequency curves including confidence intervals for requirements of load and exceedance

Note that the BMP has been designed so that the target is met with 95% confidence; not just met on the average. If uncertainty were not used in sizing the BMP, the “average” load as predicted by a BMP performance model would have been used to meet the target, but we can see that the uncertainty in that prediction at the 95% confidence level would have been three times of the target value. However by sizing the BMP so that the upper 95% confidence interval meets the target, we can be fairly certain that the load-frequency target value for watershed pollutant load will be met. Recall that

includes not only the load discharged from the BMP, but also the runoff load that bypasses the BMP when it is full.

A generic BMP design procedure based on probability was developed from the case study described in the previous section. This procedure is outlined in Figure 4.7. For this BMP design procedure, a long term record of hourly precipitation plus descriptive watershed data shown in Table 4.2 are required; and it is necessary to specify a target load-frequency value for pollutant load discharges from the watershed. This study used the STORM model as the watershed model because it is a simple model with which to do continuous simulation. BMP performance was modeled using the $k-C^*$ model with uncertainty analysis incorporated. If effluent load or concentration values from the stormwater system can satisfy a target safety probability of pollutant load or concentration, then BMP size including volume or surface area can be decided. When a BMP does not meet the estimated safety probability, an informed design modification can be made to satisfy the target probability.

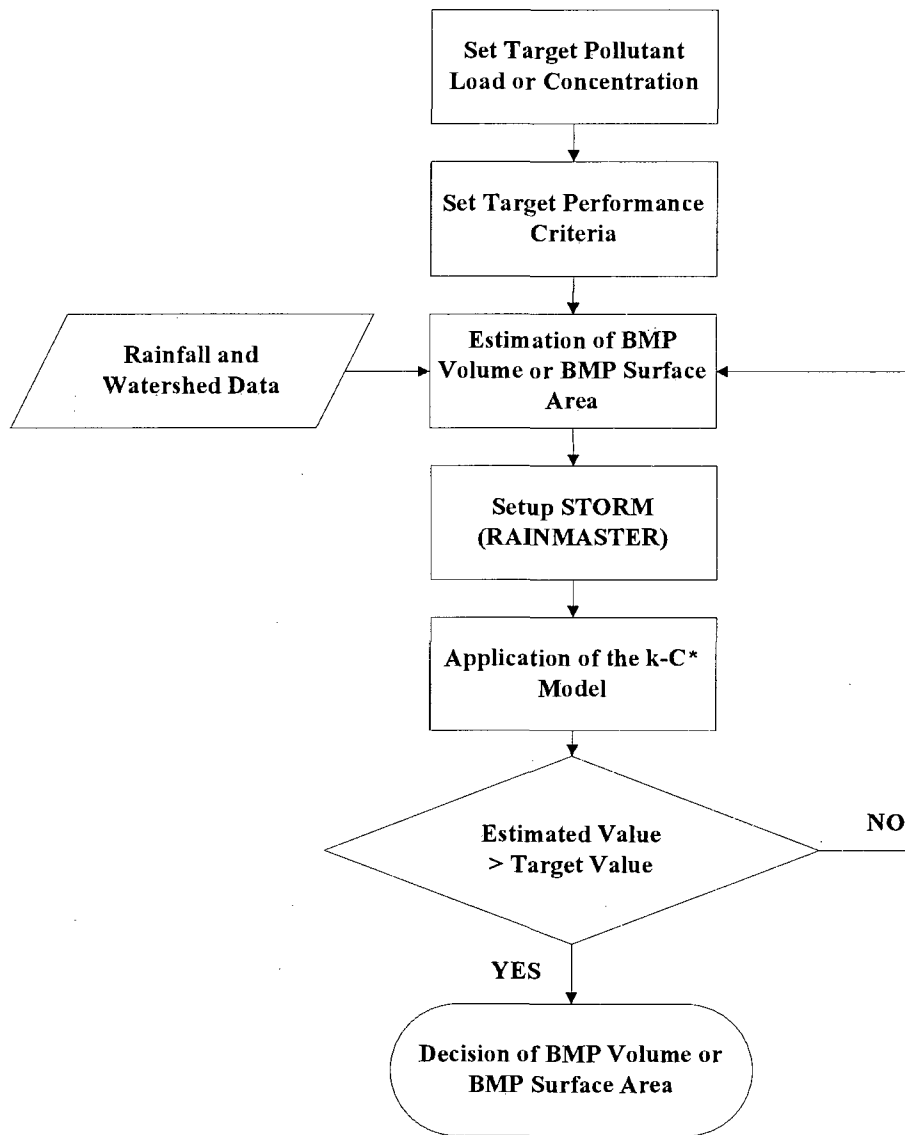


Figure 4.7 Flowchart of generic BMP design for a given target and safety

4.5 Discussion

The stormwater storage-release system is a classical system researchers have used to illustrate and explain the treatment and storage of stormwater runoff in BMPs before its release to receiving waters. Past literature has focused on BMP release rates to quantify their treatment performance. Much of this past literature has focused on the application of the first-order decay model, which employs the rate of release and a first order decay coefficient, to describe BMP treatment.

However, the rate of release varies in actual BMPs depending on the inflow rate of runoff, the BMP volume, and other BMP characteristics. Moreover, the first-order model cannot consider the irreducible minimum concentration or background concentration, C^* , for effluent EMC. Therefore, it is necessary that the geometric characteristics of the BMP, particularly BMP surface area, and C^* , the background concentration, be investigated further to better characterize BMP performance. For these reasons, this study applied the $k-C^*$ model in the modeling of BMP performance. The $k-C^*$ model is a popular model and has been applied by many researchers in the modeling of wastewater wetland performance since its introduction by Kadlec and Knight (1996). This study applied the $k-C^*$ model and uncertainty analysis to better characterize BMP treatment efficiency in detention basins and retention ponds.

The STORM model was employed for hydrologic simulation of the stormwater storage-release system for a hypothetical watershed. The STORM model was selected because its underlying algorithm is straightforward, it can perform continuous simulation, and it can model divided bypass flow on a storm-event basis. The output from STORM was used to drive the $k-C^*$ model, computing the volume and frequent of discharge loads

from the BMP and the volume and frequency for runoff discharges that bypass the BMP. Uncertainty analyses was applied to the runoff concentration values, and the k coefficient in the $k-C^*$ model to produce a probabilistic estimate of the pollutant loads released from the BMP and of loads bypassing the BMP. The LFC method was used here for the assessment of watershed performance with respect to meeting a TMDL which is expressed as an allowable exceedance frequency of the watershed pollutant load, frequency. Confidence intervals in the LFC can be suggested as one of the Margin of Safety (MOS) estimation methods in TMDL. In this study, LFCs incorporated uncertainty analysis in the estimation of safety probabilities for systems with and without BMPs. BMP performance was modeled through multi-year simulation and the difference between LFCs for the system with the BMP and without the BMP was quantified using probabilistic methods.

Based on LFCs results from Section 4.5 and Figures 4.6, this study suggests a methodology for pollutant load reduction to meet TMDLs expressed as load exceedance frequency targets. Depending on the target water quality standard (concentration or load), the BMP size can be designed. This methodology showed that BMP performance can be quantified and suggests a strategy for environmentally sustainable development.

4.6 Conclusions

Conclusions from this study are:

- The volume of detention basins should be considered when quantifying the pollutant load removal rates, but surface area of detention basins is not significant and does not need to be considered. However, volume and surface area of retention ponds should be considered when quantifying pollutant removal rates because both characteristics are significant to pollutant removal due to the presence of the permanent pool. These results should be reflected when BMPs are designed.
- LFCs can be used to represent changes in pollutant loading as well as BMP performance for sustainable water quality in a specific watershed by quantifying the difference between a watershed with BMPs and a watershed without BMPs. Also, confidence intervals in LFCs can be used to MOS estimation in TMDL.
- Finally, a methodology for sizing BMPs to reduce watershed runoff pollutants to specific loads was suggested and outlined as a case study depending on target pollutant load and exceedance per year.

4.7 References

- Adams, B. J., and Papa, F. (2000). *Urban stormwater management planning with analytical probabilistic models*, Wiley, New York.
- American Society of Civil Engineers and US Environment Protection Agency (ASCE & US EPA) (2002). "Urban stormwater best management practice (BMP) performance monitoring: A guidance manual for meeting the national stormwater BMP database requirements.", Report prepared by GeoSyntec Consultants and the Urban Water Resources Research Council of ASCE in cooperation with the Office of Water, US EPA.
- Arabi, M., Govindaraju, R. S., and Hantush, M. M. (2007). "A probabilistic approach for analysis of uncertainty in the evaluation of watershed management practices." *Journal of Hydrology*, 333(2-4), 459-471.
- Barrett, M. E. (2005). "Performance comparison of structural stormwater best management practices." *Water Environment Research*, 77(1), 78-86.
- Bonta, J. V., and Cleland, B. (2003). "Incorporating natural variability, uncertainty, and risk into water quality evaluations using duration curves." *Journal of the American Water Resources Association*, 39(6), 1481-1496.
- Braskerud, B. C. (2002). "Factors affecting phosphorus retention in small constructed wetlands treating agricultural non-point source pollution." *Ecological Engineering*, 19(1), 41-61.
- Burges, S. J., and Lettenmaier, D. P. (1975). "Probabilistic methods in stream quality management" *Water Resources Bulletin*, 11(1), 115-130.
- California Department of Transportation (CalTrans) (2003). "Storm water BMP handbook - new development and redevelopment, appendix B: general applicability of effluent probability method", January. Available at <http://www.cabmphandbooks.com>.
- California Stormwater Quality Association (2003). *California Stormwater BMP Handbook*, (WWW.cabmphandbooks.com).
- Cleland, B. (2002). "TMDL development from the "Bottom Up" – Part II: using duration curves to connect the pieces." National TMDL Science and Policy – WEF Specialty Conference, Phoenix, AZ.
- Cleland, B. (2003). "TMDL development from the "Bottom Up"–Part III: duration curves and wet-weather assessments." Proceedings of the Water Environment Federation, National TMDL Science and Policy Water Environment Federation, 1740-1766.
- Cunnane, C. (1978). "Unbiased plotting positions—a review." *Journal of Hydrology*, 37, 205–222.

- Driscoll, E. D. (1983). "Performance of detention basins for control of urban runoff quality." International Symposium on Urban Hydrology, Hydraulics, and Sediment Control, University of Kentucky.
- Franceschini, S., and Tsai, C. W. (2008). "Incorporating reliability into the definition of the margin of safety in total maximum daily load calculations." *Journal of Water Resources Planning and Management-ASCE*, 134(1), 34-44.
- Heineman, M. C. (2004). "NetSTORM—A computer program for rainfall-runoff simulation and precipitation analysis." World Water and Environmental Resources Congress 2004 Part of Critical Transitions in Water and Environmental Resources Management, ASCE, Salt Lake City, Utah.
- Huber, W. C. (2006). "BMP Modeling Concepts and Simulation." EPA600R06033; PB2007102054, Oregon State Univ., Corvallis.
- Hydrologic Engineering Center (HEC) (1977). "STORM storage, treatment, overflow runoff model user's manual." CPD-7, U.S. Army Corps of Engineers, Davis, CA.
- Kadlec, R. H. (2000). "The inadequacy of first-order treatment wetland models." *Ecological Engineering*, 15(1-2), 105-119.
- Kadlec, R. H. (2003). "Effects of pollutant speciation in treatment wetlands design." *Ecological Engineering*, 20(1), 1-16.
- Kadlec, R. H., and Knight, R. L. (1996). *Treatment Wetlands*, Lewis Publishers, Boca Raton.
- Lee, J. G., Heaney, J. P., and Lai, F. H. (2005). "Optimization of integrated urban wet-weather control strategies." *Journal of Water Resources Planning and Management-ASCE*, 131(4), 307-315.
- Lin, Y. F., Jing, S. R., Lee, D. Y., Chang, Y. F., Chen, Y. M., and Shih, K. C. (2005). "Performance of a constructed wetland treating intensive shrimp aquaculture wastewater under high hydraulic loading rate." *Environmental Pollution*, 134(3), 411-421.
- Melching, C. S., and Anmangandla, S. (1992). "Improved 1st-order uncertainty method for water-quality modeling." *Journal of Environmental Engineering-ASCE*, 118(5), 791-805.
- Minton, G. R. (2005). *Stormwater Treatment : Biological, Chemical, and Engineering Principles*, Resource Planning Associates, Seattle, Washington, U.S.A.
- National Climate Data Center (NCDC) (2008). Retrieved from the World Wide Web <http://www.ncdc.noaa.gov/oa/ncdc.html>.
- Nehrke, S. M., and Roesner, L. A. (2004). "Effects of design practice for flood control and best management practices on the flow-frequency curve." *Journal of Water Resources Planning and Management-ASCE*, 130(2), 131-139.

- Nix, S. J., and Heaney, J. P. (1988). "Optimization of storm water storage-release strategies." *Water Resources Research*, 24(11), 1831-1838.
- O'Donnell, K. J., Tyler, D. F., and Wu, T. S. (2005). "TMDL Report: Fecal and Total Coliform TMDL for the New River,(WBID 1442)." Watershed Management to Meet Water Quality Standards and Emerging TMDL (Total Maximum Daily Load) Proceedings of the Third Conference 5-9, Atlanta, Georgia.
- Patry, G. G., and Kennedy, A. (1989). "Pollutant washoff under noise-corrupted runoff conditions." *Journal of Water Resources Planning and Management-ASCE*, 115(5), 646-657.
- Roesner, L. A. (1982). "Quality of urban runoff." Urban storm water hydrology (water resources monograph 6), D. F. Kibler, ed., American Geophysical Union, Washington D.C.
- Roesner, L. A., Nichandros, H. M., Shubinski, R. P., Feldman, A. D., Abbott, J. W., and Friedland, A. O. (1974). "A Model for evaluating runoff-quality in metropolitan master planning." Technical Memorandum No.23 (NTIS PB-234312), ASCE Urban Water Resources Research Program, New York, NY.
- Rohrer, C. A. (2004). "Modeling the Effect of Stormwater Controls on Sediment Transport in an Urban Stream," M.S. Thesis, Colorado State University, Fort Collins.
- Rousseau, D. P. L., Vanrolleghem, P. A., and De Pauw, N. (2004). "Model-based design of horizontal subsurface flow constructed treatment wetlands: a review." *Water Research*, 38(6), 1484-1493.
- Schueler, T. R. (1996). "Irreducible pollutant concentrations discharged from urban BMPs." *Watershed Protection Techniques*, 2(2), 369-372.
- Segarra-Garcia, R., and Basha-Rivera, M. (1996). "Optimal estimation of storage-release alternatives for storm-water detention systems." *Journal of Water Resources Planning and Management-ASCE*, 122(6), 428-436.
- Segarra-Garcia, R., and Loganathan, V. G. (1992). "Storm-water detention storage design under random pollutant loading." *Journal of Water Resources Planning and Management-ASCE*, 118(5), 475-491.
- Shirmohammadi, A., Chaubey, I., Harmel, R. D., Bosch, D. D., Munoz-Carpena, R., Dharmasri, C., Sexton, A., Arabi, M., Wolfe, M. L., Frankenberger, J., Graff, C., and Sohrabi, T. M. (2006). "Uncertainty in TMDL models." *Transactions of the Asabe*, 49(4), 1033-1049.
- Song, Q., and Brown, L. C. (1990). "Do model uncertainty with correlated Inputs." *Journal of Environmental Engineering-ASCE*, 116(6), 1164-1180.

- Stiles, T. C. (2001). "A simple method to define bacteria TMDLs in Kansas." ASIWPCA / ACWF / WEF TMDL Science Issues Conference: On-site Program, St Louis, Missouri, 375-378.
- Strecker, E. W., Quigley, M. M., Urbonas, B. R., Jones, J. E., and Clary, J. K. (2001). "Determining urban storm water BMP effectiveness." *Journal of Water Resources Planning and Management-ASCE*, 127(3), 144-149.
- Tung, Y. K., and Hathhorn, W. E. (1988). "Assessment of probability-distribution of dissolved-oxygen deficit." *Journal of Environmental Engineering-ASCE*, 114(6), 1421-1435.
- Tung, Y. K., and Mays, L. W. (1981). "Risk models for flood levee design." *Water Resources Research*, 17(4), 833-841.
- Urban Drainage and Flood Control District (UDFCD). (2001). "Urban Drainage and Flood Control District Drainage Criteria Manual (USWDCM)." Volume I, Denver, Colorado.
- U.S. Environmental Protection Agency(US EPA) (2002). "Urban stormwater BMP performance monitoring: A guidance manual for meeting the national stormwater BMP database requirements.." Washington, DC.
- U.S. Environmental Protection Agency(US EPA) (2007). "An approach for using load duration curves in the development of TMDLs ", Washington, DC.
- Winer, R. (2000). "National pollutant removal performance database for stormwater treatment practices (Second Edition)." Center for Watershed Protection, Ellicott City , Maryland
- Wong, T. H. F., Fletcher, T.D., Duncan, H.P., Coleman, J.R., and Jenkins, G.A. (2002). "A model for urban stormwater improvement conceptualization." the Ninth International Conference on Urban Drainage, E. W. Strecker and W. C. Huber, eds., ASCE, Portland, Oregon.
- Wong, T. H. F., Fletcher, T. D., Duncan, H. P., and Jenkins, G. A. (2006). "Modelling urban stormwater treatment - A unified approach." *Ecological Engineering*, 27(1), 58-70.
- Wong, T. H. F., and Geiger, W. F. (1997). "Adaptation of wastewater surface flow wetland formulae for application in constructed stormwater wetlands." *Ecological Engineering*, 9(3-4), 187-202.
- Yen, B. C., and Tang, W. H. (1976). "Risk-safety factor relation for storm sewer design." *Journal of the Environmental Engineering Division-ASCE*, 102(2), 509-516.
- Zhang, H. X., and Yu, S. L. (2004). "Applying the first-order error analysis in determining the margin of safety for total maximum daily load computations." *Journal of Environmental Engineering-ASCE*, 130(6), 664-673.

5 CONCLUSIONS, CONTRIBUTIONS, AND RECOMMENDATIONS

5.1 Conclusions

BMPs have been widely used to control stormwater runoff and nonpoint source pollution in watersheds. However, the performance of BMP with respect to reduction of stormwater pollutant loads is not easily estimated. Thus, much research has tried to clearly explain BMP performance. This study proposed the $k-C^*$ model as the BMP performance model and applied this model to hydrologic factors, BMP geometry, and pollutant concentration. Uncertainty analysis was applied to the model to account for the many uncertainties associated with these variables.

The proposed methodology in this study suggests predicting output based on a storm event and overcomes the limitations and drawbacks of the current $k-C^*$ model. The proposed model was applied to TSS measurements from detention basins and retention ponds taken from the International BMP database to evaluate performance. For this model, the effect of BMP surface area and inflow on effluent EMC was investigated. Finally, BMP performance of pollutant loading removal in the stormwater system was also evaluated.

Specific conclusions were drawn from the research:

- (1) The $k-C^*$ model is essentially a model for wetland performance. This study incorporates this model with uncertainty analysis to represent BMP performance of TSS removal in detention basins and retention ponds. This approach, which

includes uncertainty analysis, shows confidence intervals and PDFs of effluent EMC. Decision makers can obtain more information from the output of the model on the reliability of estimated BMPs effluent discharge.

- (2) The effects of BMP surface area and inflow based on the $k-C^*$ model are that effluent EMC decreases with increasing BMP surface area and increases with decreasing inflow. However, the magnitudes of these changes are different for detention basins and retention ponds. Effects of BMP surface area and inflow on the effluent EMC is not large in detention basins, but retention ponds show noticeable effects of BMP surface area and inflow on effluent EMC.
- (3) Stormwater system performance can be evaluated using LFCs with confidence intervals when the $k-C^*$ model with uncertainty analysis is used. TSS load removal strategies can be suggested for a case study.
- (4) The TSS removal in detention basins is more strongly correlated with BMP volume rather than BMP surface area. However, the TSS removal in retention ponds is dependant on both BMP volume and BMP surface area. Moreover, results in detention basins show better efficiency than in retention ponds even though retention ponds usually show better performance than detention basins in other studies (Barrett, 2005; Winer, 2000). This is due to the small number of datasets and these dataset are regionally biased. For example, all detention basins dataset are chosen in California and 78% of retention ponds dataset are selected in Colorado. It makes possibility that BMP performances are affected by regional factors such as elevation, weather, geomorphology, soil characteristics, etc.

Therefore, it is necessary to apply a larger number of datasets which is selected in entire nations to validate the performance of detention basins and retention ponds.

5.2 Summary of Contribution

This study suggested BMP performance, which contains many uncertain variables, could be evaluated using the $k-C^*$ model with uncertainty analysis. The effects of BMP size and inflow to BMP performance are investigated with the modified model. In addition, the loading removal efficiency of BMPs for stormwater systems based on an event was investigated. The contributions of this study include:

- (1) The model proposed in this study can predict stormwater BMP performance by event with the use of confidence intervals. This is an improvement over the current BMP performance models. The current BMP performance models make predicting simulations difficult. Particularly, the prediction of stormwater events is more difficult because these models usually consider annual average values as input variables.
- (2) The effects of BMP geometry and inflow on BMP performance are very important because these factors are related to BMP design. However, there are few attempts to quantify their effects so far. This study shows that the effect of BMP surface area and inflow can be evaluated based on TSS removal BMP performance using the $k-C^*$ model.
- (3) This study quantifies BMP performance based TSS loading removal of detention basins and retention ponds using the $k-C^*$ model while

incorporating uncertainty analysis in representative stormwater systems of a watershed.

5.3 Recommendation

Three recommendations are suggested for further study:

- (1) It is necessary to apply other pollutants, such as total phosphorus and total nitrogen, to the $k-C^*$ model while incorporating uncertainty analysis to enhance the evaluation of the suggested model for predicting BMP performance.
- (2) It is necessary to apply the $k-C^*$ model while incorporating uncertainty analysis on an intra-storm event base to predict more detail. If it is possible, the BMP design method based on a storm event can be suggested.
- (3) Most of all, it is necessary to collect many more datasets to assure the results of the model because a larger number of data can create more typical results.

5.4 References

- Barrett, M. E. (2005). "Performance comparison of structural stormwater best management practices." *Water Environment Research*, 77(1), 78-86.
- Winer, R. (2000). "National pollutant removal performance database for stormwater treatment practices (Second Edition)." Center for Watershed Protection, Ellicott City, Maryland

Appendix II. Collected Data for Detention Basins

Sites	C _{in} (mg/L)	C _{out} (mg/L)	Q _{in} (m ³ /s)	Q _{out} (m ³ /s)	q	Calibrated k
15/78, CA	500	62	0.00602	0.00252	1.1864	2.6612
	370	70	0.00369	0.00213	0.3272	0.5863
	340	76	0.00356	0.00295	0.0622	0.1001
	270	38	0.01912	0.00491	1.6914	3.7691
	250	32	0.00077	0.00012	0.2485	0.5938
	240	66	0.00096	0.00062	0.0884	0.1248
	200	38	0.00569	0.00308	0.4437	0.8495
	200	26	0.00608	0.00401	0.1900	0.4703
	160	38	0.00386	0.00279	0.3414	0.5731
	130	32	0.01341	0.00267	0.3376	0.5727
	120	28	0.00070	0.00040	0.5328	0.9645
	120	36	0.00502	0.00379	0.3153	0.4548
	120	30	0.00100	0.00084	0.6055	1.0322
	100	46	0.00382	0.00249	0.0850	0.0779
	100	22	0.00370	0.00191	0.5374	1.0828
	5/605 EDB, CA	98	32	0.00215	0.00145	0.3265
48		14	0.00281	0.00242	0.5028	1.1320
Manchester, CA	110	32	0.00685	0.00667	0.5451	0.8254
	91	50	0.00030	0.00016	1.8925	1.3353
	400	33	0.01507	0.00091	1.0649	3.0144
	330	76	0.00377	0.00254	0.1121	0.1770
	300	84	0.01310	0.00148	0.3866	0.5280
	280	100	0.00203	0.00096	0.6701	0.7362
	270	58	0.00067	0.00015	0.2740	0.4629
	190	59	0.00145	0.00010	0.5713	0.7434
	190	94	0.00189	0.00039	0.9631	0.7340
	170	28	0.00266	0.00050	1.3134	2.8694
	170	48	0.00544	0.00031	0.9831	1.4133
	170	62	0.00039	0.00026	0.4430	0.4979
605/91 edb, CA	94	38	0.00342	0.00170	0.5192	0.5704
	92	18	0.00201	0.00043	0.9739	2.2666
	110	19	0.00136	0.00018	1.0966	2.6406
	85	59	0.00462	0.00071	1.5359	0.6538
	80	49	0.00096	0.00021	0.5067	0.2964
	61	24	0.00339	0.00060	4.1137	5.3180
	41	14	0.00346	0.00038	1.4281	2.9243

Appendix III. Collected Data for Retention Ponds

Sites	Cin (mg/L)	Cout (mg/L)	Qin (m ³ /s)	Qout (m ³ /s)	q	Calibrated k
La Costa WB, CA	240	28	0.00038	0.00028	0.0295	0.0753
	190	12	0.00058	0.00034	0.0450	0.2024
	60	12	0.00170	0.00116	0.1315	0.4234
	240	12	0.00176	0.00086	0.1361	0.6458
	170	28	0.00186	0.00087	0.1445	0.3156
	270	18	0.00273	0.00054	0.2116	0.7367
Lakewood RP(96), CO	618.75	338	0.00008	0.00008	0.4639	0.2869
	577.25	104.25	0.00017	0.00017	0.9161	1.6443
	343.25	168	0.00018	0.00018	0.9768	0.7290
	247	136	0.00009	0.00009	0.5049	0.3190
	180.25	44	0.00314	0.00314	17.3616	27.9679
Lakewood RP(97-98), CO	96	66	0.00012	0.00012	0.1195	0.0513
	580	24	0.00014	0.00014	0.1386	0.5138
	316	70	0.00016	0.00016	0.1584	0.2580
	356	229	0.00021	0.00021	0.2166	0.0991
	107	100	0.00034	0.00034	0.3425	0.0257
	272	69	0.00044	0.00044	0.4445	0.6626
	522	108	0.00079	0.00079	0.8038	1.3290
	223	173	0.00085	0.00085	0.8667	0.2319
	135	123	0.00086	0.00086	0.8731	0.0881
	199	119	0.00092	0.00092	0.9357	0.5150
	404	227	0.00152	0.00152	1.5412	0.9192
	342	102	0.00233	0.00233	2.3698	3.0413
	1030	88	0.00276	0.00276	2.8020	7.2036
	432	103	0.00312	0.00312	3.1718	4.7971
	143	139	0.00406	0.00406	4.1243	0.1259
302	70	0.00591	0.00591	6.0045	9.5015	